| 1. Report No.<br>FHWA/TX-06/0-4946-1 | 2. Government Accession No. | 3. Recipient's Catalog No. | |
|---|---|---|---|
| 4. Title and Subtitle<br>DYNAMIC TRAFFIC FLOW MODELING FOR INCIDENT DETECTION AND SHORT-TERM CONGESTION PREDICTION: YEAR 1 PROGRESS REPORT | | 5. Report Date<br>September 2005 | |
| | | 6. Performing Organization Code | |
| 7. Author(s)<br>Kevin Balke, Nadeem Chaudhary, Chi-Lueng Chu, Shamanth Kuchangi, Paul Nelson, Praprut Songchitruksa, Dvahg Swaroop, and Vipin Tyagi | | 8. Performing Organization Report No.<br>Report 0-4946-1 | |
| 9. Performing Organization Name and Address<br>Texas Transportation Institute<br>The Texas A&M University System<br>College Station, Texas 77843-3135 | | 10. Work Unit No. (TRAIS) | |
| | | 11. Contract or Grant No.<br>Project 0-4946 | |
| 12. Sponsoring Agency Name and Address<br>Texas Department of Transportation<br>Research and Technology Implementation Office<br>P.O. Box 5080<br>Austin, Texas 78763-5080 | | 13. Type of Report and Period Covered<br>Technical Report:<br>September 2004 – August 2005 | |
| | | 14. Sponsoring Agency Code | |
| 15. Supplementary Notes<br>Project performed in cooperation with the Texas Department of Transportation and the Federal Highway Administration.<br>Project Title: Dynamic Traffic Flow Modeling for Incident Detection and Short-Term Congestion Prediction<br>URL: http://tti.tamu.edu/documents/0-4946-1.pdf | | | |

16. Abstract

The purpose of this report is to summarize the research activities that were performed during the first year of this research project. In conducting this research, the research team split into several independent groups, each focusing on different aspects of the problem. One group has been focused on using weather and traffic flow conditions as predictors of incident conditions. Their activities are summarized in Chapter II. Other groups have been focused on developing models for producing short-term forecasts of potential congestion, using current measured traffic conditions. The results of these activities are summarized in Chapter III. Finally, we are beginning the process of developing a prototype tool that operators can use in a control center to display forecasted conditions. The beginnings of a high-level, functional specification for the tool are provided in Chapter IV.

| 17. Key Words<br>Incident Predictors, Traffic Modeling, Short-Term Congestion Prediction | 18. Distribution Statement<br>No restrictions. This document is available to the public through NTIS:<br>National Technical Information Service<br>Springfield, Virginia 22161<br>http://www.ntis.gov | | |
|---|---|---|---|
| 19. Security Classif.(of this report)<br>Unclassified | 20. Security Classif.(of this page)<br>Unclassified | 21. No. of Pages<br>120 | 22. Price |

Form DOT F 1700.7 (8-72) Reproduction of completed page authorized

# DYNAMIC TRAFFIC FLOW MODELING FOR INCIDENT DETECTION AND SHORT-TERM CONGESTION PREDICTION: YEAR 1 PROGRESS REPORT

by

Kevin Balke, Ph.D., P.E.
Center Director, TransLink®
Texas Transportation Institute

Paul Nelson, Ph.D.
Research Associate
Texas Engineering Experiment Station

Nadeem Chaudhary, Ph.D., P.E.
Senior Research Engineer
Texas Transportation Institute

Praprut Songchitruksa, Ph.D.
Assistant Research Scientist
Texas Transportation Institute

Chi-Lueng Chu
Graduate Student Worker
Texas Transportation Institute

Dvahg Swaroop, Ph.D.
Associate Professor
Department of Mechanical Engineering
Texas A&M University

Shamanth Kuchangi
Graduate Research Assistant
Department of Computer Science
Texas A&M University

Vipin Tyagi
Ph.D. Candidate
Department of Mechanical Engineering
Texas A&M University

# DISCLAIMER

This research was performed in cooperation with the Texas Department of Transportation (TxDOT) and the Federal Highway Administration (FHWA). The contents of this report reflect the views of the authors, who are responsible for the facts and the accuracy of the data presented herein. The contents do not necessarily reflect the official view or policies of the FHWA or TxDOT. This report does not constitute a standard, specification, or regulation.

This report is not intended for construction, bidding, or permit purposes. The engineer in charge of the project was Kevin N. Balke, P.E. #66529.

The United States Government and the State of Texas do not endorse products or manufacturers. Trade or manufacturers' names appear herein solely because they are considered essential to the object of this report.

# ACKNOWLEDGMENTS

# TABLE OF CONTENTS

**Page**

# LIST OF FIGURES

**Page**

# LIST OF TABLES

**Page**

# CHAPTER I. INTRODUCTION

**PROJECT OBJECTIVES**

The goal of this research project is to produce a tool that TxDOT can implement in the freeway management centers that will allow them to use traffic detector information currently being generated in their freeway management systems to make real-time, short-term predictions of when and where incidents and congestion are likely to occur on the freeway network. The idea is to combine roadway network modeling, traffic flow simulation, statistical regression and prediction methodologies, and archived and real-time traffic sensor information to forecast when and where: (a) traffic conditions will exist that are likely to produce an incident and (b) platoons of traffic will merge together to create congestion on the freeway. To accomplish this goal, we have identified four objectives as part of this research effort:

1. Develop a methodology for identifying and predicting when and where incidents are likely to occur on the freeway system by comparing traffic detector data from around known incident conditions.

2. Develop a model to predict traffic flow parameters 15 to 30 minutes into the future based on current and historical traffic flow conditions.

3. Develop a prototype tool that can be implemented by TxDOT in their freeway management centers that combines the ability to predict potential incident conditions and short-term congestion.

4. Conduct a demonstration of the prototype tool.

Figure 1 shows an overview of the two-year work plan that we have devised for completing this research effort. The first year of the work plan focuses on developing models needed for predicting incident potential and short-term congestion. A key task is to identify the most suitable predictors for use in these models. The second year of the project will focus on developing a prototype incident/short-term congestion (ISTC) prediction tool that TxDOT can implement in their control centers.

```
┌──────────────────┐     ┌──────────────────┐     ┌──────────────────┐
│ Task 1.  Identify│ ──▶ │ Task 2.  Develop │ ──▶ │ Task 3.  Correlate│
│ Candidate Incident│     │ Incident Predictor│     │ Incident Predictors│
│    Predictors    │     │                  │     │   with Actual    │
│                  │     │                  │     │     Freeway      │
│                  │     │                  │     │ Management Data  │
└──────────────────┘     └──────────────────┘     └──────────────────┘

┌──────────────────┐     ┌──────────────────┐     ┌──────────────────┐     ┌──────────────────┐     ┌──────────────────┐
│ Task 4  Assess   │ ──▶ │ Task 5.  Select/ │ ──▶ │ Task 6.  Correlate│ ──▶ │ Task 7.  Develop │     │ Prepare Year     │
│ Approaches for   │     │    Develop       │     │ Congestion Prediction│   │   Functional     │     │ 1  Research      │
│ Predicting Short-│     │   Congestion     │     │ Model with Actual │     │ Specifications for│    │    Report        │
│ Term Congestion  │     │ Prediction Model │     │ Freeway Management│     │ Prototype Tool   │     │                  │
│                  │     │                  │     │      Data        │     │                  │     │                  │
└──────────────────┘     └──────────────────┘     └──────────────────┘     └──────────────────┘     └──────────────────┘
```

```
┌──────────────────┐     ┌──────────────────┐     ┌──────────────────┐     ┌──────────────────────┐
│ Task 8.  Develop │ ──▶ │ Task 9.  Test and│ ──▶ │ Task 10.         │     │ Deliver Prototype    │
│ Prototype Incident/Short-│ │ Refine ISTC    │     │ Demonstrate      │     │ ISTC Software Tool   │
│ Term Congestion (ISTC)│  │ Prediction Prototype│  │ Prototype ISTC  │     │ and Documentation    │
│ Prediction Tool  │     │    Tool          │     │ Prediction Tool  │     └──────────────────────┘
└──────────────────┘     └──────────────────┘     └──────────────────┘
                                                   ┌──────────────────┐     ┌──────────────────┐
                                                   │ Task 11.  Develop│     │ Prepare Year     │
                                                   │   User's Guide   │     │ 2  Research      │
                                                   │                  │     │    Report        │
                                                   └──────────────────┘     └──────────────────┘
```

**Figure 1.  Sequence of Proposed Work Tasks.**

## SCOPE AND ORGANIZATION OF REPORT

The purpose of this report is to summarize the research activities that were performed during the first year of this research project. In conducting this research, the research team split into several independent groups, each focusing on different aspects of the problem. One group has been focused on using weather and traffic flow conditions as predictors of incident conditions. Their activities are summarized in Chapter II. Other groups have been focused on developing models for producing short-term forecasts of potential congestion, using current measured traffic conditions. The results of these activities are summarized in Chapter III. Finally, we are beginning the process of developing a prototype tool that operators can use in a control center to display forecasted conditions. Chapter IV provides the beginnings of a high-level, functional specification for the tool.

# CHAPTER II. MODELING INCIDENT PREDICTORS AND CONDITIONS

**IDENTIFICATION OF CANDIDATE INCIDENT PREDICTION MODELS**

A precursor is a variable that is derived from traffic stream data whose variations can indicate or point to a desirable pattern in traffic flow behavior. Recent research in incident prediction has widely used the concept of precursors in its models for predictions. Several researchers have worked with various precursors and tested the potential of those precursors for incident prediction.

Traffic volume has traditionally been a precursor of interest to many researchers for statistically relating to crash frequency. This precursor has been statistically quite significant, and research using models with volume has shown to be capable of describing 60 percent of the incidents (1). However, longer aggregation time involved in deducing traffic volumes has been a restriction of using volume as a precursor in real-time prediction systems. Volume has been predominantly useful in highway or intersection safety oriented studies.

Hourly flow, which is a shorter time aggregation of volume, is another precursor that has been used by a couple of researchers to predict accident rate. The results of models involving hourly flow have indicated some definitive correlation between hourly flow and accident rate, as in the work of Hiselius (2) an increasing rate of accidents with hourly flow is indicated. Segregating hourly flow rate by vehicle type, Hiselius also observed a constant increase in accident rate with hourly flow in the case of cars, but a decreasing rate with hourly flow in the case of trucks (2). Another study (3) also affirms that hourly flow provides a better understanding of the interactions like incidents; however, there has not been elaborate work on hourly flow as a precursor and a convenient prediction model for real-time applications.

Time headway has been tried as a casual precursor. Research shows that shorter headways have been the reason for collisions (4). However, again, there has been no convincingly explanatory model for use of this precursor in real-time incident prediction systems.

Research has found that the coefficient of variation in speed (CVS) along the lane to be sensitive in predicting accidents (5, 6, 7, 8, 9). Most of the models using CVS as a precursor have found very satisfactory correlation with accidents. Abdel-Aty et al. (8) have documented that their model's crash prediction level was around 62 percent, and similarly convincing results

have been reported in most of the other models, too. In all the studies involving CVS, the provision to aggregate the precursor values over an optimally small time period has been an advantage in sensing and predicting the variation of traffic behavior. However, there were a few studies (9) that have taken a totally opposite stand with regard to the ability of CVS as an incident precursor. Several reasons can be attributed to such a difference in conclusion, such as method of obtaining speed data, aggregation interval, and statistical methodology. However, in comparison to other precursors, CVS is the most likely choice for further investigating the use of CVS in real-time prediction models.

Traffic density is another parameter that has a good correlation in explaining incidents and is usually used in conjunction with CVS (7, 8). After a careful review, our research team has chosen density and coefficient of speed variation along the lanes (CSV) as the potential candidates for further investigation and use in the model for this project.

**MODELING INCIDENT PREDICTORS AND CONDITIONS**

Literature in the area of incident modeling and prediction is extensive, particularly for accident modeling. Many modeling approaches were proposed to help predict and detect incidents. Among all types of incident, accident has received the most attention from researchers due to its impacts economically and emotionally. Various approaches to modeling and predicting crashes boil down to two major categories: aggregate analysis versus disaggregate analysis. In the aggregate approach, crashes are aggregated temporally and spatially for the analysis. For example, one can examine the relationship between annual crash frequency on a particular freeway segment and freeway geometry. In contrast, a disaggregate approach views individual crashes as units of analysis. Recent availability of archived data from sensor devices such as inductive loop detectors and weather station sensors made possible the disaggregate approach used nowadays. Past studies for incident prediction using the disaggregate approach emphasized the real-time applications such as freeway safety performance monitoring tools and real-time crash precursors. Recent efforts in the area of incident modeling are summarized below.

Lee et al. (7) developed a log-linear model using categorical variables for incident prediction. They found in-lane coefficient of variation of speeds and traffic densities to be significant incident predictors. They also reported across-lane CVS to be statistically

insignificant. Their research indicated that practitioners consider different sizes of moving average window for different indicators.

Oh et al. (5) employed a nonparametric Bayesian classification method to predict real-time accident likelihood using loop detector data. They tested mean and standard deviation of flow, occupancy, and speed for the ability to predict crashes. A standard deviation of speed was found to outperform other indicators as a real-time crash precursor. The proposed method, however, may have limited potential for field implementation. First, only a single indicator was used in the model, which makes it unlikely to capture a variety of traffic conditions leading to crashes. Second, a selection of accident likelihood threshold is arbitrary. Third, the method is still inefficient; in other words, it produces a significant rate of false alarm.

Golob and Recker (10) applied nonlinear canonical correlation with cluster analysis to determine how any traffic flow condition on an urban freeway can be classified into mutually exclusive clusters (regimes) that differ in terms of likelihood of crash by types. Although they did not conduct a full-scale validation of their modeling approach, they did find that accurate estimation of crash rates heavily depends on the quality of loop data.

Giuliano (11) studied the frequency, patterns, and duration of incidents on a high-volume urban freeway. Models of incident duration were estimated using analysis of variance (ANOVA) with natural logarithm of duration being a dependent variable. She found incident duration to vary by incident type, lane closure, and time of day.

Madanat et al. (12) developed binary logit models for likelihood prediction of two types of freeway incidents: accidents and overheating vehicles. They considered both loop and environment data in their model development. They found peak period, temperature, rain, speed variance, and merge section to be significant predictors of overheating incidents. For the crash prediction model, only three variables were found to be statistically significant, which are rain, merge section, and visibility.

Although researchers have conducted a number of studies in the area of incident management in the past, relatively few have considered the use of both loop and environment data for real-time incident prediction. Weather and environment data were analyzed in a fairly aggregate picture, such as wet versus dry or daytime versus nighttime. Time-varying environment-related variables such as visibility and precipitation are now obtainable from many weather stations but are rarely addressed in the analysis. A methodology that utilizes these two

data sources for the incident prediction may lead to advancement in the capability to predict and detect incidents. As such, there is a need to explore the feasibility of predicting incidents using both real-time loop detectors and environment data. The researchers hope that this project will shed light on critical conditions that may lead to incident occurrences. Successful results and findings from this project would lead to a field implementation that aims to better the freeway incident management system. This, in turn, would help increase freeway productivity and freeway safety overall, which is the ultimate goal of this project.

We attempted to answer two important questions in this task:

- Given weather and loop detector data, how can we predict the likelihood of incidents?
- Are certain types of incidents more likely to occur than others for a given set of data conditions?

To answer these questions, we conducted this project as described in the following section.

**Methodology**

Freeway incidents can be classified into two categories for analytical purposes: in-lane and non-in-lane incidents. In-lane incidents are those that cause disruption to mainline traffic streams. They can vary significantly in levels of disruption. For example, multilane blocking vehicle overturns are usually more disruptive than single-lane blocking rear-end crashes. Loop data conditions prior to incidents may be used to predict these in-lane incidents. On the other hand, non-in-lane incidents such as vehicle stalls or shoulder disablements are not easily observed through the changes in loop data conditions. Therefore, weather and environment data can play an important role in predicting these types of incidents.

The modeling methodology in this project is structured as shown in Figure 2. We first analyzed the relationship between weather and environment data and incident types. Incident types are difficult to predict using loop data because their impact may not be observable and certain types of incident may have no impact at all. Environment data such as time of day and lighting conditions can be very helpful in predicting the type of incident that is most likely to occur under a certain set of conditions. As a following step, we examined the loop data for their ability to predict and detect in-lane incidents. Only accidents were considered in this analysis, while congestion and stall incidents were excluded. Congestion incidents were excluded at this

6

stage for two reasons: (a) their patterns of occurrences are fairly recurring, and (b) the occurrence mechanism of accidents is quite different from congestions. Stall or disablement, although frequent, is found to have negligible impact on the loop data. In the final step, based upon the findings in both steps of the analyses, we will develop an incident prediction model integrating weather, environment, and loop data conditions.
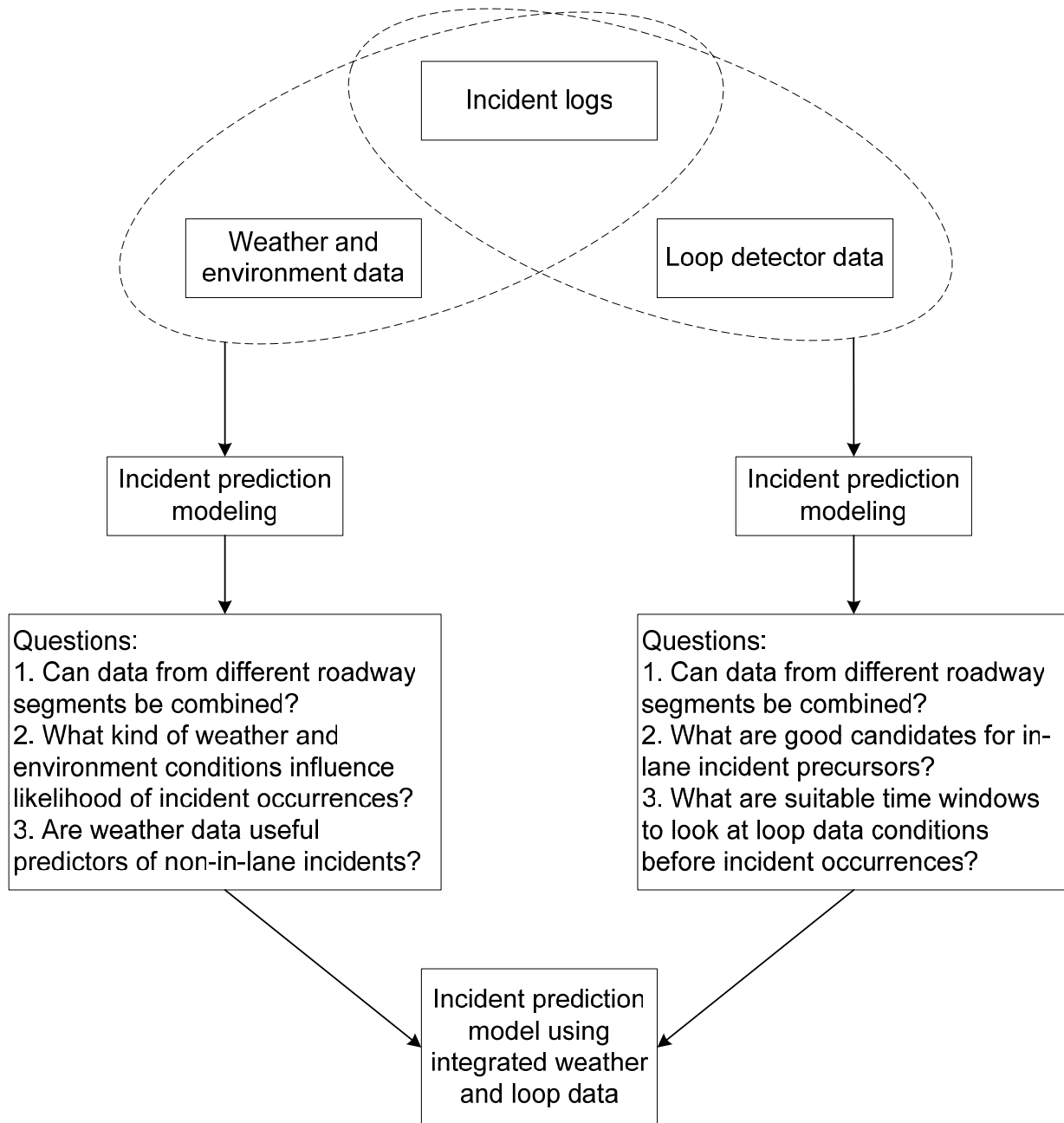


**Figure 2. Modeling Methodology.**

There are two types of outcomes in which we are interested: (a) likelihood of incident occurrences and (b) likelihood of a particular incident type. Both types of outcome are discrete and qualitative by nature; therefore, a typical linear regression approach would not be suitable in this case. Discrete outcome modeling approaches are becoming more common as a convenient statistical analysis tool to address problems of this nature. For example, researchers have used binary probit models to examine the factors influencing rear-end versus side-swipe accidents and single-vehicle versus multi-vehicle accidents (13). They also used ordered probit models to describe the severity of accident injuries (13). The outcome of this class of models is a probability associated with a set of explanatory variables, and this predicted probability in turn determines the outcome.

In this project, logit models were selected for the analyses for the following reasons:

- Logit models have closed-form expressions.
- Logit and probit models give similar results (14). Therefore, the use of probit models does not give any significant advantages over logit models.
- Logit models are computationally convenient for real-time implementation.

In this project, the binary logit model was used when two incident types are considered. Multinomial logit (MNL) and nested MNL were considered in cases where there are more than two incident types. The nested MNL model addresses the problem of independent of irrelevant alternatives (IIA) by placing the outcomes that are expected to share common unobserved disturbances in the same nest (15).

The standard multinomial logit formulation is of the form:

$$P_n(i) = \frac{\exp[\boldsymbol{\beta}_i \mathbf{X}_{in}]}{\sum_{\forall I} \exp(\boldsymbol{\beta}_I \mathbf{X}_{In})}. \tag{1}$$

where,

$P_n(i)$ = the probability of observation $n$ having discrete outcome $i$,

$\mathbf{X}_{in}$ = a vector of measurable characteristics that determine the outcome for observation $n$,

$\boldsymbol{\beta}_i$ = a vector of estimable parameters for discrete outcome $i$, and

$I$ = all possible outcomes for observation $n$.

The binary logit model is a special case of multinomial logit model when only two discrete outcomes are being considered.

The nested MNL model requires the assumption of generalized extreme value distribution for disturbance terms. The nested MNL model can be expressed mathematically as:

$$P_n(i) = \frac{\exp[\boldsymbol{\beta}_i \mathbf{X}_{in} + \phi_i LS_{in}]}{\sum_{\forall I} \exp[\boldsymbol{\beta}_I \mathbf{X}_{In} + \phi_I LS_{In}]},$$ (2)

$$P_n(j \mid i) = \frac{\exp[\boldsymbol{\beta}_{j|i} \mathbf{X}_{jn}]}{\sum_{\forall J} \exp[\boldsymbol{\beta}_{J|i} \mathbf{X}_{Jn}]}, \text{ and}$$ (3)

$$LS_{in} = \ln\left[\sum_{\forall J} \exp(\boldsymbol{\beta}_{J|i} \mathbf{X}_{Jn})\right].$$ (4)

where,

$P_n(i)$ = the unconditional probability of observation $n$ having discrete outcome $i$,

$X$ = the vectors of observable characteristics that determine the likelihood of discrete outcomes,

$\boldsymbol{\beta}$ = vectors of estimable parameters,

$P_n(j|i)$ = the probability of observation $n$ having discrete outcome $j$ conditioned on the outcome being in outcome category $i$,

$J$ = the conditional set of outcomes,

$LS_{in}$ = the inclusive value (logsum), and

$\phi$ = an estimable parameter.

**Analysis of Weather Data**

Numerous studies in the past reported that there exists a statistically significant relationship between weather conditions and traffic accidents. Madanat et al. (12) found visibility, rain, and temperature as useful predictors for certain types of incidents. Khattak et al. (13) examined differential impacts of adverse weather on crash types on limited-access roadways. Binary probit models were estimated for single- versus two-vehicle crashes and for rear-end versus side-swipe crashes. Injury severity was also analyzed using ordered probit

models. Shankar et al. (16) explored the effects of roadway geometrics, weather, and other seasonal effects on accident frequencies using a negative binomial model. Several weather-related factors such as maximum rainfall and number of rainy days were found to be significant. In addition, interactions between weather and geometric variables also were found to be important determinants of accident frequencies. Both studies by Khattak et al. (13) and Shankar et al. (16) were aggregate analysis; therefore, loop detector data were not considered in the studies. Brodsky and Hakkert (17) studied the risk of road accident in rainy weather. The results indicated that the added risk of an injury accident in rainy conditions can be substantial. Furthermore, the hazard could be even greater when a rain follows a dry spell.

However, past studies were primarily aggregate analyses. For example, the monthly accident frequency and annual number of accidents were typically used as dependent variables. A set of explanatory variables including the weather data was used to describe the variability in the frequency and type of accidents. This traditional modeling approach was useful for identifying factors contributing to frequency and various types of accidents for highway design and planning purposes; however, it is of limited use for real-time prediction of incidents in freeway operations. In addition, the weather stations in many metropolitan cities in the United States are capable of reporting the weather conditions on an hourly basis. Therefore, the first task is to examine the relationship between the incident types and environment variables.

We first examined the relationship between hourly weather records and types of incident. Given that an incident has already taken place on a freeway, we need to determine what kind of incident is most likely based on current weather and environment data. We begin with data descriptions used in the study. Then, several logit models were estimated for each individual roadway as well as combined data. Subsequently, results and findings from the analysis are discussed.

*Data*

In the analysis of weather and environment data, we considered three freeway sections in Austin, Texas (see Figure 3), which are (a) IH-35, (b) Loop 1, and (c) US 183.

We used incident logs and weather station data to create a data set for incident type modeling. We obtained incident logs from 2002 to 2004 for the selected roadway sections. Incident logs are recorded manually by freeway operators; therefore, human errors and unreported incidents are not unexpected, particularly during the hours without monitoring. Each

incident log contains useful information about each incident occurrence. In general, each log will approximately tell where, when, and what type of incident was happening. Note that there is a lag time between actual incident occurrence and reported times. Literature indicated that this lag time varies depending on type of incident. Major incidents such as multilane-blocking accidents usually have a short lag time, while minor incidents such as shoulder disablements are likely to have a long lag time. It is worth noting that incident logs of Austin freeways also contain a number of "test" incidents. These incidents are logged by operators only for testing purpose and, thus, must be removed prior to the analysis.
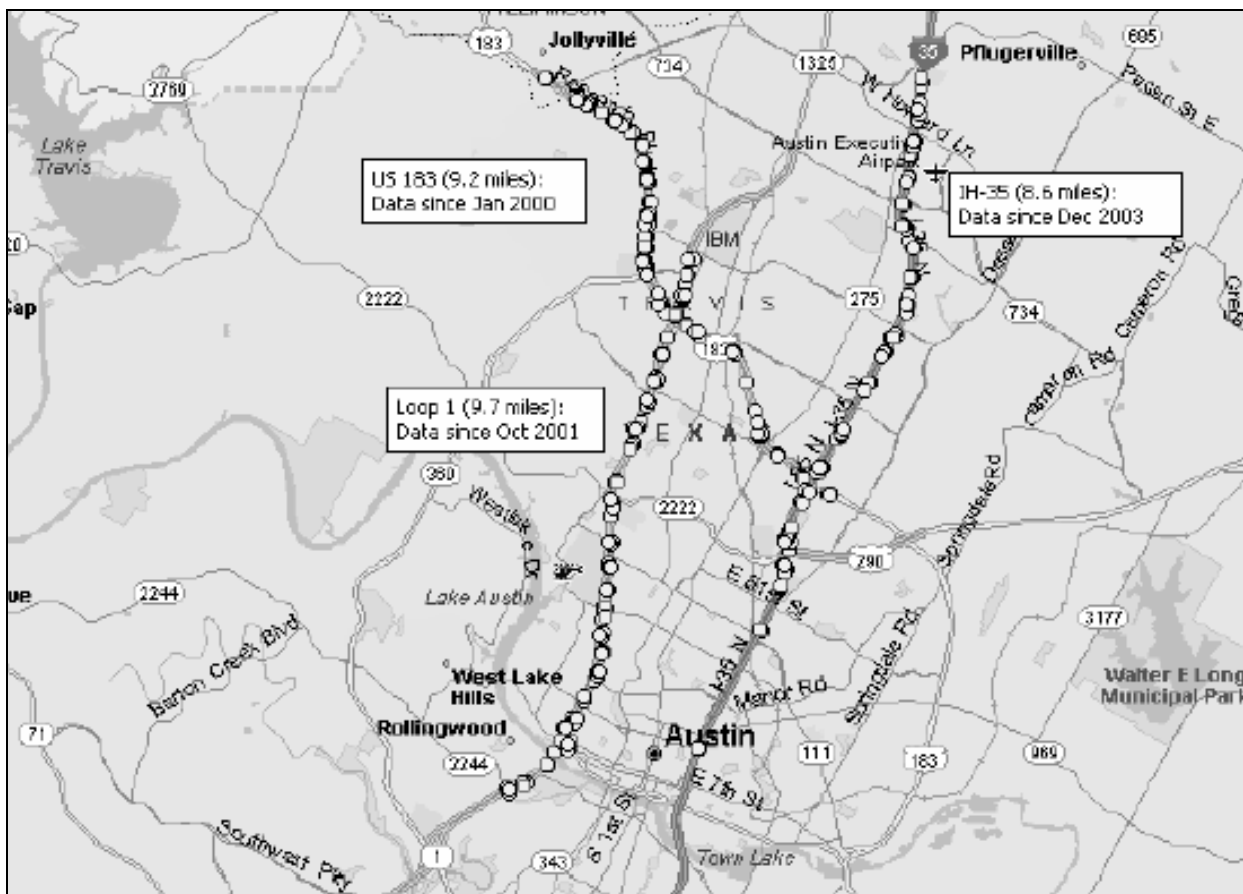


**Figure 3. Map of Studied Locations.**

Another source of data is weather stations. These climatological data are provided by the National Climatic Data Center (NCDC), and they can be accessed online (18). There are three weather stations in the vicinity of selected freeways: (a) Camp Mabry, (b) Austin-Bergstrom International Airport, and (c) Georgetown Airport. We selected the Camp Mabry station as it is

situated relatively closer to the studied freeways than the other two stations. Weather records are usually archived on an hourly basis. The data are archived at more frequent intervals (every 10 to 20 minutes) during special weather events such as heavy fog and thunderstorm. Hourly and special report types are denoted in weather records as "AA" and "SP," respectively.

Applications of weather forecast in freeway operations are not as extensive as in those of air traffic control. Weather records are used in this project to represent weather conditions during incident occurrences. Note that these weather stations may not exactly represent the true weather conditions at considered freeway segments due to spatial weather irregularities. However, it should give fairly accurate weather conditions during special weather events. Weather condition data are typically qualitative, and some are ordinal. For example, a weather type "TS" would represent moderate thunderstorm while TS+ and TS- indicate heavy and light thunderstorm, respectively. The data are recorded in text format. In addition, there can be a combination of weather types. For instance, if a thunderstorm and a haze are occurring at the same time, the weather type record will be "TS HZ." In order to perform the analysis, these text formats must be recorded as dummy variables, and a combination of weather types must be split into a set of single indicator variables.

Logged date and time of incident occurrences were matched with the nearest hourly weather records. These two sources of data were combined into one single table for the analysis. In addition, we obtained the daily sunrise and sunset times in 2004 to determine the lighting condition at the time of incident occurrence. Since changes in these times are insignificant year over year, we assumed the 2004 sunrise and sunset times to be representative of the other years as well.

*Model Development*

Three major types of incidents reported in incident logs are: (a) congestion, (b) collision, and (c) stall. A single-level MNL model was not suitable in this case since congestion incidents tended to follow a regular pattern. Therefore, incident types are classified into two categories: (a) recurring and (b) non-recurring. This classification scheme places collision and stall incidents in the same branch. A nest structure as shown in Figure 4 was used for the estimation of nested MNL models.
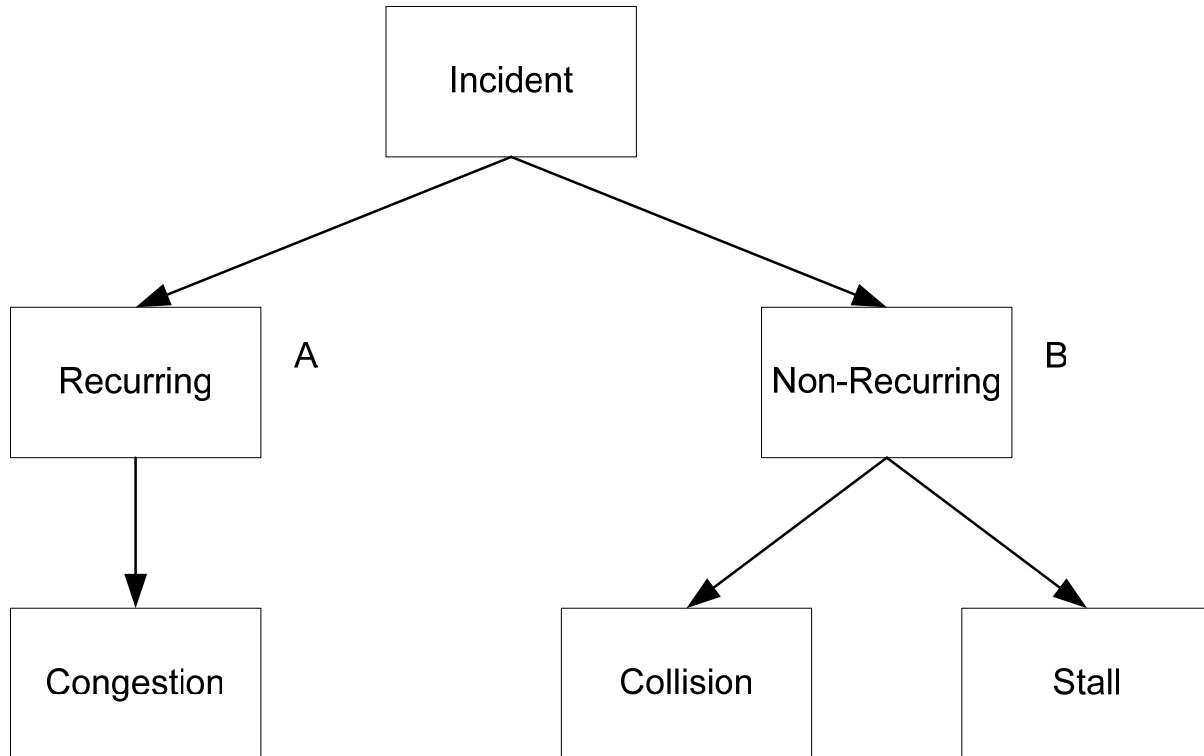
**Figure 4.  Nest Structure for Studied Incident Types.**

First, we estimated the models separately for each of the studied freeways. Due to inadequate sample size of congestion incidents on IH-35, we estimated a binary logit model for differential impacts of weather and environment conditions on collision versus stall incidents. For the other two roadways, nested MNL models were estimated using the proposed nest structure in Figure 4. Finally, we combined the data from all the selected roadways to estimate an overall nested MNL model. Estimation results are presented in the next section. The models were estimated using an econometric analysis software package called LIMDEP.

*Results*

Estimation results from US 183 and combined data are presented in Table 1 and Table 2, respectively. To interpret the results, a positive coefficient estimate indicates that the presence of such a variable would increase the likelihood of a particular incident type. For the non-recurring incident branch, a positive coefficient estimate increases the likelihood of a collision incident. Similarly, a positive coefficient estimate in the recurring (congestion) branch signifies an increase in the likelihood of congestion.

**Table 1. Estimated Nested MNL Model for US 183.**

| Variable | Estimated Coefficient | t-ratio | P-value |
|---|---|---|---|
| *Estimated model for the nest alternative (collision vs. stall)* | | | |
| Constant | -0.2225 | 0.1018 | 0.0288 |
| Nighttime indicator (1 if nighttime; 0 if otherwise) | 0.8985 | 0.3816 | 0.0185 |
| Poor visibility indicator (1 if visibility is 4 miles or less; 0 if otherwise) | 0.8973 | 0.3802 | 0.0183 |
| | | | |
| *Estimated model for the branch choice (recurring vs. non-recurring)* | | | |
| Direction indicator (1 if northbound; 0 if southbound) | -0.4818 | 0.2120 | 0.0231 |
| Morning peak indicator (1 if time is from 7:15 AM to 9:15 AM; 0 if otherwise) | 1.5587 | 0.2015 | 0.0000 |
| Nighttime indicator (1 if nighttime; 0 if otherwise) | 2.0333 | 0.3517 | 0.0000 |
| Clear sky indicator (1 if the sky is clear below 12000 ft; 0 if otherwise) | 0.6616 | 0.1918 | 0.0006 |
| Natural log of visibility | -0.7540 | 0.1037 | 0.0000 |
| Rain indicator (1 if there is a presence of rain; 0 if otherwise) | -1.3242 | 0.5778 | 0.0219 |
| | | | |
| *Inclusive value parameters* | | | |
| Recurring nest (fixed at 1.0 because there is only one alternative) | … Fixed parameter … | | |
| Non-recurring nest | | | 0.7109 |
| | | | |
| Number of observations | 702 | | |
| Restricted log-likelihood | -800.59 | | |
| Log-likelihood at convergence | -671.08 | | |

The confidence levels of each variable can be determined from the t-ratios or P-values. The t-ratios are obtained by dividing estimated coefficients with respective standard errors. A higher absolute value of t-ratios implies a higher confidence level. A P-value can be compared directly to a specified significance level. For example, a P-value of 0.07 would be statistically significant at 5 percent significance level but insignificant at 10 percent significance level.

Table 1 is an example of a nested MNL model estimated for an individual roadway. The inclusive parameter estimate of a non-recurring nest substantially departs from 1.0, indicating that a nested MNL model is a suitable choice.

As expected, congestion was more likely to occur during the morning peak and in the southbound direction toward Austin. The increase in congestion likelihood is partly explained by home-to-work trips in the morning in the southbound direction. Home-to-work trips are more likely to occur over a short period of time in the morning, thus creating congestion. They are also

less flexible than work-to-home trips. Poor visibility is found to increase the likelihood of congestion and collision. A congestion incident is more likely to occur during clear sky conditions while a presence of rain increases the likelihood of collision and stall incidents. A positive coefficient estimate of nighttime indicator implies that a collision incident is more likely to take place than a stall incident at night.

**Table 2. Estimated Non-nested MNL Model for Combined Data.**

| Variable | Estimated Coefficient | t-ratio | P-value |
|---|---|---|---|
| *Estimated model for the collision incident* | | | |
| Constant | -0.1922 | 0.0743 | 0.0097 |
| Nighttime indicator (1 if nighttime; 0 if otherwise) | 1.0348 | 0.2340 | 0.0000 |
| Poor visibility indicator (1 if visibility is 4 miles or less; 0 if otherwise) | 0.4295 | 0.1761 | 0.0147 |
| Summer indicator (1 if month is from June to August; 0 if otherwise) | -0.3803 | 0.1219 | 0.0018 |
| Morning peak indicator (1 if time is from 7:15 AM to 9:15 AM; 0 if otherwise) | 0.3367 | 0.1274 | 0.0082 |
| | | | |
| *Estimated model for the congestion incident* | | | |
| Direction indicator (1 if northbound; 0 if southbound) | -1.2455 | 0.1383 | 0.0000 |
| Morning peak indicator (1 if time is from 7:15 AM to 9:15 AM; 0 if otherwise) | 2.5567 | 0.1354 | 0.0000 |
| Nighttime indicator (1 if nighttime; 0 if otherwise) | 3.0778 | 0.2429 | 0.0000 |
| Clear sky indicator (1 if the sky is clear below 12000 ft; 0 if otherwise) | 0.9543 | 0.1176 | 0.0000 |
| Natural log of visibility | -0.7616 | 0.0588 | 0.0000 |
| | | | |
| Number of observations | 2182 | | |
| Restricted log-likelihood | -2391.68 | | |
| Log-likelihood at convergence | -1922.06 | | |

However, the estimated coefficient of nighttime indicator for a congestion alternative is positive. This result is counterintuitive as it implies that congestion is more likely to occur at night. There are two possible reasons for this. First, evening peak periods may occur after sunset. Second, this could be due to a false specification of the model in which a constant is omitted for the congestion branch. The addition of a constant would, however, render the model inestimable as it will become over-identified. The nighttime indicator may be capturing the effect of the omitted constant and, thus, be yielding a counterintuitive sign.

Congestion incidents on US 183 in 2004 were excluded from the modeling consideration due to an excessive number of reported congestions, which is likely to be attributed to changes in occupancy thresholds for congestion during the studied period. Estimation results are similar to the model for Loop 1 (not shown here). The natural logarithm of visibility was found to be more statistically significant than the original values. The log of visibility is used instead of the original values in order to account for the scaling effect. For example, a one-mile decrease in visibility from two to one is likely to have more significant impact on incident likelihood than a decrease from nine to eight miles.

We combined data from all the selected freeways and then estimated the nested MNL model for three types of incidents. The inclusive parameter value of the estimated model was 0.971, thus indicating that it can be reduced to a non-nested MNL model. Table 2 shows the estimated non-nested MNL model using the combined data. Aggregating data can help mitigate the bias caused by the overrepresentation of congestion or the under-representation of collision in the sample. One concern regarding data aggregation is that each selected freeway must share common characteristics that allow them to be aggregated. Observation showed that the estimated models for each selected freeway did not give any contradictory results.

Table 2 shows that clear sky condition, morning peak, and southbound direction increase the likelihood of congestion. A presence of rain was no longer statistically significant when using combined data. A coefficient estimate of nighttime indicator is counterintuitive, which is possibly due to an omitted constant as aforementioned. Similarly, we found that the natural logarithm of visibility was a better variable than visibility itself. A decrease in log of visibility tends to increase the probability of non-recurring incidents. In addition, we found nighttime and visibility of four miles or lower to increase the likelihood of accident. A combination of both nighttime and poor visibility also was found to give additional rise in the likelihood of collision incident. Increase in stall likelihood during the summer season is probably explained by overheating vehicles.

In the next section, loop detector data are evaluated to determine if and how they can be used to predict freeway incidents. Loop detectors are installed extensively on Loop 1 and US 183. Loop installation is somewhat limited on IH-35. Therefore, we performed an analysis of loop detectors using only the data from Loop 1 and IH-35.

**Analysis of Loop Detector Data**

In Texas, loop detectors provide a stream of one-minute observations of volume, speed, occupancy, and truck percent. These data are used in several applications such as congestion detection, travel time estimation, etc. The majority of loop data applications are passive in that the events must happen before actions will be taken. This analysis examines whether these data carry useful information that would allow us to predict incidents. The ability to predict incidents in advance would allow the traffic management center (TMC) operators to act proactively and deploy necessary preventive measures to minimize the risk of incident occurrences. We used the loop detector data to help predict incident versus non-incident likelihoods. This analysis requires two groups of data: incident and non-incident conditions.

*Data*

The concept of incident prediction using loop detector data focuses on understanding the relationship between disruptive traffic conditions and incident occurrences. Identifying incident precursors that have a strong relationship with incidents is central to this analysis.

Only the collision incident variable is considered in this analysis for two reasons. First, the majority of incidents that involve in-lane traffic disruptions are collision incidents. Stall incidents usually cause only a slight disruption, if any, to traffic flows. Many stall incidents are on roadway shoulders, which make it difficult to observe any impacts from loop data. Second, lag time for accidents is likely to be short, thus avoiding the problem of identification of actual incident occurrence time.

We used loop detector and collision data from Loop 1 and US 183 in 2003 and 2004 in this analysis. IH-35 was excluded due to limited loop installations. Next, loop data must be associated with each collision record. Since each collision record in incident logs contains date and time of collision, direction of roadway, and description of nearby cross street, we used direction of roadway and description of nearby cross street to locate the corresponding detector identifications (IDs) and station ID from a loop detector inventory file. A program was coded to perform this task. We then examined and edited manually the matched results since differences in the spelling of cross street names in incident log and loop inventory files cannot be easily accounted for in the programming. We excluded collision records that cannot be associated with any loop detector data in the proximity from further analysis.

Once the detector IDs are determined, the loop detector data can be retrieved either by lane or by station using recorded collision date and time. A selection of pre-accident duration for the analysis of traffic dynamics requires careful consideration. Lag time, which is the time between actual and reported accident occurrence, plays an important role in this consideration. For example, if the average lag time is three minutes, this means that pre-accident duration must be at least three minutes before the reported time. Since there is no comprehensive study regarding the lag time, we consider an average lag time of five minutes as the absolute minimum in this project. The pre-accident analysis of loop data was carried out at least five minutes prior to the reported time.

*Computed Measures*

There is a large catalog of measures that can be computed from a stream of one-minute observations of loop detectors. Studies by Lee et al. (6, 7) identified the average variation of speed on each lane (CVS) and traffic density as potential crash precursors. Average variation of speed difference across adjacent lanes was also tested but was insignificant. Oh et al. (5) evaluated the five-minute average and standard deviation of flow, occupancy, and speed for their performance as indicators of disruptive traffic dynamics. Standard deviation of speed was selected as a single measure for real-time estimation of accident likelihood.

In this project, we tested average volume, average speed, average occupancy, and average variation of speed (CVS) on each lane. The computation procedure requires a specification of window size for moving averages. The computation is performed first for each individual lane detector. Then, station averaging is applied to a set of detectors that belong to the same station. A program was coded to perform this task. The program inputs require station ID, date, and size of moving average window to calculate interested measures from the loop data.

**Lane Data —** For each individual lane detector, average volume, average speed, average occupancy, and variation of in-lane speed were computed. Moving average window size can be specified in the calculation. Three-, five-, and eight-minute moving averages were tested in this analysis.

The average volume per minute is calculated as:

$$\overline{q} = \frac{\sum_{i=1}^{N} q_i}{N} \qquad (5)$$

where,

$q_i$ = one-minute volume count of $i^{th}$ interval, and

$N$ = number of one-minute intervals in a specified averaging window.

The average occupancy is calculated as:

$$\overline{o} = \frac{\sum_{i=1}^{N} o_i}{N} \qquad (6)$$

where,

$o_i$ = one-minute average percent occupancy.

Also, it should be noted that occupancy is a proportional indicator of density.

The weighted average speed is calculated as:

$$\overline{v} = \frac{\sum_{i=1}^{N} q_i v_i}{\sum_{i=1}^{N} q_i} \qquad (7)$$

where,

$v_i$ = one-minute weighted average speed of $i^{th}$ interval.

The weighted average speed has an advantage over the arithmetic mean in that zero-count intervals are not used in the calculation, thus avoiding underestimation of mean values. The weighted average speed better describes the true fluctuation of vehicles' speed over time, particularly during nighttime where there is a preponderance of zero-count intervals.

The coefficient of variation in speed is a measure of the fluctuation in traveling speed. Past studies indicate that a breakdown in traffic flow will significantly increase the CVS and, thus, the likelihood of accidents (6).

Because a speed observation can be zero when there is no vehicle, the computation of CVS can be done in many variations. To illustrate, assume that we are considering the CVS over a five-minute interval. The first case is to compute the CVS using the one-minute average speeds over a five-minute interval while each interval is weighted equally. In this manner, zero-count intervals, which are typically the case at night, will increase the value of the CVS. In other words, the CVS may be large because zero-count intervals cause abrupt changes in speed values. The second case is to compute the CVS as in the first case, but weight each interval by the volume counts. Mathematically, this can be expressed as:

$$CVS = \frac{\sigma_{v_i}}{\bar{v}} = \frac{\sqrt{\frac{1}{N}\sum_{i=1}^{N} q_i \left(v_i - \bar{v}\right)^2}}{\bar{v}}.$$

(8)

The CVS values are generally sensitive to differences in speeds in low-volume conditions. The CVS calculation using eq. (8) can be modified such that the moving weighted average speeds are used instead of one-minute average speed. As a result, CVS can be computed as:

$$CVS_{\bar{v}} = \frac{\sigma_{\bar{v}_i}}{\bar{\bar{v}}} = \frac{\sqrt{\frac{1}{N}\sum_{i=1}^{N} \left(\bar{v}_i - \bar{\bar{v}}\right)^2}}{\bar{\bar{v}}}$$

(9)

where,

$$\bar{\bar{v}} = \frac{1}{N}\sum_{i=1}^{N} \bar{v}_i.$$ $CVS_{\bar{v}}$ = the fluctuation of moving average speeds over $N$ intervals.

Eq. (9) was used for the CVS computation in this analysis to mitigate the effect of changes in speed values in low-volume conditions. This also helps decrease a false alarm rate. Other measures such as standard deviations of volume and occupancy were not analyzed, as literature does not show any promising results (5).

**Station Data** — Data from a group of lane detectors at the same location are referred to as station data. The computed lane measures are averaged across lanes to obtain station average measures. Four measures are computed as in the case of lane data. Missing and invalid data are commonly encountered in the calculation. For each one-minute interval, missing or invalid

measures in each lane detector can either be omitted or specially treated. In this project, we treat any intervals that have invalid computed lane measures as invalid intervals.

The average volume across lanes is defined by:

$$\bar{q}_s = \frac{1}{\ell} \sum_{j=1}^{\ell} \bar{q}_j. \tag{10}$$

where,

$\ell$ = the number of lanes at the station.

The average occupancy across lanes is defined by:

$$\bar{o}_s = \frac{1}{\ell} \sum_{j=1}^{\ell} \bar{o}_j. \tag{11}$$

The average speed across lanes is defined by:

$$\bar{v}_s = \frac{1}{\ell} \sum_{j=1}^{\ell} \bar{v}_j. \tag{12}$$

The average CVS across lanes is defined by:

$$\overline{CVS} = \frac{1}{\ell} \sum_{j=1}^{\ell} CVS_j. \tag{13}$$

The station average measures were computed for every minute of valid lane detector data. These data are further matched with both incident and non-incident conditions to produce a data set for model development.

*Model Development*

Incident logs contain the information about the lanes affected by incidents. TxDOT lane numbering is designated in an ascending order from median to shoulder. For example, #1, #2, and #3 signify median, middle, and shoulder lanes, respectively. Since the excessive fluctuation of individual lane measures tends to offset the benefits from microscopic loop data, the station average data were instead examined in our analysis.

Estimation of real-time crash likelihoods using a binary logit model requires a sample of two traffic conditions: incident and non-incident traffic conditions. The incidents are verified and

logged manually by TMC operators from 6:00 AM to 12:00 AM during weekdays and 12:00 AM to 6:00 AM on Saturday. Incidents that occurred outside these hours were not recorded. Full-year archived loop detector data at selected freeway segments were available for 2003 and 2004. Therefore, we limited the study periods to only weekdays in 2003 and 2004 between 6:00 AM and 12:00 AM (midnight).

In 2003, there were a total of 82 collisions reported on these two freeways. Only 54 out of 82 collisions could be paired with the freeway loop detectors in the vicinity based on the cross street descriptions in incident logs.

For non-incident traffic data, we randomly sampled the loop data from these two roadway segments during incident-free traffic conditions. To do so, we first filtered the loop data for only the days without any reported incidents. Because operators log incidents only when the TMC is operating, we constrained the sampling periods to these hours only. A 2003 data set consisted of 44 collision records and 106 non-incident records. We applied a similar procedure to the 2004 data set. A final data set for model estimation consisted of 117 collision records and 342 non-incident records from random sampling during non-incident days.

Binary logit models were estimated to predict the likelihood of accident. The developed model aims to predict real-time accident likelihoods given an observation stream of loop detector data. Explanatory variables tested in the model development include volume, occupancy, and speed as well as computed values such as CVS.

To model the collision likelihood using loop data, we need to specify two parameters properly: moving average window size and incident detection time. A large moving average window size would help eliminate minor fluctuations in traffic dynamics, but it may obscure discernible changes in traffic dynamics. A small moving average window size, on the contrary, would be more sensitive to changes in traffic conditions while also subject to excessive false alarms. How much in advance the model would be able to predict a collision depends on the incident detection time used in the model development. If we analyze the traffic conditions 10 minutes prior to the accident reported time, this would imply that the estimated model will be predicting the likelihood of collisions within the next 10 minutes. It is worth noting that excessive incident detection time would make it difficult to observe any disruptive traffic conditions that may lead to crashes. In the model calibration process, this would reduce the model goodness-of-fit as well. Conversely, shorter incident detection time may increase the

likelihood of observing disruptive traffic conditions leading to crashes, while the ability to predict the collision in advance would be limited to only the incident detection time used in the calibration.

To optimize these two parameters, different moving average windows and incident detection times were evaluated for their influence on the model goodness-of-fit. Average occupancy and average CVS are found to be statistically significant consistently, amongst others. As such, we retained these two variables for the evaluation of model goodness-of-fit for different combinations of model parameters.

The evaluation result is presented graphically in Figure 5. A combination of incident detection time of 15 minutes and 5-minute moving average was found to give the best model goodness-of-fit. Therefore, this set of parameters is used and recommended for the selection of the final model.

**Model Goodness-of-Fit**
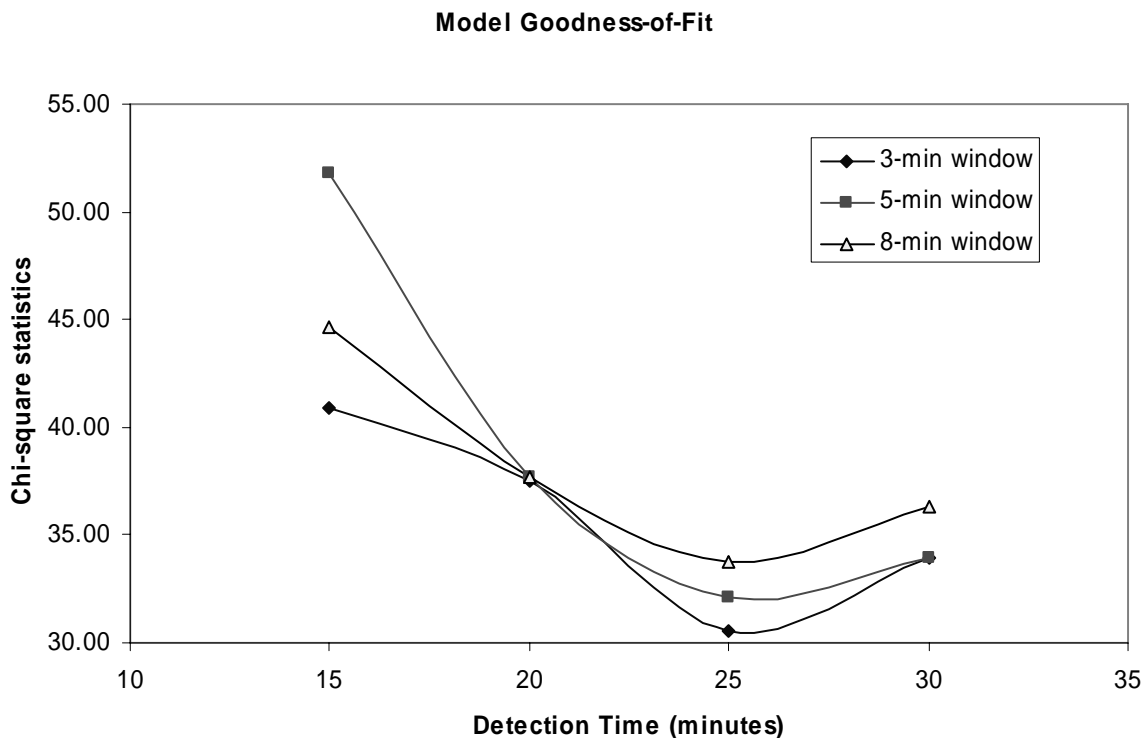


**Figure 5. Model Goodness-of-Fit.**

*Results*

Using 15-minute detection time and 5-minute moving average, the estimated binary logit model before estimation corrections is presented in Table 3. By using loop data at 15 minutes

23

prior to the reported incident occurrence, the estimated model provides an advance warning in terms of a likelihood of collision within the next 15 minutes.

**Table 3.  Estimated Binary Logit Model for Collision Incident.**

| Variable | Estimated Coefficient | t-ratio | P-value |
|---|---|---|---|
| Constant | -2.508 | -9.150 | 0.0000 |
| Average occupancy (%) | 0.139 | 4.776 | 0.0000 |
| Average CVS | 14.251 | 3.703 | 0.0002 |
| Number of observations | 380 | | |
| Restricted log-likelihood | -212.58 | | |
| Log-likelihood at convergence | -186.68 | | |

Both coefficient estimates for average occupancy and average CVS are positive. This is quite intuitive as it implies that abrupt increases in occupancy and CVS simultaneously will significantly give rise to the likelihood of collision. During a low-volume condition, CVS in general is relatively large. But, without a significant increase in occupancy, the likelihood of collision will not be much affected. Similarly, a normal increase in traffic flow during the course of the day would typically translate to an increase in average occupancy. However, average CVS will usually stay approximately unchanged, thus leaving the likelihood of collision unaffected as well.

Since the collision outcomes are overrepresented in the sample, an estimation correction must be made. The correction is straightforward, providing that a full set of outcome-specific constants is specified in the model. Under these conditions, standard logit model estimation correctly estimates all parameters except for the outcome-specific constants. To correct the constant estimates, each constant must have the following subtracted from it:

$$\ln\left(\frac{SF_i}{PF_i}\right), \tag{14}$$

where,

$SF_i$ = the fraction of observations having outcome $i$ in the sample, and

$PF_i$ = the fraction of observations having outcome $i$ in the total population.

With estimation corrections, we adjusted the constants of each outcome. We assumed that approximately 2 percent of the loop data were influenced by collision incidents. This will give $PF = 0.2$ and $SF = 117/459$.

**Model Test: Collision Incidents** — Using the estimated binary logit model in Table 3 with adjusted constants, the minute-to-minute prediction of likelihood of collision can be obtained. We tested the developed model to several sets of data with collision incidents. For example, a five-day data set at station ID 26 of US 183 from October 10–14, 2004, was input into the model. A collision incident was reported on October 12, 2004, at 1:06 PM. The predicted likelihood of collision over the same five days is shown in Figure 6.
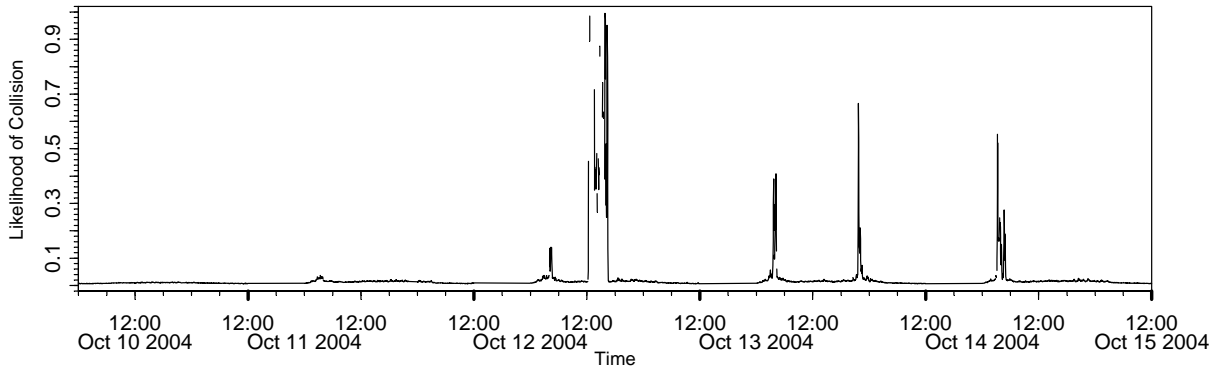


**Figure 6. Predicted Likelihood of Collisions (US 183 @ Station ID 26).**

All the test results are very encouraging as the model predicts high likelihoods of collision quite accurately. A jump in likelihood later after crashes also implies a possibility of secondary crashes. This could signal TMC operators to examine the warnings and deploy necessary preventive measures in advance.

25

**Model Test: Non-incident Conditions** — The estimated model also was tested with several data sets from non-incident days. For instance, we used five-day loop data without any incidents reported from Loop 1 at station ID 255 from April 21–25, 2003. Predicted likelihoods of collisions for the selected five days do not reveal any drastic increase in the likelihood of collision (see Figure 7). The maximum predicted likelihood is less than 0.025. This result indicates that the developed model is robust to minor fluctuations of the selected incident precursors.
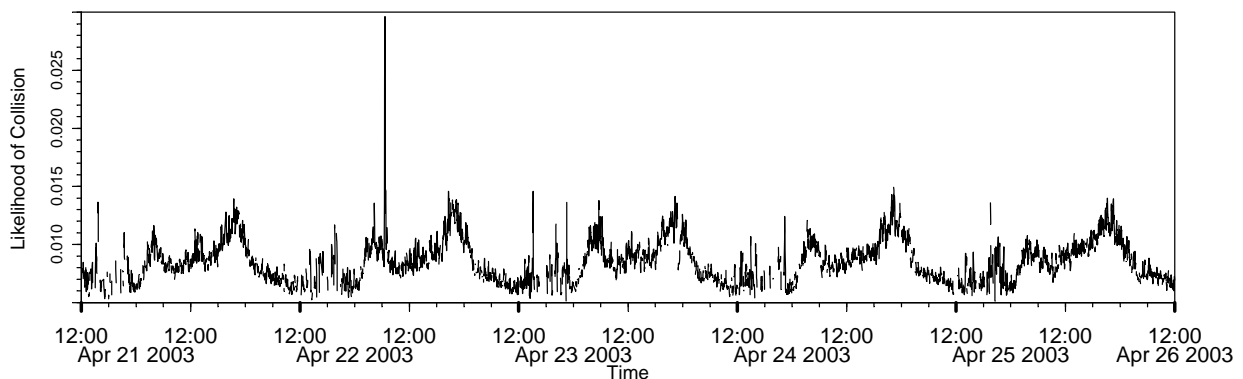


**Figure 7. Predicted Likelihood of Collisions (Loop 1 @ Station ID 255).**

From the model testing of non-incident conditions, we found that the test results are quite satisfactory as they imply a low rate of false alarms. The estimation results indicate that occupancy and average variation of speed are potential precursors of crashes. These findings are also consistent with the previous studies by Lee et al. (7).

**Next Steps**

We conducted the analyses of weather, environment, and loop data to evaluate their feasibility in predicting incident types and occurrences on freeways. First, nested and non-nested multinomial logit models were estimated to study the impacts of weather and environment data on incident types. Factors such as visibility, time of day, and lighting conditions were found to be significant determinants of incident types studied: collision, congestion, and stall. Then, we examined the loop data for their ability to predict an in-lane incident, which is a collision in this case. Coefficient of variation in speed and average occupancy were found to be promising precursors of freeway accidents. The five-minute moving average window was found to give the

best prediction results. The model was able to predict the likelihood of accident within the next 15 minutes based on a stream of loop detector data. Model testing with both incident and non-incident conditions reveals that the method produces a low rate of false alarm and is capable of predicting the likelihood of secondary crashes.

In the next step of this research, we are combining the findings and results from both analyses to develop an integrated procedure for predicting incident occurrences and their type utilizing weather, environment, and loop detector data. One possible approach is to use a series of logit model predictions in the order of information available. For example, we can predict the likelihood of incident versus no incident based on loop data and environment data. If the predicted likelihood of incident is above the warning threshold, we can feed loop data and full-information weather and environment data into a second set of models to predict the most likely incident type. Common issues encountered with data sources such as erroneous and missing data must be properly addressed in the next step. We expect that the proposed framework can be quite effective yet efficient enough for real-time implementation. This next phase is expected to be completed by the end of 2005, and the evaluation results may be available as early as the beginning of 2006.

# CHAPTER III. MODELING SHORT-TERM TRAFFIC CONGESTION

## INTRODUCTION

We begin by describing the nature of the problem using a simple sketch (Figure 8) of a freeway segment similar to the one under consideration. For illustration purposes, we consider the eastbound direction only. This segment has two entrance ramps and two exit ramps. Also shown are the frontage road and possible locations of detectors for illustration purposes.
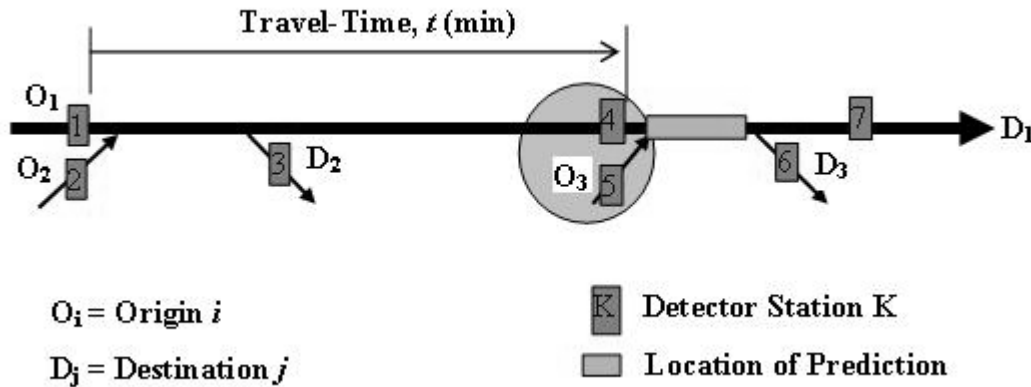
**Figure 8.  Schematic of Hypothetical Example Freeway Section.**

In the example system of Figure 8, we desire to predict traffic conditions at the downstream freeway section identified by the box. One alternate is to predict traffic conditions using freeway and on-ramp data from detectors shown in the circle (local information). However, when at least one upstream freeway section is instrumented (as in Figure 8), the accuracy of predictions can be improved by using information about vehicles that are already on the freeway but that have not arrived yet. In this regard, the reader should note that the conditions at the section of interest are dictated by vehicles arriving from origins O1, O2, and O3 minus vehicles departing to destination D2. During uncongested conditions, through vehicles detected at O1 and O2 arrive at our section of interest $t$ minutes later. Thus, for these vehicles we have arrival information $t$ minutes in advance of their actual arrival at the section of interest. Similarly, data collected at any freeway detectors farther upstream can be used to obtain even more advance information. However, this is not the case for vehicles detected at O3. These vehicles arrive at the section of interest almost immediately. With this knowledge, we can start to formulate the conceptual framework of a congestion prediction system. In a following

subsection, we will describe some scenarios to introduce concepts related to prediction based on local and advance information. The advantage of such an approach is that it provides redundancy to handle cases where a subset of detectors fails. Before proceeding, however, we will define two terms useful for the material presented in this section.

Let $T_n$ be the current time at which a prediction needs to be made $T$ (i.e., 5, 10, 15, or 30) minutes after $T_n$. The value of $T$ is known as the prediction horizon (PH). The usual approach is to first fit a mathematical model to describe a time series and then to extrapolate (or interpolate) to this model to produce a prediction into the selected time horizon. A variety of mathematical forms are available, and the exact form selected depends on the characteristics (shape, trend, cycles, etc.) of the given time series. Figure 9 and Figure 10 provide graphical illustration of the model fitting process using a series of one-minute volume data for a freeway lane. These data were collected from 4:00 to 6:00 PM.
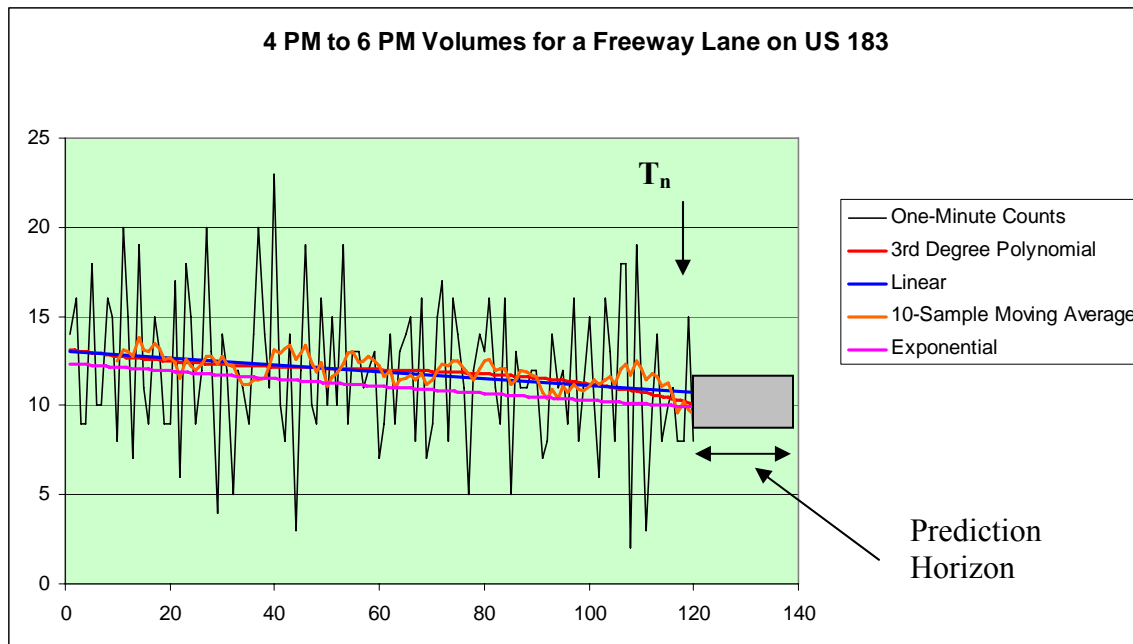


**Figure 9. An Example of Model Fitting to Time-Series Data.**
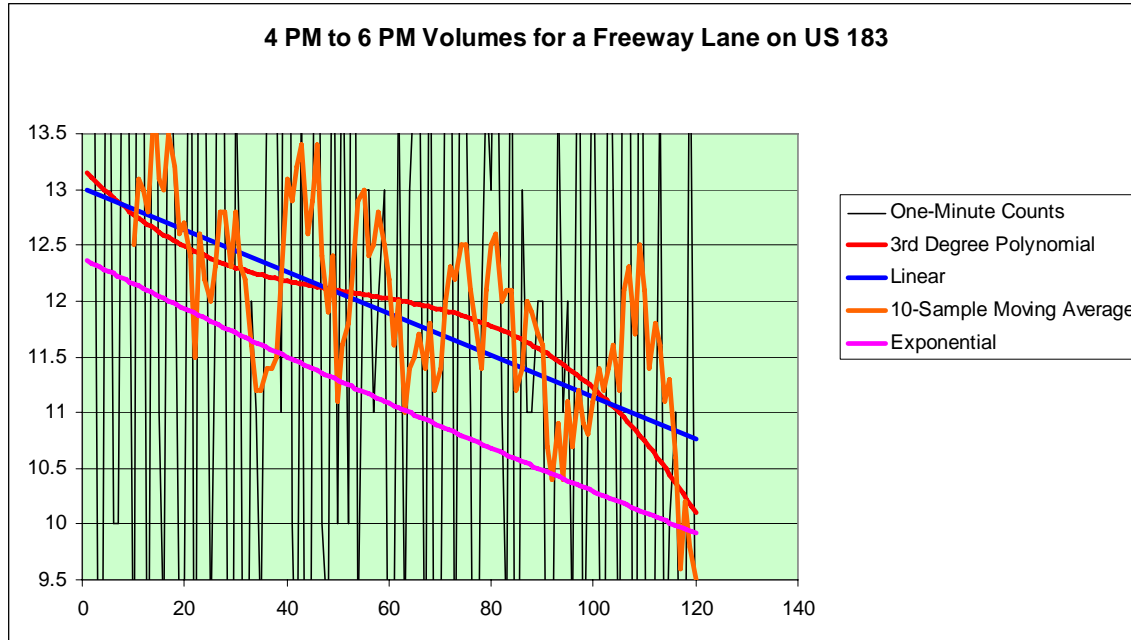
**Figure 10.  A Zoomed-In Portion of Previous Plot.**

As can be seen from a visual inspection of the plot of one-minute volume counts in Figure 10, there are significant variations in minute-to-minute values. These variations could be the result of platooning of vehicles, which can be observed even during near-congested free-flow conditions, or other factors. However, from a macroscopic perspective, the data series shows a downward trend (decreasing volumes as time passes). This trend is consistent with the reduction of traffic demand expected during this time (PM peak period) of the day.

Figure 10 shows a zoomed-in view of the four models (a third-degree polynomial, linear, 10-sample moving average, and exponential) fitted to the sample data for illustration purposes. As shown in this figure, the moving average follows the behavior of actual data, but the averaging dampens the effects of large variations in the original data. In this case, of downward trend, exponential smoothing underestimates the behavior of counts as compared to the linear model. Thus, exponential smoothing is not a good model for these data. The third-degree polynomial model is similar to the linear model except that it also captures a flat trend in the middle of the data series.

Once we select an appropriate subset of models for further evaluation, it can be used to predict the value of the fitted variable at some time in the future. It should be noted that prediction is nothing more than a projection of the model into a future time. The reader should note that the four models illustrated in Figure 10 provide different projections (predictions). A

statistical analysis can be used to test the prediction accuracy by comparing predicted and observed values. One commonly used method is to compare root mean square error (RMSE) for each model and select the model with the least error (19). RMSE is calculated as follows

$$RMSE = \sqrt{\left[\sum (measured\ volume - predicted\ volume)^2\right]/N}$$
(15)

where,

$N$ = the number of observation points.

The ability of a prediction model to predict a certain distance into the future (the prediction horizon) depends on the aggregation level of data used to develop the model. For instance, if one-minute (five-minute) data are used, the model will have a one-minute (five-minute) prediction horizon; however, the model can be used recursively to predict farther into the future by using predicted values from the previous steps. Furthermore, a prediction method can be formulated to make use of any available historical data. One such method would be to use real-time data up to time $T_n$ and historic data for time $T_n+T$ to predict traffic conditions at time $T_n+T$. The general form of such a prediction model for variable $X$ might be as follows:

$$X'_{T_N+T} = \beta X_{T_N} + (1-\beta)\hat{X}_{T_N+T}$$
(16)

where,

$X'_{T_N+T}$ = the predicted value at time $T_n+T$,

$X_{T_N}$ = the model value at time $T_n$,

$\hat{X}_{T_N+T}$ = the historical value at time $T_n+T$, and

$\beta$ = a constant in the interval $[0,1]$.

The constant $\beta$ specifies relative weight to be given to real-time and historic data. For instance, a value of 0 for $\beta$ requests the model to use historic data only, a value of 0.75 requests the model to use both real-time and historic data but with three times more weight to real-time data, and a value of 1 requests the model to ignore historic data. Furthermore, it is not difficult to develop an adaptive scheme to select or set values of $\beta$ in real time. One possible use of an adaptive application of this parameter would be for providing fail-safety in case real-time data for a detector are missing or deemed faulty according to certain tests.

**Literature Review**

Real-time assessment of freeway traffic conditions has been a subject of intense research for several decades. However, most of this work has primarily focused on detection or assessments rather than prediction of traffic conditions and incidents. The bulk of this work deals with detection of freeway breakdown, incident detection, and estimation of travel times. Here it is worth noting that accurate detection of traffic conditions is essential for providing good predictions. Thus, findings of research related to the assessment of existing traffic conditions are useful for this project as well. In the following paragraphs, we provide a summary of recent findings relevant to this project.

The definition of freeway capacity has been debated for quite some time now and there are disagreements between researchers about how to measure the capacity of a freeway section. For instance, Zhang and Levinson (20) submit that *Highway Capacity Manual (HCM) 2000* definitions of capacity are inadequate and that freeway capacity should only be measured at an active bottleneck. Based on a study of 27 sites in Minnesota, they proposed a diagnostic tool to identify congestion. Their method uses 30-second occupancy from a pair of upstream and downstream detectors. This method uses data from individual lanes and consists of two stages described below:

Step 1:

1. If minimum occupancy of all freeway detectors at a station is greater than 25 percent, the traffic at that station is in a congested state.
2. If the maximum occupancy of all freeway detectors at a station is less than 20 percent, the traffic at the station is in an uncongested state.
3. Otherwise, the traffic state at this station is in transition.

Step 2:

1. If the upstream station is congested and the downstream station is uncongested for more than five minutes, a breakdown just occurred and the segment defined by the two stations is an active bottleneck. The beginning interval of the five-minute period is identified as the start of a queue discharge period.
2. After the beginning of a queue discharge period, if both stations are uncongested for a period of five minutes, the bottleneck has recovered.

33

This research also shows that the activation of a bottleneck causes flow to drop by 2 to 11 percent. These results are similar to those published by Persaud et al. (21), who used data from a freeway in Canada. Figure 11 illustrates the freeway breakdown phenomenon recently observed by these researchers.
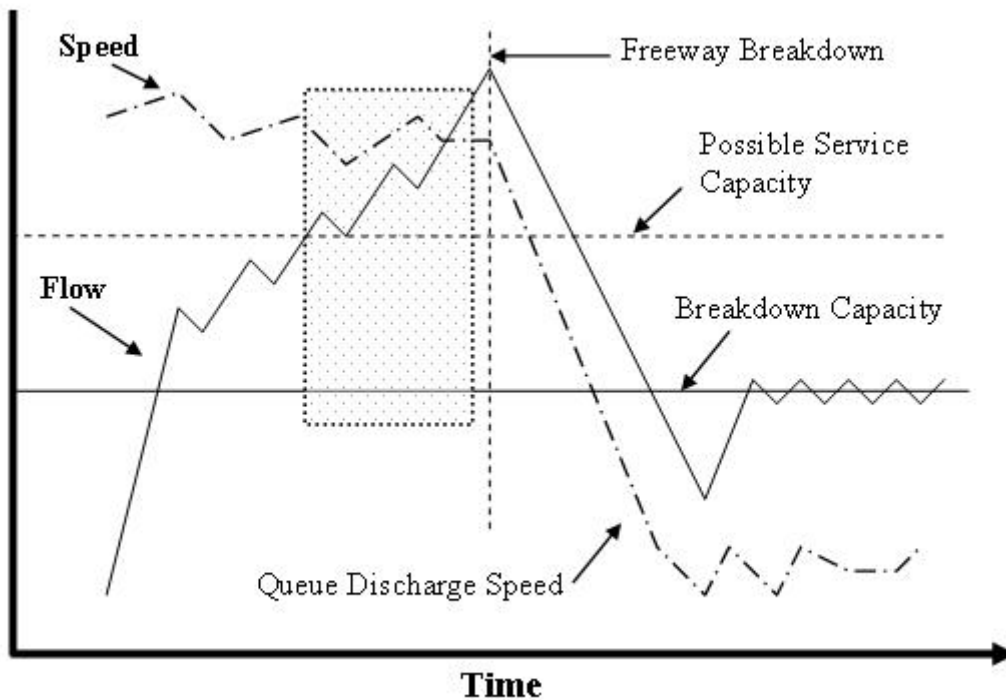


**Figure 11. Freeway Breakdown Phenomenon.**

The following points highlight the findings:

- As traffic flow increases, average speeds may decrease but generally remain near free-flow speeds.
- For a short period just before breakdown, flow may be as high as 2600 vehicles per hour (vph). This region is marked by a shaded box.
- At freeway breakdown, there is a drastic reduction in flow and speed. Vehicle speeds may even reach zero just upstream of the bottleneck. A queue condition forms.
- As the queue of vehicles discharges from the bottleneck, speeds start to increase and the freeway capacity stabilizes at the breakdown capacity level of 2100 to 2200 vph.

This two-capacity phenomenon often occurs at freeway entrance ramps where platoons of vehicles trying to enter the congested freeway create a bottleneck. The result is a reduction in service capacity. In addition, the shockwave created by a sudden drop in speed may travel for many miles upstream causing unsafe conditions. Persaud et al. (21) also calibrated a logistics model to estimate the probability of breakdown ($P_B$) as a function of one-minute flows:

$$P_B = \frac{e^U}{1 + e^U} \tag{17}$$

where,
        U = a+b*(Flow), and
        *Flow* = one-minute total volumes across all freeway lanes.

Their calibration of the model resulted in values of −11.8 and −0.003536 for the parameters *a* and *b*, respectively.

The second thrust of research has been the development and study of automatic incident detection. This research and development thrust has produced and compared the performance of a wide array of methodologies (22, 23, 24). According to the first source (22), these methodologies are based on several different technologies including: artificial intelligence, video detection, catastrophe theory, statistical methods, and pattern recognition. Numerous models have been developed within each category. The majority of these methods use speed, occupancy, and flow information from inductive loop detectors. Furthermore, field experience shows that these methods are still flawed because of low detection rates, false alarms, and undetected effects due to inclement weather.

The third thrust of research deals with the estimation and prediction of travel times on freeways. Chen et al. present a system that calculates and displays predicted travel times on designated routes in California (25). Coifman proposes a method to estimate link travel times based on point estimates (26). This approach is based on simplification of the flow-density relationship proposed by Newell (27), and it has produced good estimates in the absence of incidents. This theory is also the basis for one of the approaches used in this project, which we describe later.

**Prediction Strategies**

*Local Strategies*

The local prediction strategy uses local information only. In the example of Figure 11, prediction of traffic conditions (i.e., volume, occupancy, and/or speed) at the freeway section of interest at a time $T$ minutes from current time ($T_n$) will require $T$-horizon predictions of data from detector stations 4 and 5 (shown inside the circle in Figure 8). These predictions could be done for data from each detector (speed trap in this case), or for combined data for all lanes. The next step would be to combine these individual predictions to predict traffic conditions at the section of interest. How to combine the data to obtain predictions for the section of interest depends on the time series itself (volume, occupancy, or speed). For instance, volume can be simply added; however, elaborate schemes are needed to predict occupancy and speed. As an example, downstream speed is a function of not only the speed time series at detector 4, but also volumes measured at both detectors 4 and 5.

If an appropriate model is used, a local prediction strategy will generally work well under free-flow conditions; however, the accuracy of predictions will not be good in the presence of bottlenecks or incidents upstream or downstream of the detector stations. The reason is that such situations can suddenly change the pattern of the time series, requiring additional information that cannot be collected at the local level. One advantage of a local strategy is that it requires little calibration. In other words, these strategies are less sensitive to detectors consistently under- or overestimating the data.

*System-Based Strategies*

System-based strategies combine data from a group of adjacent detectors to predict traffic conditions at a freeway section of interest. These methods can be analytical or simulation based. In this section, we discuss these methods by providing examples of how local information can be combined to develop a system-based strategy.

**Analytical Strategies** — The following two examples show how local information can be combined to develop a system-based strategy using an analytical approach. The first example is the free-flow case that occurs when $T$ is equal to $t$ (the free-flow travel time in Figure 8). In this case, we can use actual data from detector stations (DSs) 1, 2, 3, and 5 collected until $T_n$. Data collected from DSs 1 and 2, after appropriate adjustment for vehicles leaving the system at

DS 3, provide information about the vehicles that are already on the freeway and that are expected to arrive at the section of interest $t$ minutes from now. For traffic measured at DS 5, however, a $T$-horizon prediction will need to be made using data collected until time now ($T_n$). These two groups of sources can be combined now to predict traffic conditions at the section of interest $T$ minutes into the future. If the travel time is different (significantly smaller or larger) from the prediction horizon, extrapolation or interpolation of mathematical model representing the time series data from DS 1 and 2 will need to be made.

The second example occurs with freeway congestion at a specific location. If an incident or bottleneck occurs just upstream of DS 4 and causes a queue condition, the arrival of vehicles from DS 1 to DS 4 will be delayed. In such a case, the actual travel time between DS 1 and DS 4 will have to be estimated using data collected at DS 4 as well. The use of cumulative flows is one such approach. It is based on the theory developed by Newell (27). The use of cumulative flows is one of several approaches being investigated by the research team for this project. It compares the expected traffic flow from DS 2 to actual traffic measured at DS 4 to determine the number of vehicles accumulated (and consequently delay) in the section between the two detector stations. Up to this point, the research team's work has focused on the assessment of the current conditions (that is, at time $T_n$) at various sections of the freeway. A more detailed description of the cumulative flow methodology designed for this project and the initial test results are provided in another section of this report.

**Simulation Models** — Computer models are frequently used to assess the conditions of roadway facilities. These models can be categorized as macroscopic, mesoscopic, and microscopic. Another way of categorizing such models is by using the functionality provided by them. The two main categories are traffic flow and traffic assignment. In recent years, hybrid traffic-assignment-flow models also have emerged.

Macroscopic models are based on simplified mathematical formulations that attempt to describe the average behavior of a group of vehicles over specified time duration (i.e., 1, 5, or 10 minutes). Examples of these include speed-flow, speed-density, and flow-density models. The speed prediction models being investigated by members of this research team also fall in this category. The objective of these models is to estimate average vehicle speed in a freeway section using speed and volume data from detector stations at the upstream and downstream ends of the section. Macroscopic models are extremely efficient from a computational point of view.

Microscopic models are the most detailed in that they incorporate behavior (car following, lane changing, merge, diverge, etc.) of individual vehicles in small time steps (one second or even one-tenth of a second). Because of the level of detail simulated, these models are also the most intense from a computational point of view.

Mesoscopic models fall somewhere between macroscopic and microscopic models, depending on the detail simulated. Most models in this category deal with aggregate behavior of a group of vehicles but perform simulation in small steps similar to the microscopic models.

Regardless of its type, a simulation model requires a given set of input data for all sources and destinations for the system under investigation to assess the internal state of the system corresponding to the provided data. Proper use of a simulation model requires verification that the model is producing results that mimic field conditions. This verification process is known as "calibration."

If we were to simulate the conditions of the freeway in Figure 8 using one-hour data collected until time $T_n$, we would need to provide one-hour volume data from detector stations 1, 2, and 5. We also would need information about where this traffic is going (i.e., proportions of traffic from $O_1$ exiting to destinations D1, $D_2$, and $D_3$). Some simulation models have the ability to calculate this origin-destination (O-D) information using counts from entrance and exit detectors using methods such as the gravity model, while others require the user to provide the correct O-D matrix. It should be noted that O-D patterns change by time of day. We also will need free-flow or desired speeds for each freeway section and detailed geometric information required by the model. Assuming that we have accurate data, a one-hour simulation will assess internal conditions (speeds, volumes, and occupancy) at any selected point on the freeway. Most microscopic simulation models allow the user to create a data collection point, which can be used to find out how well the model simulates observed conditions. For instance, a comparison of data for a simulated detector at DS 4 with actual data collected at DS 4 (Figure 8) will provide the user the ability to determine if the selected model needs calibration. Most simulation models provide parameters that can be tweaked to produce simulation results to match real conditions. Several simulation runs may be needed until the user is satisfied with the results of a simulation model.

In the above example, using data until $T_n$ will only tell about conditions until that time. To use a simulation model for prediction requires that predicted data be used. In the case of our

example, we will have to perform local predictions of data collected from DSs 1, 2, 3, 5, 6, and 7 and use these predicted data to simulate future conditions. Figure 12 illustrates the conceptual framework for a prediction system based on a simulation model.
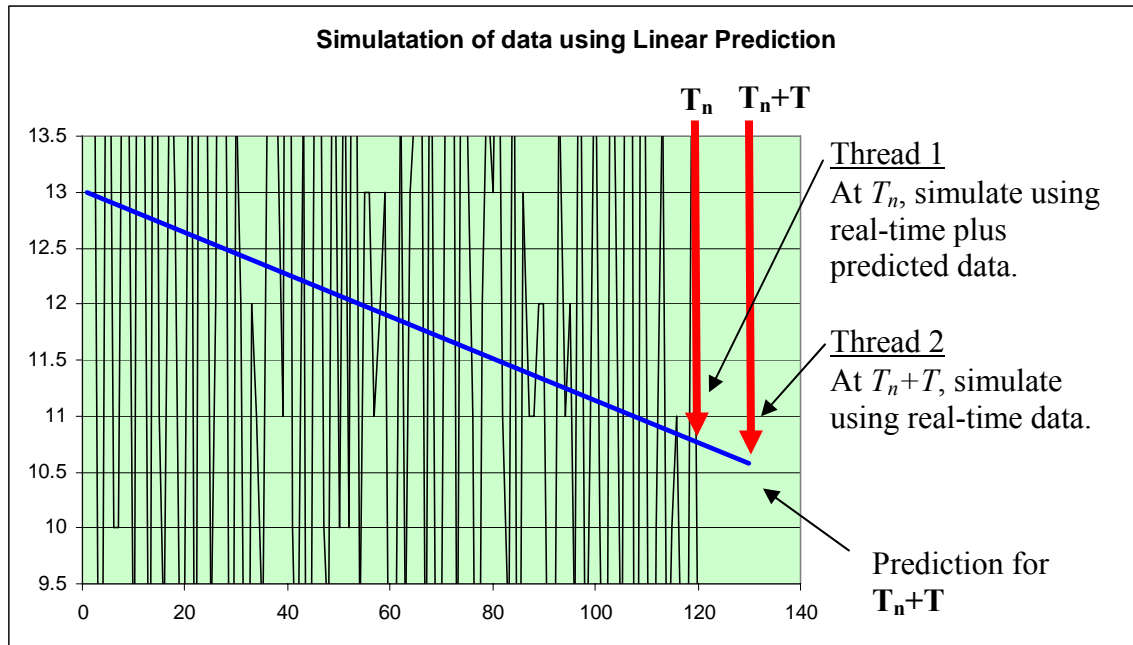


**Figure 12. Conceptual Framework for a Microsimulation-Based Prediction System.**

As shown in Figure 12, two simulation threads will have to be run. One thread uses data collected until $T_n$ plus prediction until $T_n+T$ to predict future conditions of the system. The second thread is run at time $T_n+T$ using actual data collected until this time. This latter run is made to verify the accuracy of prediction and to use in real-time adaptive calibration of future predictions. Although this framework is simple from a conceptual point of view, development of a prediction system using existing simulation models is complicated because this method requires changing input data in real time, a feature most existing simulation models do not support. The following paragraph provides a description of some of the currently available simulation models and their capabilities.

Microscopic traffic flow simulation models include CORSIM (28), VISSIM (29), and PARAMICS (30). These models use static data and are incapable of accommodating any traffic diversion due to traffic congestion and incidents. Traditional traffic assignment models, on the other hand, are for planning purposes and do not provide detailed analysis of traffic flow. Therefore, these models are not of use in this project. Recent years have seen the evolution of

39

hybrid models that combine the features of the above types of models. Examples of these models include DYNASMART (31) and MITSIM (32). The strength of these two models is their ability to change traffic assignments based on the behavior of simulated traffic. However, all five models described above are designed for off-line use. As such, they require static input data that cannot be combined with real-time data on the fly. Recent extension of DYNASMART to DYNASMART-X fills this void. DYNASMART-X combines real-time data with static data to make traffic assignments in real time. Projects are underway to field-test this tool.

## DATA ISSUES

Currently, lane-by-lane volumes and occupancies, speed, and truck percentages are collected for Austin freeways on a one-minute basis. A prediction system can be designed to use lane-by-lane data or aggregate data for all lanes. However, it is worth investigating which subset of these data is the most useful. This section is devoted to the analysis of information contained in Austin data. Information theory was used for this purpose.

### Background on Information Theory

Different variables such as traffic volume, occupancy, and speed/speed variation have been used in different traffic and incident prediction models. However, it is often debated as to which variable(s) is (are) better suited for this purpose. To gain a better understanding of the usefulness of available data, we analyzed a subset of real data from Austin, Texas, using a methodology based on information theory. This methodology, proposed by Foo et al. (33), applies information theory to study the value of each variable.

In information theory, the value of a variable is measured by entropy and mutual information contained in a set of variables. Entropy is a measure of the amount of uncertainty in a random variable, and it is defined as:

$$H(X) = -\sum_{x} p(x)\log p(x), \qquad (18)$$

where,
  $H(X)$ = the entropy of variable $X$, and
  $p(X)$ = the probability density of $X$.

Data with larger entropy values are more valuable than those with smaller values.

Mutual information between two variables, $X$ and $Y$, measures how much information variable $X$ contains about $Y$. More formally, it is a measure of the reduction of uncertainty of $Y$ due to the knowledge of $X$ and is defined as:

$$I(X,Y) = \sum_x \sum_y p(x,y) \log \frac{p(x,y)}{p(x)p(y)} \qquad (19)$$

where,

      $I(X,Y)$ = the mutual information between $X$ and $Y$, and

      $p(X,Y)$ = the joint probability density of $X$ and $Y$.

For example, assume that we have three variables, $A$, $B$, and $X$, and $I(A,X) = 0.9$ and $I(B,X) = 0.5$. Then, we can claim that $A$ tells more about $X$ than $B$. Therefore, $A$ is a better predictor of $X$ than $B$.

## Empirical Study

To study the value of each variable, namely, volume, occupancy, and speed, we selected the northbound section of US 183 from Carver Avenue to Fathom Circle in Austin, Texas. The data used in this analysis were collected from 6:00 AM to 9:00 AM on February 4, 2002, (Monday) through February 7, 2002 (Thursday).

## Analysis of Entropy

We calculated entropy of volume, occupancy, and speed; and joint entropy of volume and occupancy, volume and speed, and occupancy and speed for each detector in the study section. Using 0.05 as the significant level, we performed pair wise t-tests between the entropies of two variables, $X$ and $Y$.

Define $d_i = x_i - y_i$ as the difference between the $i$-th observation of $x$ and the $i$-th observation of $y$, and $\mu_D$ as the mean of $d$; then the hypothesis testing procedures is as follows:

    $H_0$: (null hypothesis):         $\mu_D = 0$.

    $H_1$: (alternate hypothesis):    $\mu_D > 0$.

Rejection Rule with 0.05 significant level ($\alpha = 0.05$):

    Reject $H_0$ if t-Statistic > $t_\alpha = 1.65$.

Table 4 presents the mean entropy of each variable, and Table 5 summarizes the results of the pair wise t-tests.

**Table 4.  Mean Entropy.**

| Variable | Mean Entropy |
|---|---|
| Volume | 3.87 |
| Occupancy | 2.85 |
| Speed | 1.44 |
| Volume and Speed | 4.90 |
| Occupancy and Speed | 4.03 |

**Table 5.  Results of Pair Wise t-tests of Variable *X* and *Y*.**

| Variable *X* | Variable *Y* | t-Statistic | t Critical Value |
|---|---|---|---|
| Volume | Occupancy | 60.45 | 1.65 |
| Volume | Speed | 37.12 | 1.65 |
| Occupancy | Speed | 24.04 | 1.65 |
| Volume | Volume and Speed | -52.1971 | 1.65 |
| Occupancy and Speed | Volume and Speed | -39.22 | 1.65 |

From Table 4 and Table 5, it is obvious that the entropy of volume is significantly larger than that of occupancy (with t-Statistic = 60.45) and that of speed (with t-Statistic = 37.12). Thus, the value of volume is significantly higher than that of the other two variables.

However, when joint effects of variables are considered, we find that the joint entropy of volume and speed is significantly larger than that of volume and that of occupancy and speed. Thus, it is better to use both volume and speed than just volume alone or occupancy and speed. In summary, information on volume and speed is more valuable than other variables.

**Analysis of Mutual Information**

Table 6 presents the mean mutual information between volume, occupancy, and speed for the study section. Note that the mutual information between volume and occupancy is the largest among all pairs of variables. This is an expected finding because volume and occupancy are highly related. On the other hand, mutual information between volume and speed and that between occupancy and speed are relatively small. In other words, knowing either volume or occupancy is not sufficient to predict speed.

**Table 6.  Mean Mutual Information between Variables *X* and *Y*.**

| Variable *X* | Variable *Y* | Mean Mutual Information |
|---|---|---|
| Volume | Occupancy | 1.844 |
| Volume | Speed | 0.39 |
| Occupancy | Speed | 0.27 |

As suggested by Foo et al. (33), we also can estimate the prediction power of each variable by using time-shifted mutual information. For instance, time-shifted mutual information of volume can be the mutual information between the volume for the past one minute and the volume for the next one minute. Recall that mutual information between *X* and *Y* measures how much information *X* contains about *Y*. Therefore, time-shifted mutual information of *X* measures how much information *X* at the current time contains about *X* at a future time. Table 7 summarizes the results of the time-shifted mutual information calculated for each variable.

**Table 7.  Mean Time-Shifted Mutual Information.**

| Variable | Mean Time-Shifted Mutual Information |
|---|---|
| Volume | 3.43 |
| Occupancy | 2.56 |
| Speed | 1.28 |

Note that volume has the largest time-shifted mutual information. By performing pair wise t-tests, we confirmed that time-shifted mutual information of volume is significantly larger than that of occupancy (with t-Statistic = 59.71) and that of speed (with t-Statistic = 37.33). Therefore, we conclude that volume has better prediction power than the other two variables.

**Conclusions**

Based on the empirical study, we suggest using volume and speed as the key variables for developing our prediction model. The reasons for this recommendation are summarized below.

First, volume and speed have the largest entropy among all the variables. Thus, information on volume and speed has significantly higher value than other variables. Besides, mutual information between volume and speed indicates that volume and speed are not strongly dependent; neither are occupancy and speed. Since volume does not contain much information about speed (and vice versa), we need information on both volume and speed. On the contrary, mutual information between volume and occupancy is very large, and thus, volume may serve as a proxy for occupancy (and vice versa). Since volume has larger entropy and larger time-shifted

mutual information than occupancy has, as well as the fact that the joint entropy of volume and speed is larger than that of occupancy and speed, we conclude that volume is a better variable to use than occupancy.

## AUTOMATION OF *HCM* ANALYSIS TECHNIQUES FOR FREEWAY OPERATIONS

Under Task 4 of the project proposal ("Assess Approaches for Predicting Short-Term Congestion") one of the alternatives to be assessed was "automating the *Highway Capacity Manual (HCM)* analysis techniques for analyzing freeway operations." We carried out such an assessment, specifically directed toward the technique described in Chapter 22 of *HCM 2000* (34), "Freeway Facilities." The results of that assessment are described below, following the next paragraph, which is intended to provide an understanding of the context of Chapter 22 of the *HCM* within the overall suite of *HCM* chapters devoted to various types of analyses related to freeways.

Chapter 13 ("Freeway Concepts") of *HCM 2000* is an introduction to such basic concepts as "capacity and quality of service for freeways." In the introduction to this chapter it is further stated that "this chapter can be used in conjunction with the methodologies of Chapter 22 (Freeway Facilities), Chapter 23 (Basic Freeway Segments), Chapter 24 (Freeway Weaving), and Chapter 25 (Ramps and Ramp Junctions)." However, the basic methodologies of most of these chapters are limited to the undersaturated case, presumably based upon considerations such as "unlike free flow, queue discharge and congested flow have not been extensively studied…" (*HCM 2000*, p. 13-5), and the statement (same page, in regard to an instance of a flow/speed relationship representing three separate regimes: "undersaturated," "queue discharge," and "oversaturated") that "analysts are cautioned that although the relationship…may provide a general predictive model for speed under queue discharge and oversaturated flows, it should be considered conceptual at best." However, as this task is prediction of congestion, and therefore consideration of oversaturated flows is inherent within the task, any methodology applicable to this task requires centrally consideration of oversaturated cases and the resulting congested flow.

With very much respect to the various authors of the cited chapters of *HCM 2000*, we believe the inapplicability of the methodologies presented to oversaturated flows stems from the very strong tradition of presenting in *HCM 2000* only methodologies that are suitable for hand implementation. The fact is that queue discharge and oversaturated flow are relatively well

44

understood theoretically, but any realistic procedure for their analysis is quite impractical to implement manually. Among the chapters listed above only Chapter 22 breaks significantly with the *HCM* tradition of providing analysis techniques only for the undersaturated case.

In regard to the procedures provided in Chapter 22, the following statement (p. 22-42) is made: "The analyst could, given enough time, analyze a completely undersaturated time-space domain manually, although this is highly unlikely. *It is not expected that an analyst will ever manually analyze a time-space domain that includes oversaturation.* [Emphasis added.] For heavily congested freeway facilities with interacting bottleneck queues, a simulation model might be more applicable." We believe these considerations suggest the Chapter 22 procedure is particularly appropriate to be considered for the automation envisioned in the current project. The principal reason that oversaturation is unlikely to be analyzed manually is the complexity of the corresponding procedure of Chapter 22 of *HCM 2000*. The computational module provided for oversaturated segments is described via a highly iterative 35-step four-page flowchart. However, the basic technology for its implementation as a computer automation is well developed.

**Overview of Chapter 22 Methodology**

The Chapter 22 methodology is based upon the kinematic-wave model (KWM), the original "hydrodynamic model" of vehicular traffic flow. This model was discovered independently by Lighthill and Whitham (35) and by Richards (36). The required inputs to any application of the KWM are a (position-dependent) flow-density function (or any equivalent via the fundamental relationship flow = speed*density), the time-dependency of the demand at all entrances to the facility being modeled, the time-dependent capacity at all exits, the densities throughout the facility at some "initial" time, and of course the facility geometry.

The Chapter 22 methodology uses in the undersaturated regime (i.e., densities below the 45 pc/mi/ln at which an assumed capacity flow is assumed to be reached for any given free-flow speed) a certain (family of, depending upon various adjustment factors) flow-density function(s), as described in Chapter 23 (Exhibit 23-3, p. 23-5, and eq. [23-4]). In the oversaturated regime it uses a linear extrapolation from the capacity point to a jam density of 190 pc/mi/ln. The latter is adapted from Newell (27).

A module is provided to estimate entrance and exit demands from 15-minute traffic counts. (These demands need not be the observed flows because of possible effects of congestion.) Alternately, estimated demands can be applied if desired (e.g., for purposes of planning applications).

We recommend a simplified queuing analysis for purposes of providing the initial density profile, termed "background density." This is determined by first taking flows upstream of any bottleneck equal to the sum of the total (net) initial upstream demand, and flows downstream of a bottleneck equal to the capacity of that bottleneck. The background densities are then taken as those densities corresponding to that flow as a free flow, i.e., the lower of the two densities that correspond to that flow on the prevailing flow-density function. This procedure essentially assumes that the facility is free of congestion at the initial time, which is one of the limitations of the methodology. (See item *iii* below.)

Even given these quantities, analytic solutions are known only for very simple cases, particularly very simple facility geometries. However, even these analytic solutions are quite valuable for purposes of benchmarking computational solutions. Therefore, the Chapter 22 methodology ultimately invokes a computational procedure in which the conceptually continuous time and space variables are replaced by discrete counterparts. The facility itself is divided into "segments," with two or more adjacent segments joined at "nodes." Nodes may be points at which merges or diverges occur, or they may be points of spatial inhomogeneity of the roadway (e.g., a lane drop), or they may be inserted simply in order to accurately capture spatial inhomogeneity of the traffic flow over a homogeneous section of freeway.

Time discretization is accomplished by introducing a time step. The objective of the discrete computational process is to compute, at each time step, the flows at all nodes and the mean densities within each segment. This computation is accomplished in order of increasing time, and from upstream to downstream within each time step, beginning at entrant mainline nodes. At each time step the flow at a given node is updated as the minimum of a number of different potential flows, each of which takes into account one particular constraint on the flow at that node, and is computable on the basis of densities and flows at either the preceding time step or at the current time step but at upstream nodes or segments.

A number of limitations of the Chapter 22 methodology are expressly noted. Those that seem most relevant to the objectives of TxDOT Project 0-4946 are:

i. "Multiple overlapping bottlenecks are an example" that "certain freeway traffic conditions cannot easily be analyzed by the methodology" (p. 22-1).

ii. "The freeway facility methodology is limited to the extent that it can accommodate demand in excess of capacity. The procedures address only local oversaturated flow situations, not system-wide oversaturated flow conditions" (p. 22-1).

iii. "The completeness of the analysis will be limited if freeway segments in the first time interval, the last time interval, and the first freeway segment do not all have demand-to-capacity ratios less than 1.00" (p. 22-1).

iv. "The demand-capacity ratios should be less than 1.0 for all cells along the four boundaries of the time-space domain. If they are not, further analysis may be flawed and in some cases should not be undertaken" (p. 22-13).

## Perspective on Chapter 22 Methodology and the KWM

The essential ingredients of the KWM are the equation of continuity (conservation of vehicles), and a flow-density relationship, often termed a "fundamental diagram" (FD), or "traffic stream model." The conservation law is widely accepted, even though as it appears within the KWM it incorporates the idea that the motion of discrete vehicles can be represented in terms of quantities (densities and flows) that vary continuously with space and time. In fact, Papageorgieu (37) has described the equation of conservation of vehicles as "the only accurate physical law available for traffic flow." However, researchers have raised serious doubts regarding the validity of fundamental diagrams. This has contributed to doubts regarding the validity of KWMs, although there also have been doubts raised from other considerations. These two sources of doubt regarding the KWM are discussed respectively in the next two paragraphs.

The principal source of doubt about FDs arises simply from the fact that repeated measurements (e.g., 38, 39) do not support them. Cassidy and Windover (40) have argued that this could be attributable to the data analysis methodologies employed, particularly to the use of variables (e.g., densities and flows) obtained by aggregating over fixed time intervals. It is interesting that this state of uncertainty about the proper place of fundamental diagrams within transportation science and engineering remains in considerable doubt more than 70 years after they were initial proposed by Greenshields (41).

Doubts about the validity of the KWM also have been raised because of the use of incorrect discrete computational approximations. The most common instance of an incorrect computational approximation is, in the terminology of the Chapter 22 methodology, the (intuitively appealing) approximation of the flow between adjacent segments during a time step as the flow corresponding to the density in the upstream segment at the beginning of that time step. For uncongested flows this approximation produces adequate approximations, given suitable segment lengths and time steps. However, under congested conditions this approach can considerably overestimate the flow from an uncongested upstream segment to a congested downstream segment, as occurs in queue formation; likewise, it can considerably underestimate the flow from a congested upstream segment to an uncongested downstream segment, as occurs in queue discharge. See Ross (42, 43) and Newell (44) for an instance of incorrect inference regarding the KWM that was drawn from this approach, and the related discussion.

These doubts regarding the KWM gave considerable encouragement to the development of alternative models, including alternative hydrodynamic models, microscopic models, and most recently the increasingly popular mesoscopic models. Nonetheless, the KWM has retained considerable credibility among transportation engineers and scientists, as witnessed by its incorporation in the *HCM*. We suspect the reasons behind this include the following:

- The KWM reproduces qualitatively many phenomena observed in traffic flow, including queue formation (propagation of shock waves), queue discharge, queue dissipation (e.g., from declining upstream demand), and even interaction of queues although one of the quotations above suggests the Chapter 22 implementation of a KWM solution has difficulty with such interactions.
- Under steady-state demands that lead to system-wide conditions of undersaturated flow, the intuitive and familiar capacity analysis that underlies much of the *HCM* is simply the steady-state form of the KWM. Note however that steady-state analyses never are appropriate when oversaturation prevails because oversaturation by definition is associated with growth of queues, and therefore time-varying behavior.

Nelson and Kumar (45) showed that for the Godunov computational approximation to the KWM the appropriate boundary conditions consist of specification of the demand at entrant boundaries during free flow immediately downstream of those boundaries, and of the supply at exiting boundaries during conditions of congested flow immediately upstream of those

boundaries. Lebacque (46) has extended this result to the KWM itself. These theoretical results raise some issues in regard to the treatment of boundary conditions within the Chapter 22 methodology. Specifically, within these specifications of boundary conditions there is no suggestion of the requirement that the demand-capacity ratios be less than 1 that is highlighted in the limitations *iii* and *iv* above. This naturally raises the question of the extent to which these limitations on the demand-capacity ratio are absolutely required. We return further to this issue in the discussion of boundary conditions with the following subsection "Requirements for Application to Predict Short-Term Congestion."

Similarly, there is no inherent restriction on the initial conditions for the KWM that corresponds to the limitation that the demand-capacity ratios all be less than 1 at the initial and terminal times. However, the simplified queuing analysis that is used to establish the initial density profile certainly is most reasonable when there are no oversaturated flows at the initial time. Further, the measures of effectiveness calculation that seems to be the principal objective of the Chapter 22 methodology certainly is most reasonable when both the initial and the terminal states have no oversaturated flows, even locally.

Finally, although we have described the Chapter 22 methodology above as based upon computational solution of the KWM, we should clarify that it is *not* so described within the chapter itself. Although it is reasonable to view the methodology in this manner, it also is reasonable to view it as a modification of classical queuing analysis to incorporate the effects of congestion, particularly the finite storage capacity of segments (i.e., the nonzero length of vehicles). In effect any modification of queuing theory, in the context of traffic flow, to take into account these factors also can be viewed as a computational approximation to the KWM.

**Status of Related Automation Efforts**

The history of traffic flow theory is replete with instances of incorrect methodologies used for the computational solution of the KWM, but correct methods have been known and employed for some time. P. Michalopoulos and J. P. Lebacque (references presently unavailable, but work done *circa* 1984) seem to have been independently the first to apply correct computational schemes to traffic flow. The Godunov method that seems to have first been so employed by Lebacque has emerged as the method of popular choice, presumably in large part because its essential ingredients have a reasonably natural interpretation within traffic flow

theory. This method has subsequently been rediscovered by others (47, 48) For completeness we should mention that much of the natural interpretation of the Godunov method within its application to traffic flow was developed initially in the latter work.

The French code STRADA (49), which employs the Godunov method, seems to be the closest thing to a commercial application code that employs a computational solution (via the Godunov method) to the KWM as its computational engine. This code is regarded by its authors as a research code, but it seems to have been widely employed within France for purposes of analysis of various kinds of traffic operations.

Results from computational solution of a KWM are most naturally presented as a space-time diagram of density, speed, or flow. Figure 13, from Nelson and Kumar (45), is an illustrative instance of such a presentation. Very briefly, the test scenario underlying this diagram consists of a one-hour simulation of a 13-mile section of freeway, with a lane drop at five miles, a second lane drop at nine miles, an initially uniform density corresponding to free flow below the capacity of either of the two bottlenecks, and entrant demand undergoing several jump increases during the simulation (cf. the density increases along the line distance = 0 that corresponds to the entrant section). The demand jump at $t = 0.1$ hours generates a queue discharge wave that ultimately activates the nine-mile bottleneck, at around $t = 0.25$ hours. A shock subsequently propagates upstream and serves as the upstream boundary of a congested region of enqueued flow at a density of about 190 vpm over the downstream portion of the two-lane section between the five-mile and nine-mile stations. This shock grows in strength (i.e., the queue grows faster) as it is joined by the queue-discharge waves from subsequent jumps in entrant demand. The queue-discharge wave originating from the entrant demand jump at $t = 0.5$ hours activates the five-mile bottleneck before the shock wave propagating upstream reaches that bottleneck. The queue thus generated has a density of about 210 vpm over this three-lane section of freeway, but that jumps to over 300 vpm when the shock propagating upstream from the nine-mile station arrives. The arrival of this latter shock is an instance of "interacting bottleneck queues," and this diagram shows there is no inherent limitation that precludes such interactions from being treated via an appropriate computational solution of the KWM.
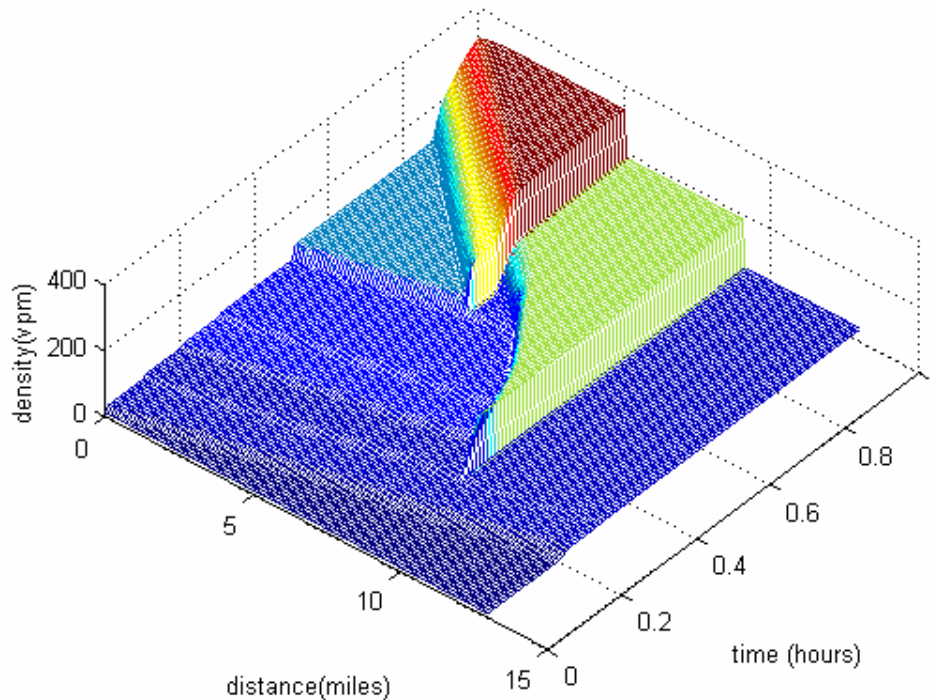
**Figure 13. Space-Time Diagram of Densities for Test Scenario 2 of Nelson and Kumar (45).**

## Requirements for Application to Predict Short-Term Congestion

There are two significant research issues associated with implementation of a predictive model based upon computational solution of the kinematic-wave model to provide a timely prediction of development of congested flow. (Here "timely" means sufficiently far in advance of the anticipated time of actual development to permit countermeasures to be taken to prevent that development.) The first is a computational implementation issue, relating to precisely what measurements should be used as input to that computation, that clearly is solvable, but that in its implementation seems to involve issues not heretofore explored. The second issue is related to how far in advance traffic flow can be predicted with sufficient precision to warrant implementation of countermeasures. The latter is really the central research issue that underlies the feasibility of implementing the potentially high-payoff techniques being explored in this project.

*Where to Make Measurements*

This issue is best illustrated by means of a simple example. Suppose it is desired to predict, using the kinematic-wave model and based upon measurements occurring at times prior to $t = T$, the state of traffic flow over a section of roadway extending from position $x = 0$ to $x = L$, and at a specified subsequent time $T+\Delta T$. Exactly what measurements should be employed as the required input data to permit the computational solution (of the KWM) necessary to provide this prediction?

The classical mathematic view of this prediction problem is that we would need to know the initial densities along the segment $0 \leq x \leq L$ at the "initial" time $t = T$, and the flows at the boundaries $x = 0,L$ between times $t = T$ and $t = T + \Delta T$. (More precisely, mathematically the flow at the upstream boundary is only needed at times during which free flow prevails there, and the flow at the downstream boundary is only required for periods during which congestion prevails there. In practice both are available, subject to the considerations discussed following, which raises an additional issue of how best to use the "excess" information to achieve more reliable predictions.) However, this statement of the required boundary data requires use of measurements *after* time $t = T$, which is contrary to the objective described in the preceding paragraph. How do we modify the requirements on the boundary data to accomplish this objective?

One possibility would be to use historical boundary data (e.g., from similar days of the week, under similar weather conditions) to provide the required boundary data. This solution clearly is feasible and probably should be used at least as a base case in any study of this issue. However, it seems contrary to the implicit objective of basing predictions upon best available current data, which is available up to time $T$.

An alternative approach to this problem is to trade spatial proximity of measurements in order to employ measurements made at earlier times. More precisely, suppose in the above highly idealized situation we elect to employ flow measurements made at upstream position $x = -a < 0$ and downstream position $x = L+b>L$, with historical data employed only after time $t = T$. Then the flow in the targeted section $0 \leq x \leq L$ is actually independent of the historical data, provided the upstream measurement section is sufficiently far away from the entrant section $x = 0$ (i.e., $a > \Delta T/v_{ff}$, where $v_{ff}$ is free-flow speed) and the downstream measurement section is sufficiently far away from the exit section $x = L$ (i.e., $b > \Delta T/w_u$, where $w_u$ is the maximum [in

absolute value] upstream wave speed [typically about 20 mph]). This observation permits predictions that realistically depend only upon measurements taken far enough in advance to permit countermeasures.

In more realistic situations (e.g., presence of on-ramps) it is unlikely that we will be able to completely avoid use of historical data. However, it seems likely that considerations such as that of the preceding paragraph can at least minimize the dependence upon historical data, which is a desirable step.

The preceding discussion has focused upon boundary data, but some mention is appropriate for the initial conditions (i.e., densities at time $t = T$). The obvious approach is to estimate those conditions from the data available, at and immediately prior to that time, from detectors located on the targeted section. This will be only an estimate (i.e., will contain errors), principally because of the spatial sparseness of these detectors. This approach will contribute to the unreliability of the predictions, which is the next topic of discussion.

*Reliability of Predictions*

At best the KWM, like any other macroscopic model, provides a mean value of the traffic flow, where this mean is over some large set ("ensemble") of potential realizations, all of which are consistent with the measurements that necessarily must be employed. For small elapsed prediction times (the "$\Delta T$" of the preceding discussion) most of these realizations will lie close to the predicted means, and therefore presumably the predictions will lie close to most instances of reality. However, as time elapses the underlying statistical distribution will spread out (its variance will increase), and the predictions made will be less and less accurate, for more and more cases. The central question underlying this project is whether the time over which the predictions remain reasonably reliable is larger than the minimum time required to implement countermeasures.

It is appropriate to note that the question of reliability of short-term traffic predictions has been addressed in the literature (50, 51). However, much of these prior discussions have been directed toward predictions of travel time, for which persistence is reasonably reliable, and therefore historical data provide a reasonable basis. By contrast, the objective of the present task is precisely to predict the *onset* of congestion, which is to say occurrence of a lack of persistence, which is a more difficult matter to achieve.

**INPUT-OUTPUT ANALYSIS OF CUMULATIVE FLOWS**

This document presents a simple methodology for evaluating the operating states of a freeway using cumulative flow data from pairs of adjacent detectors along the freeway. The methodology is based on the works by Newell (27) and Cassidy and Windover (40).

This document is organized as follows. First, we provide background on using cumulative flow and moving time coordinates system. Next, we analyze the behavior of two quantities—flow-in-process and delayed-flow—under different traffic conditions and propose a methodology for identifying traffic flow states. Then, we provide a demonstration of the use of this methodology using detector data obtained from computer simulation. Next, we apply the proposed methodology to a subset of real data from Austin, Texas, and discuss data accuracy and data integrity issues identified during this stage. Finally, we describe a software tool being developed to automate the analysis of data.

## Background

This section provides an overview of cumulative flow and moving time coordinates (MTC) systems, which are the foundations of the proposed methodology described in the next section. Readers interested in further details are referred to Newell (27) and Cassidy and Windover (40).

### Cumulative Flow

Cumulative flow is the measure of the total number of vehicles passing over a detector from some referenced time (i.e., since 8:00 A.M.). Define:

$A(x,t)$ = cumulative number of vehicles that have passed detector location $x$ by time $t$,

$x_u$ = an upstream detector location,

$x_d$ = a downstream detector location, and

$y$ = freeway section of interest bounded by $x_u$ and $x_d$.

For any section $y$, we can construct an input-output diagram by drawing the cumulative flow curves, $A(x_u, t)$ and $A(x_d, t)$, with respect to time as shown in Figure 14. This input-output diagram is a very useful tool for analyzing the characteristics of freeway traffic flow in section $y$. More specifically, the vertical distance between the two curves at some time $t_j$ is the total number of vehicles in section $y$ at that time. In this document, we define this quantity as flow-in-process

of section $y$. Furthermore, the horizontal distance between the curves at height $j$ represents the travel time of the $j$th vehicle from $x_u$ to $x_d$.
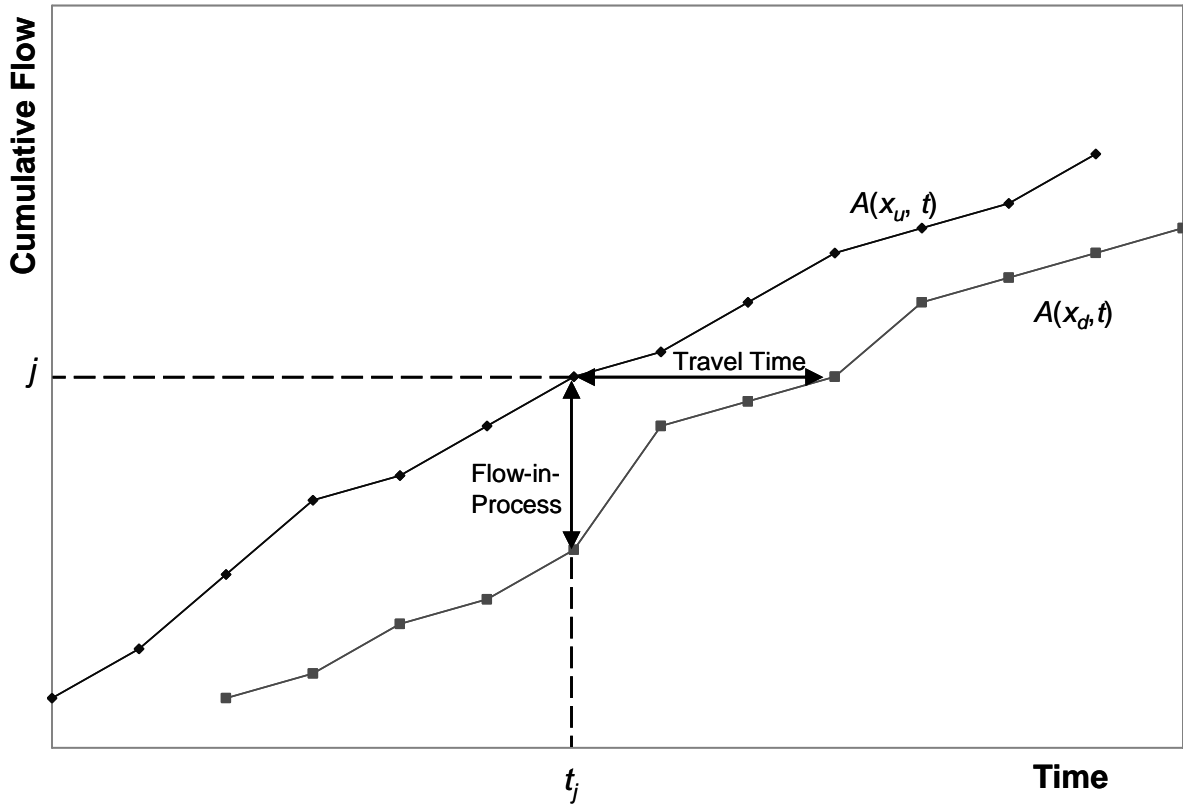


**Figure 14.  Input-Output Diagram.**

*Moving Time Coordinates System*

Even though the input-output diagram provides us with information on flow-in-process and travel time, additional information can be obtained by using an MTC system.

Define moving time, $t'(x,t)$, as follows:

$$t'(x,t) = t + v(x_d - x) \tag{20}$$

where,

$t$ = the actual data collection time (i.e., 8:00 AM, 8:01 AM, 8:02 AM, etc.) at $x_u$, and

$v$ = the average free-flow travel time per unit distance (i.e., per foot, per meter, etc.) from $x_u$ to $x_d$.

We can now define new cumulative flow curves as follows:

$$A'(x_u, t') = A(x_u, t' - v(x_d - x_u)) \tag{21}$$

and

$$A'(x_d, t') = A(x_d, t'). \tag{22}$$

This transformation is equivalent to shifting the upstream curve $A(x_u,t)$ (in Figure 14) to the right by an amount equal to the free-flow travel time from $x_u$ to $x_d$. In this MTC system, a vehicle traveling at $v$ takes zero time to travel from $x_u$ to $x_d$ in the absence of delay inside section $y$. Figure 15 illustrates cumulative curves of Figure 14 in an MTC system. As shown in Figure 15, the vertical distance between the two curves at any time $t_j$ represents current delay to vehicles in section $y$. In this document, we refer to this quantity as delayed flow.
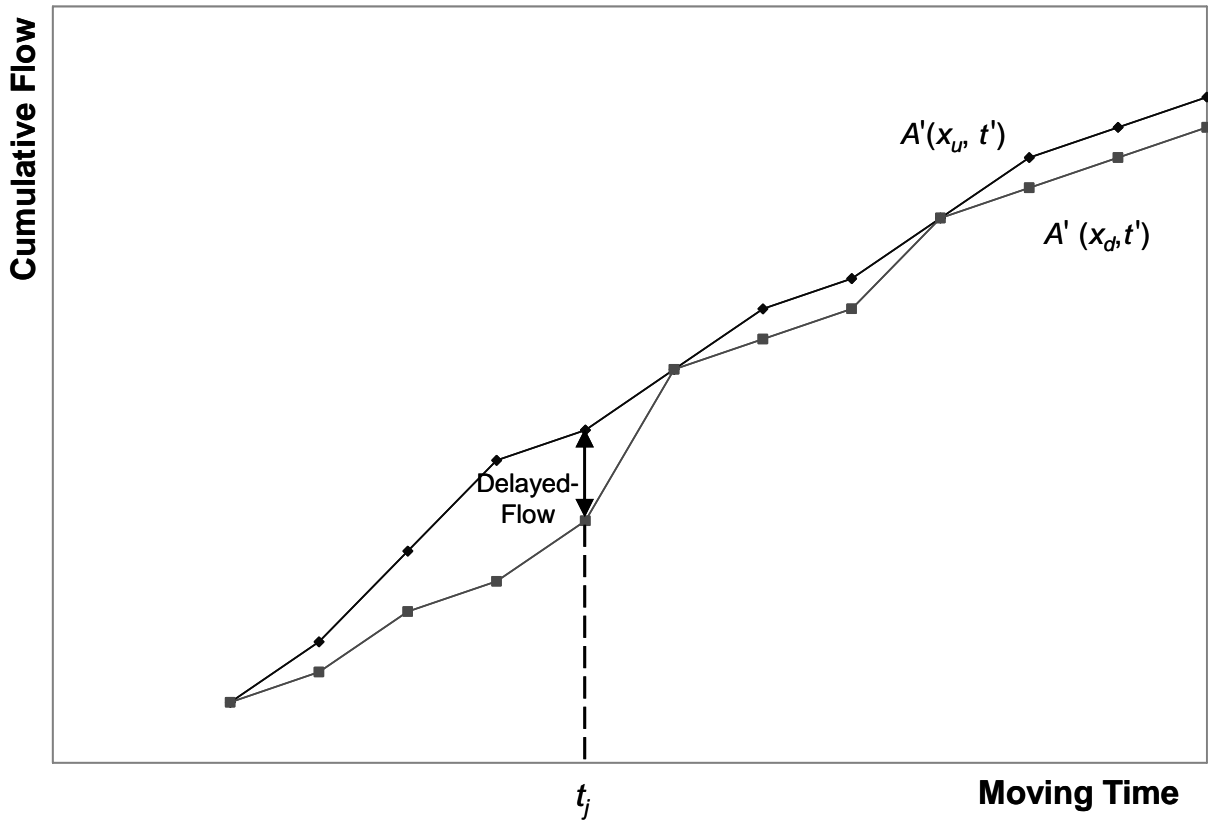


Figure 15.  Input-Output Diagram Using Moving Time Coordinates System.

**Proposed Methodology**

*Characteristics of Flow-in-Process and Delayed-Flow*

In this section, we discuss characteristics of flow-in-process and delayed-flow under different traffic conditions on a freeway section.

First, consider a perfect case where the following occurs:

- vehicles arrive uniformly at $x_u$,
- vehicles arrive at a constant rate at $x_u$, and
- vehicles travel from $x_u$ to $x_d$ at the average free-flow speed.

In this case, the two cumulative curves will be parallel (Figure 16a), and the upstream cumulative curve will superimpose the downstream cumulative curve in the MTC system (Figure 16b). As a result, flow-in-process will be constant and delayed-flow will be zero.
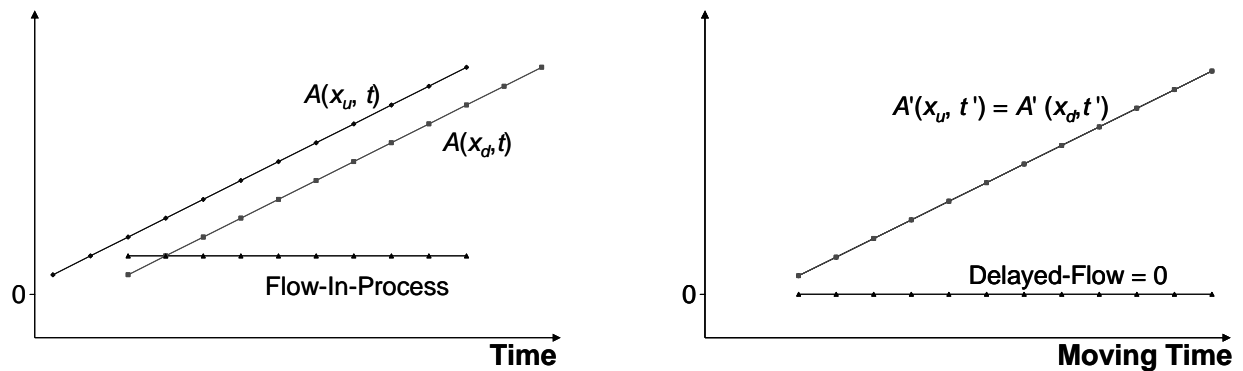


**Figure 16. Constant Vehicle Flow.**

Suppose there is an increase in traffic flow at time $t$, while the travel time is not affected. In this case, there will be more vehicles traveling in the section starting at time $t$. As a result, there will be a jump in flow-in-process while delayed-flow will remain zero (Figure 17). Similarly, if traffic flow decreases at time $t$ without affecting travel time, there will be a decrease in flow-in-process while delayed-flow will remain unchanged (Figure 18).
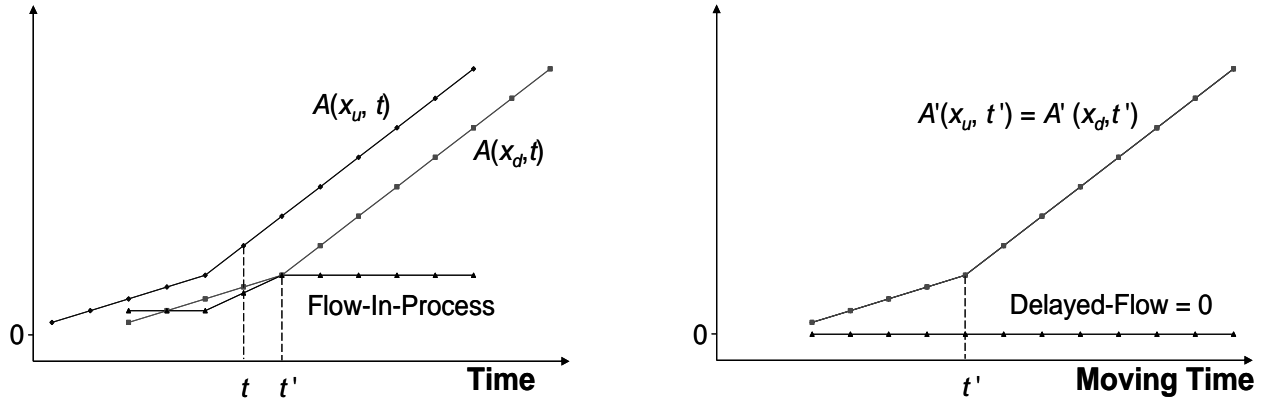
57

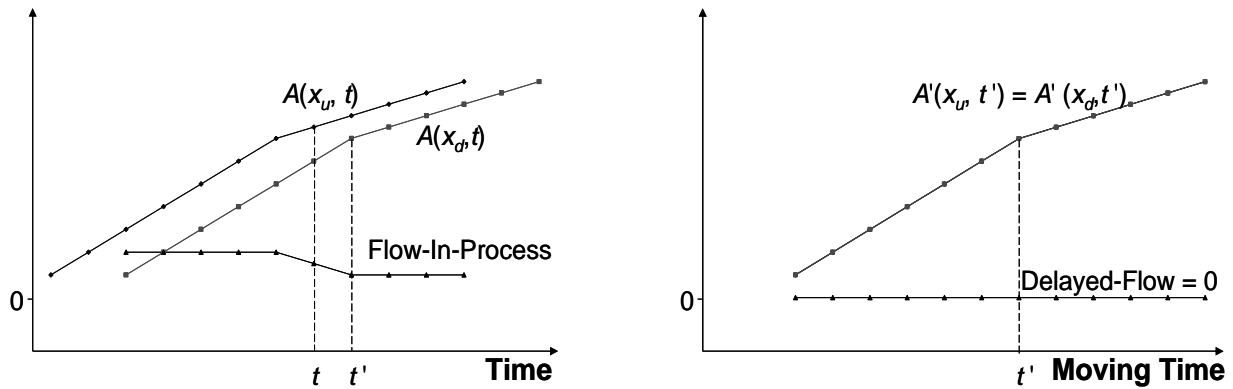**Figure 17. Increase Vehicle Flow.**



**Figure 18. Decrease Vehicle Flow.**

Now, suppose that an incident occurs in the section at time $t_1'$ resulting in increased travel time between the two detector locations. In the MTC system, this situation will cause the cumulative flow from $x_d$ to be lower than that from $x_u$, resulting in a positive delayed-flow. When the incident clears at some time $t_2' > t_1'$, the number of vehicles leaving the downstream detector location will increase, resulting in a decrease in flow-in-process and delayed-flow. Examples of the input-output diagrams and the corresponding flow-in-process and delayed-flow for the case described above are illustrated in Figure 19.

If the shock wave resulting from the incident reaches $x_u$, the operation of the adjacent upstream freeway will be compromised. This spillback of congestion into the upstream freeway section can be identified by doing a similar analysis for that section.

58
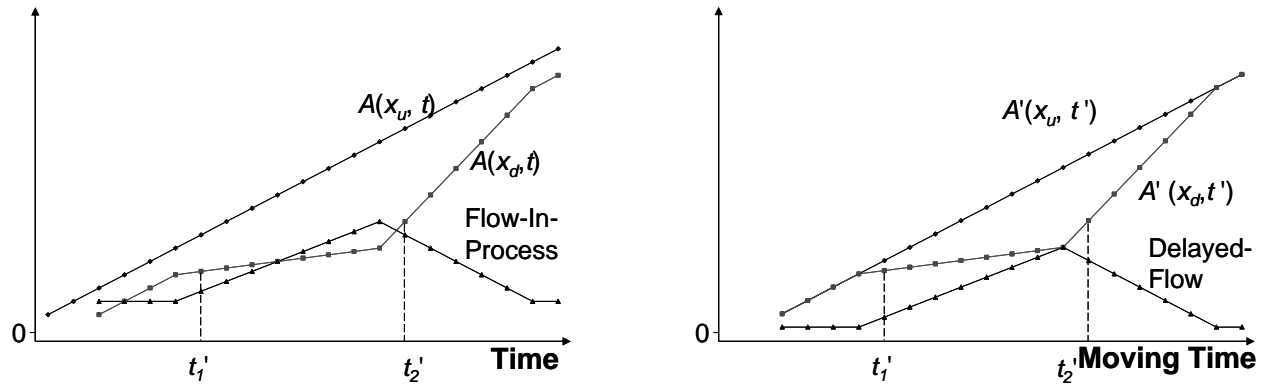
**Figure 19.  Incident at Freeway Section without Spillback.**

Figure 20 illustrates the effects of spillback on the affected freeway sections. Figure 20a presents the input-output diagrams for section $y_d$ (section where the incident occurs). Figure 20b shows the input-output diagrams for the upstream section $y_u$. In this example, the incident occurs at $t_1'$, and the shock wave spills back to the upstream section $y_u$ at $t_1$. The figure also shows that the incident clears (that is, flow-in-process at section $y_d$ starts to decrease) at $t_2'$ while the effects of the incident in the upstream section start to subside at $t_2 > t_2'$.

The reader should note that input-output diagrams of section $y_u$ (Figure 20b) are similar to those in Figure 19, indicating the effect of the incident does not reach further into the upstream section. Should the shock wave reach the upstream section of $y_u$, Figure 20b will be similar to Figure 20a.

*Methodology*

Based on the analysis in the previous section, we proposed evaluating the current operating states of the freeway system by monitoring the flow-in-process and delayed-flow of each adjacent pair of detectors along the freeway starting from the farthest downstream section $y_n$, back to the farthest upstream freeway $y_1$ (Figure 21).
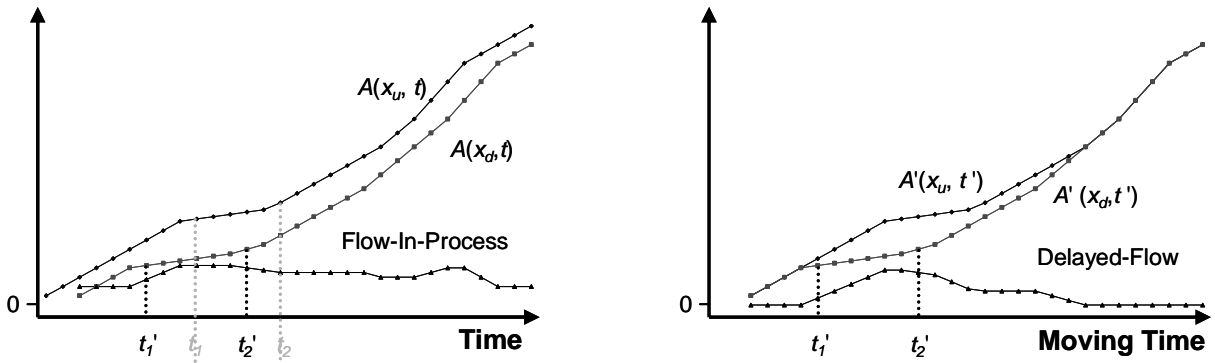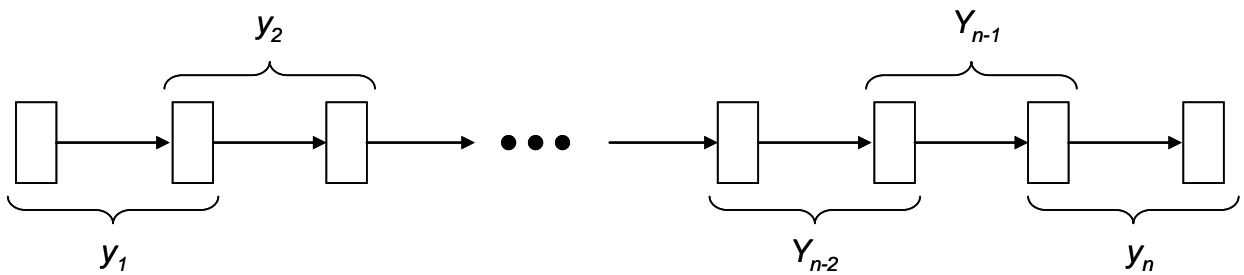
(a)Input-output diagrams for section $y_d$.
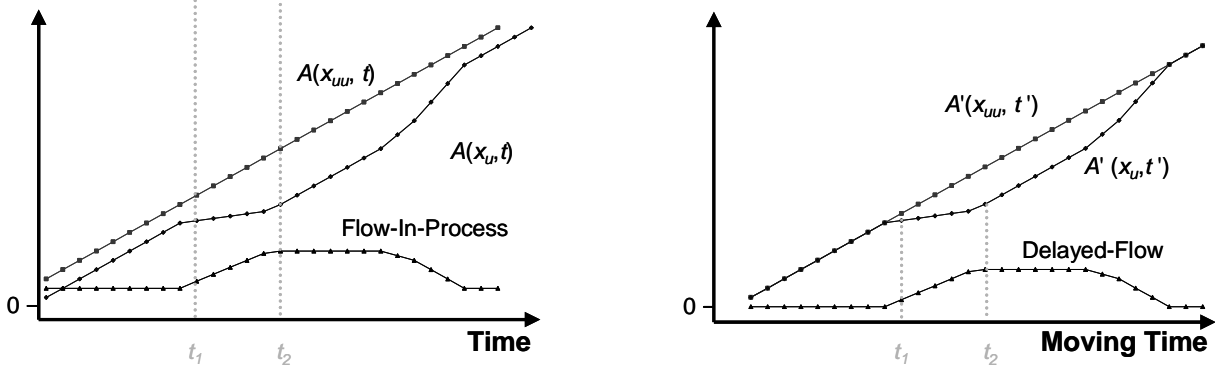


(b) Input-output diagrams for upstream section $y_u$.

**Figure 20.  Incident at Freeway Section with Spillback.**



**Figure 21.  Freeway Detector System.**

As discussed in the previous section, the flow-in-process and delayed-flow can identify whenever there is a volume change on any freeway section. Therefore, these indicators can identify start and end of peak flow periods as well as incidents. In addition, analysis of areas under the elevated sections of a delayed-flow curve may quantify the amount of delay at each freeway section. However, this issue needs further investigation. For instance, if an incident

occurs at freeway section $y_i$, monitoring delayed-flow for that section will identify the incident. Also, delayed-flow of upstream section $y_{i-1}$ will identify when the shock wave from section $y_i$ arrives at section $y_{i-1}$. Furthermore, the effects of the shock wave reaching farther upstream (i.e., section $y_{i-2}$) can be identified using data from that section. For this reason, our proposed methodology evaluates the system from the farthest downstream freeway section to the farthest upstream freeway section. There are three primary advantages of this proposed methodology. These advantages are listed below.

- It is scalable and can be applied to freeways with different sizes.
- Using the principle of flow conservation, it can be applied to freeway sections with different configurations (Figure 22).
- It depends on a limited amount of information, i.e., volume counts and free-flow speed.
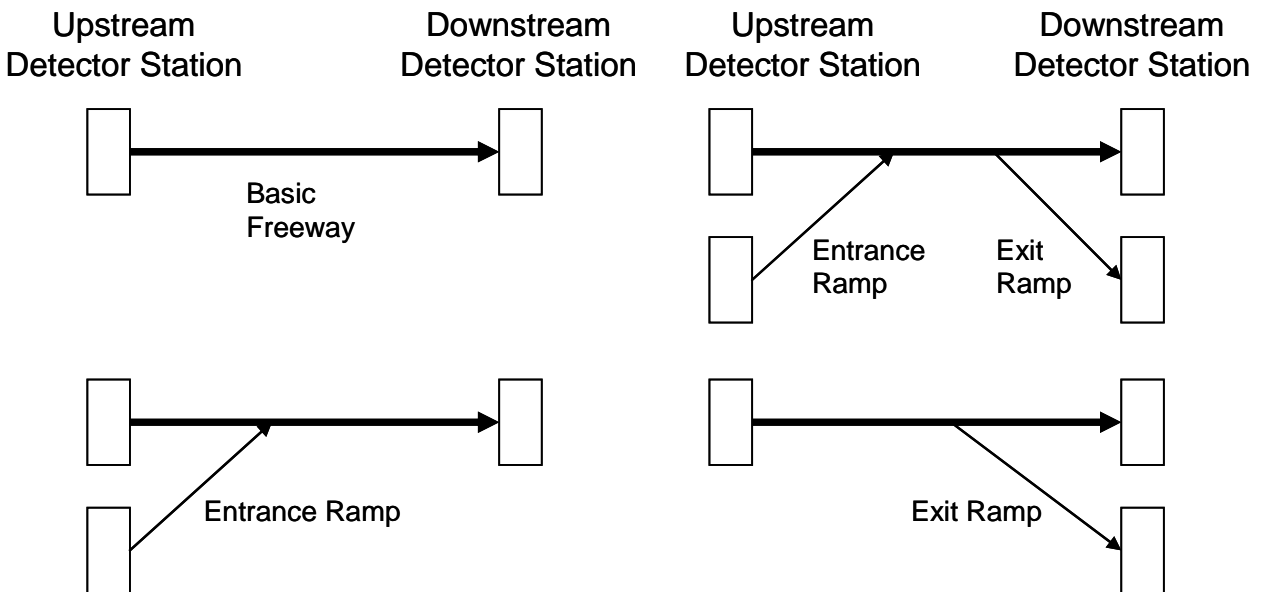


**Figure 22. Different Freeway Configurations.**

## Illustration Using Simulation

In this section, we illustrate the proposed methodology by applying it to count data obtained from computer simulation using VISSIM 4.00 (52). The simulated system is a three-lane freeway with four basic freeway sections in the study area (Figure 23). In addition, the freeway speed was uniformly distributed in the range of 55 and75 vehicles per hour.
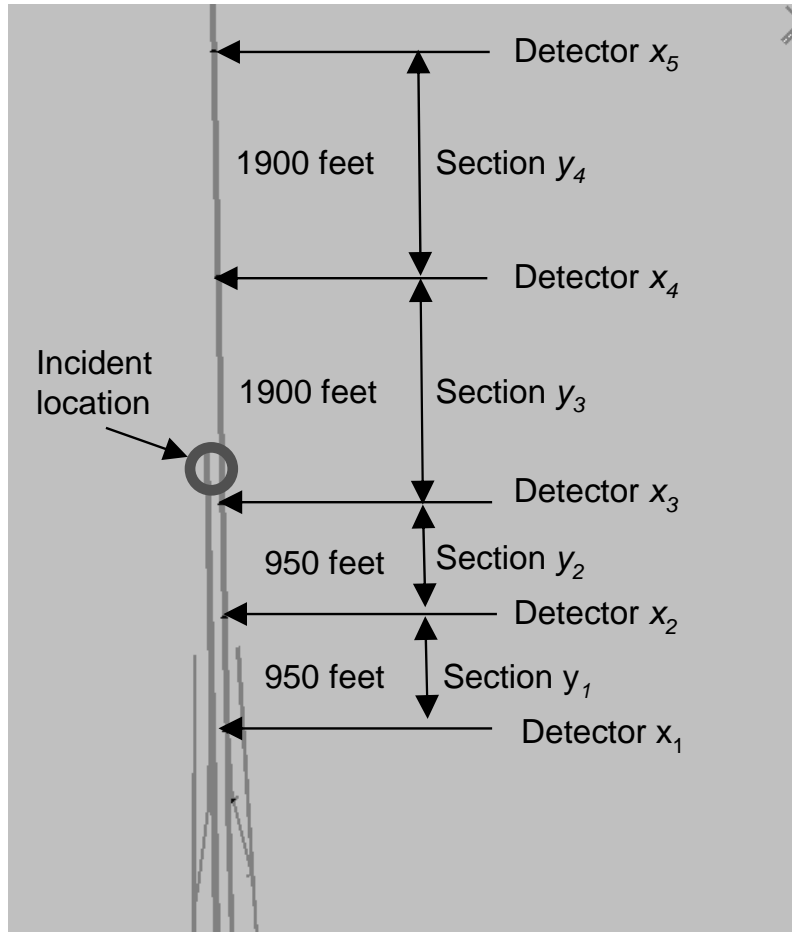


**Figure 23. Freeway System.**

We divided the simulation into three time periods. Table 8 provides the durations and arrival rates for these periods. The reader should note that the arrival rate increases significantly after the first 15 minutes of simulation. The period of high demand lasts for 30 minutes, at which point the arrival rate drops to the initial rate. For the study described here, we conducted one one-hour simulation without any incident and one one-hour simulation with a single 10-minute incident, which started 1800 seconds into the simulation and blocked the middle lane only. As

illustrated in Figure 23, the incident occurred at section $y_3$ immediately downstream of detector station $x_3$.

**Table 8.  Arrival Rate Distribution.**

| From (seconds) | To (seconds) | Arrival Rate (vph) |
|---|---|---|
| 0 | 900 | 4000 |
| 900 | 2700 | 7500 |
| 2700 | 3600 | 4000 |

Figure 24 shows the flow-in-process and delayed-flow plots for the no-incident scenario. Here, the curves of flow-in-process and delayed-flow with respect to time are not piecewise linear as in the previous section. This difference is because vehicle arrivals are random as opposed to the uniform arrivals assumed for previous illustrations. Furthermore, individual vehicles travel at different speeds and not the average free-flow speed as assumed earlier. These characteristics are similar to that observed in the real world. Nevertheless, the reader should note that the curves of flow-in-process and delayed-flow can be approximated by piecewise linear curves to produce curves similar to those presented in the previous section.

In Figure 24, the flow-in-process for each section increased sharply some time after 900 seconds of simulation and reduced sharply some time after 2700 seconds of simulation time. In general, this result agrees with the arrival (demand) data presented in Table 8. The reader will notice that the elevated portion of the flow-in-process curves do not start at 900 seconds but are slightly shifted to the right. This shift is equal to the travel time from the vehicle entry point into the system to the detector locations and shows when the increased traffic started impacting each section. Also note that flow-in-process of sections $y_3$ and $y_4$ are larger than those of sections $y_1$ and $y_2$ during the period with increased traffic flow. In general, longer sections result in larger flow-in-process, which is defined as vehicles traveling in the section at a particular time. Since section $y_3$ and $y_4$ are longer than sections $y_1$ and $y_2$, it is expected that the flow-in-processes of sections $y_3$ and $y_4$ are larger than those of sections $y_1$ and $y_2$. Despite a significant increase in demand, however, delayed-flow remains approximately the same at all freeway sections during the entire simulation period. This is because no disruptions occurred on any section.
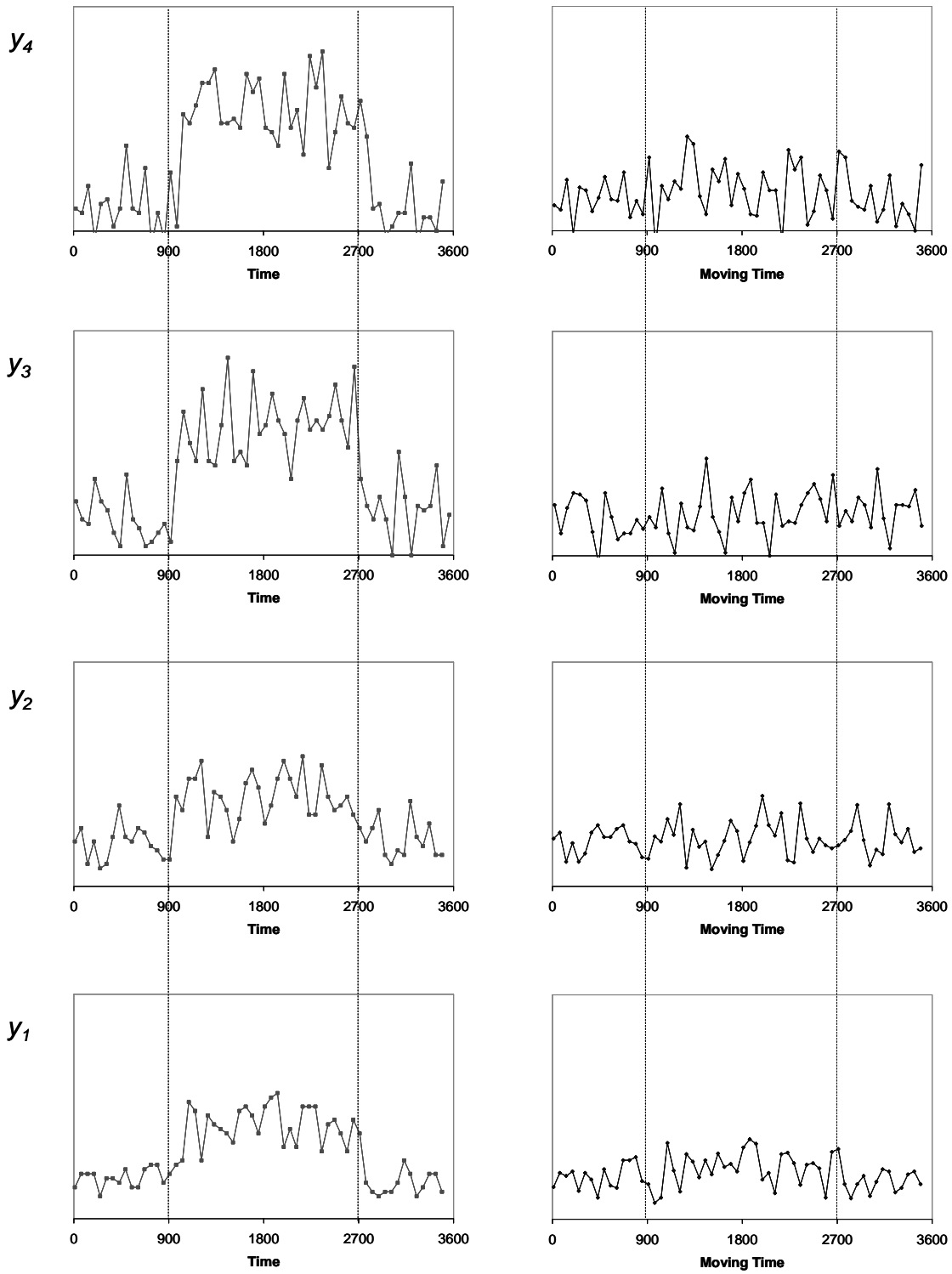
**Figure 24. Scenario without Incident.**

Figure 25 presents the flow-in-process and delayed-flow plots for the scenario with incident. Notice that the behaviors of flow-in-process and delayed-flow plots for each section are similar to that in Figure 24 until 1800 seconds. In other words, these plots detect an increase in traffic and no increase in delay. At around 1800 seconds, delayed-flow of section $y_3$ increases significantly, which indicates an incident. Later, delayed-flow and flow-in-process of upstream sections, $y_2$ and $y_1$, also increase, while the delayed-flow of section $y_3$ does not drop. It serves as a signal that the shock wave created by the incident has reached the upstream sections.

More detailed information can be obtained by magnifying the scale of plots for sections $y_1$, $y_2$, and $y_3$ (Figure 26). Figure 26a shows how time lags in peaks of delayed-flow at adjacent sections identify the progression of the shock wave. Note that delayed-flow of downstream section $y_4$ is not affected, while the flow-in-process decreases during the incident. This happens because fewer vehicles enter section $y_4$ during the incident.

Similarly, Figure 26b shows time lags between the times at which congestion starts to clear at adjacent sections. Since the incident lasted for 600 seconds, we would expect that delayed-flow for the section with incident quickly drops to the level prior to the incident. This is the case for section $y_3$ at time 2400 seconds. Delayed-flows of sections $y_1$ and $y_2$ do not drop to the expected levels until several minutes after the incident cleared. This result is not surprising.

In this section, we presented the application of the proposed methodology by simulating a basic freeway section. Additional research to verify the methodology via computer simulation for other configurations of freeway sections (Figure 21) is currently underway. This ongoing work includes simulations with different locations and durations of incidents. The results obtained so far have produced similar results.

**Application of Proposed Methodology to Real Data**

This section documents the application of the proposed methodology to two sites along northbound US 183 in Austin, Texas. The first site includes the detector stations located at Guadalupe Street, Lamar Boulevard, and Lazy Lane, and the second site consists of detector stations located at Tweed Court and Pavilion Boulevard. Data used here were collected by the Texas Department of Transportation in 2002. The study sites are illustrated in Figure 27.
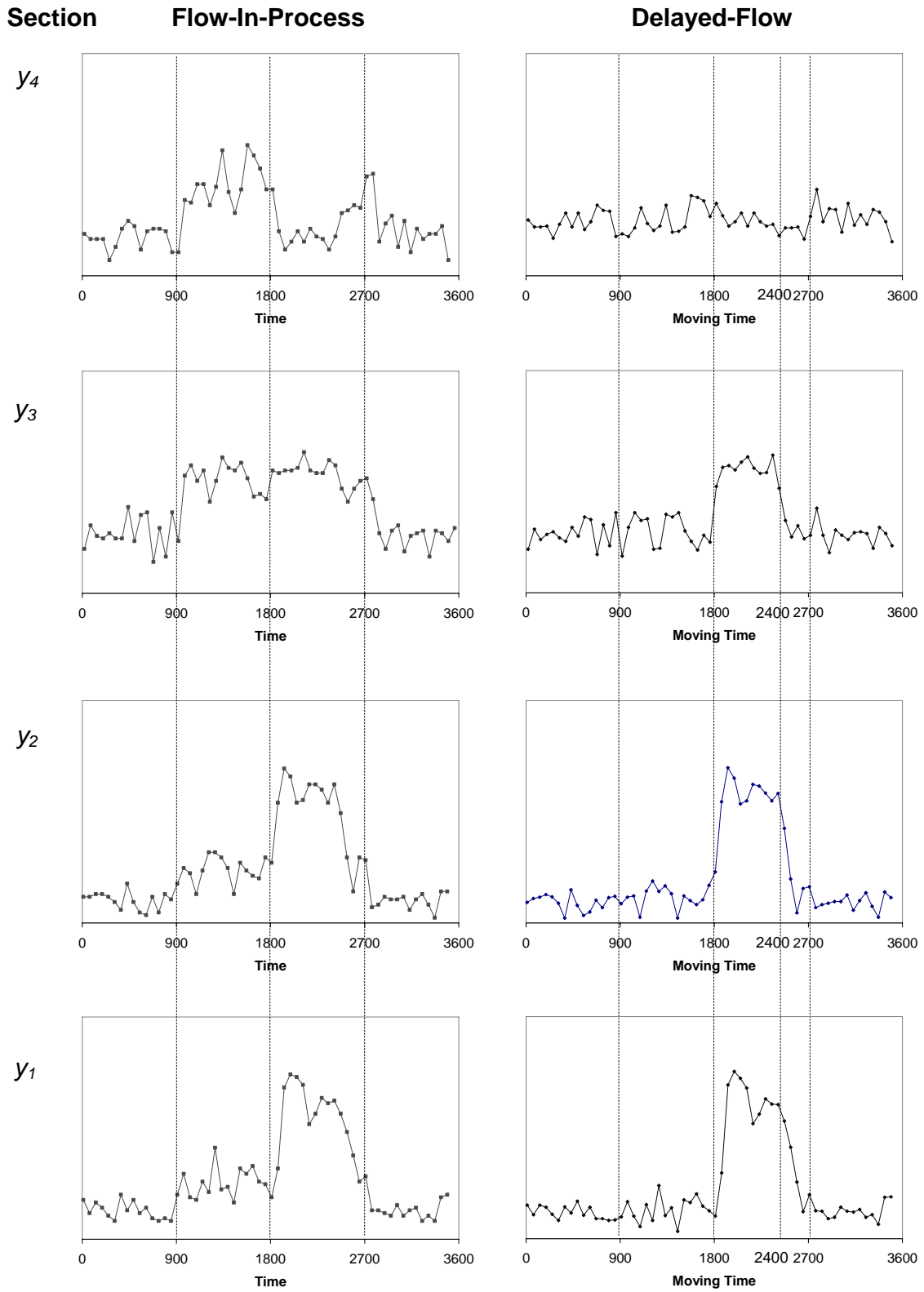
**Figure 25. Scenario with Incident.**
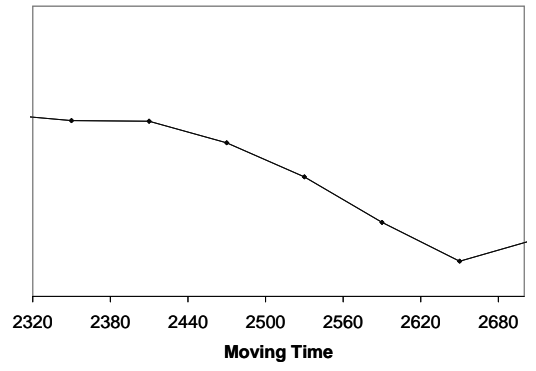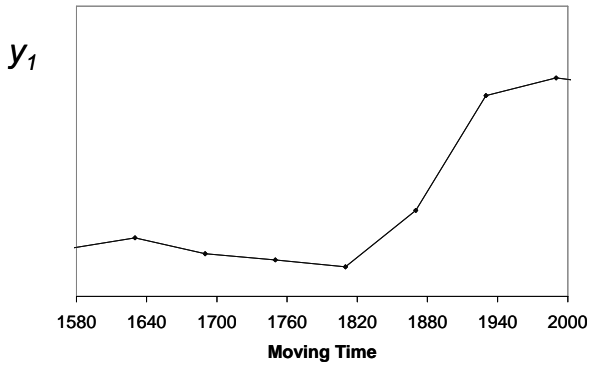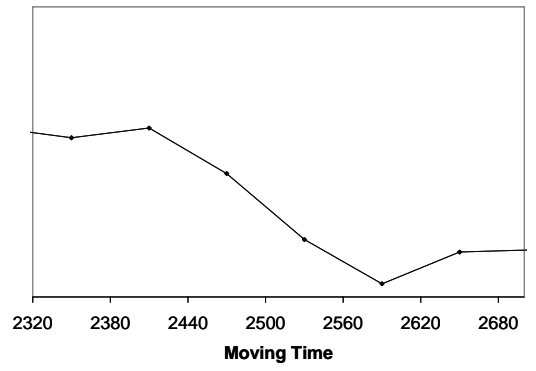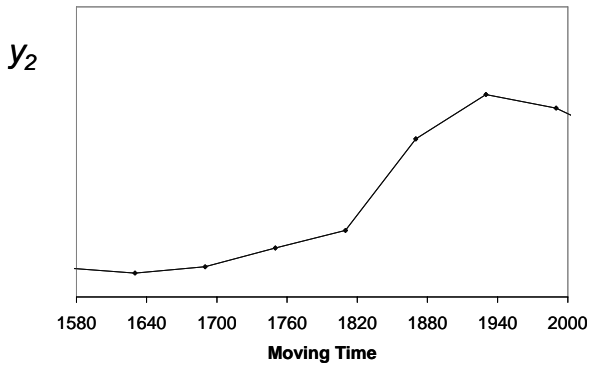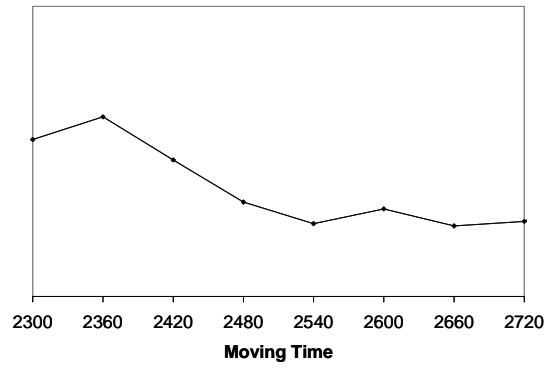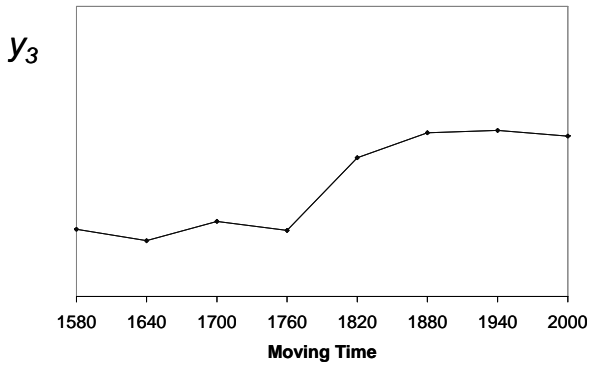
**(a) Incident occurrence**  **(b) Incident termination**

**Figure 26. Delayed-Flow during the Beginning and Ending of the Incident.**

67

Lazy
Lane

Lamar
Boulevard

Guadalupe
Street

Pavilion
Boulevard

Tweed
Court

**Figure 27.  Study Sites on US 183, Austin, Texas.**
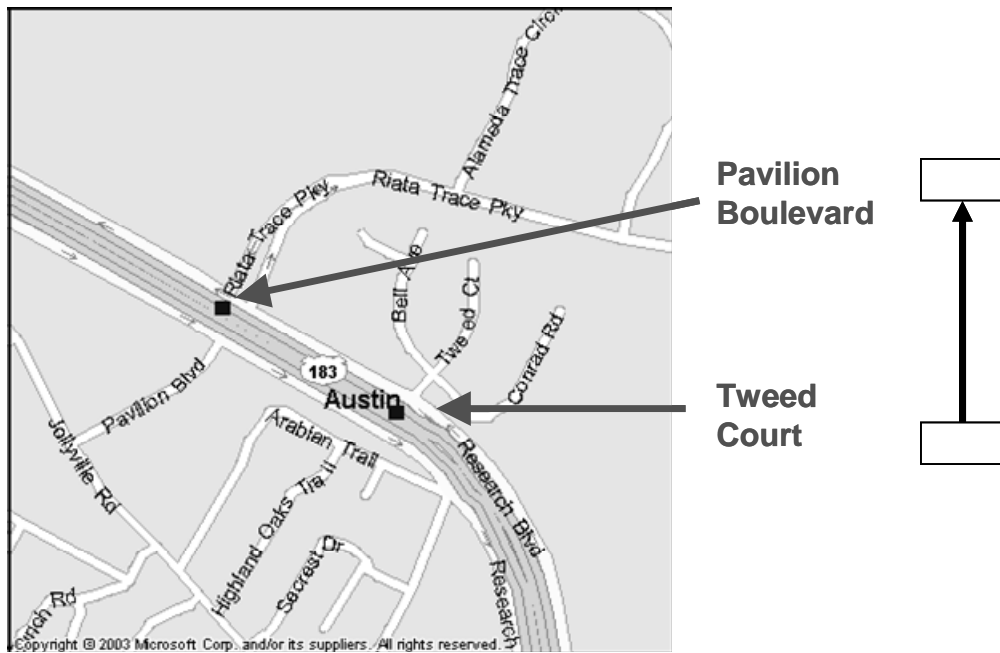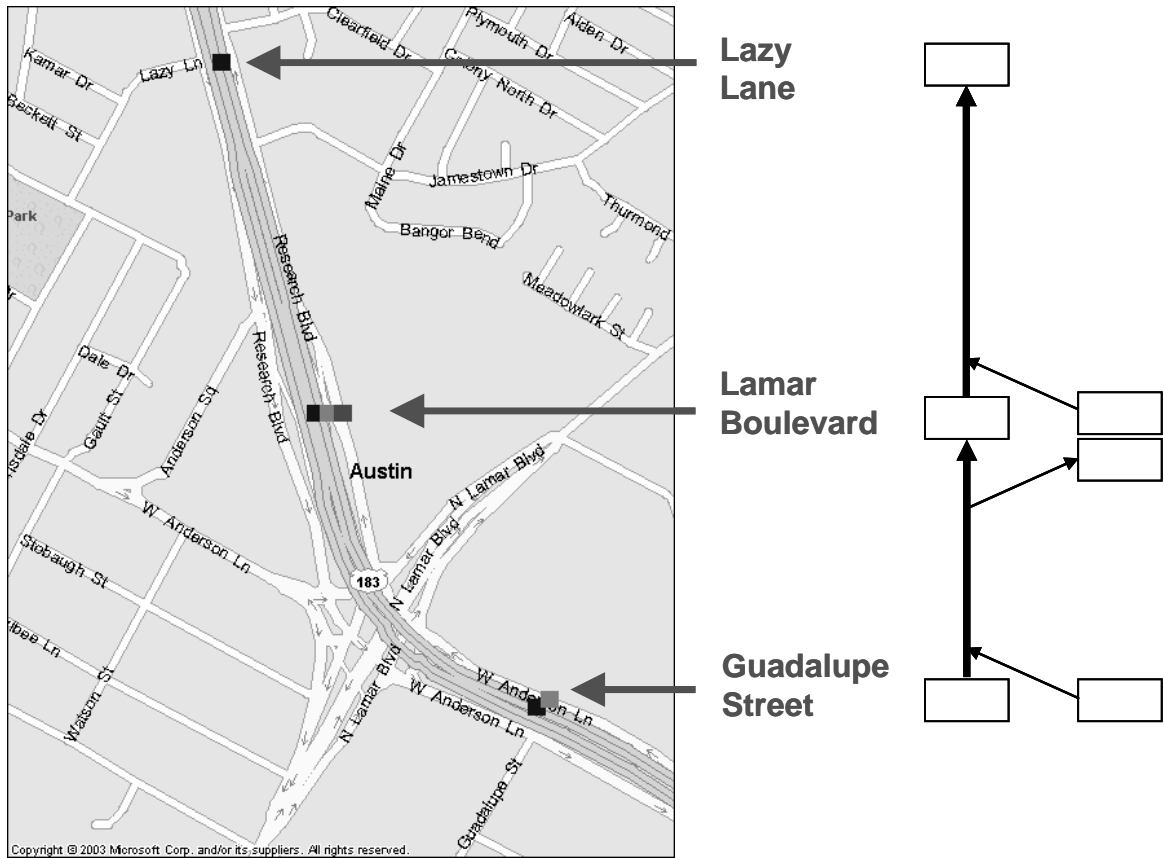
At the first site, there are three lanes on the freeway, and the approximate distance between adjacent detector stations at Guadalupe Street, Lamar Boulevard, and Lazy Lane is a half mile. The second site also has three lanes on the freeway, and the detector stations at Tweed Court and Pavilion Boulevard are about a quarter mile apart. Detector stations at all these locations collect lane-by-lane traffic counts and occupancies, average speeds, and truck percentage over one-minute intervals. The average free-flow speed is 70 mph. Data analyzed for the first site (Guadalupe-Lamar-Lazy) were from 14:00 to 18:00 on June 4, 2002 (a Tuesday); data of the second site (Tweed-Pavilion) were from 02:00 to 04:00 on January 5, 2002 (a Saturday).

*Guadalupe-Lamar-Lazy Site*

Figure 28 presents the flow-in-process and delayed-flow plots for this site. To evaluate this site, we first study the downstream section (from Lamar Boulevard to Lazy Lane). In this section, both flow-in-process and delayed-flow increase steadily at an approximate rate of 100 vehicles per hour from 14:00 to 17:00, and jump to around 500 vehicles from 17:00 to 18:00. Recall that flow-in-process is defined as the number of vehicles that are traveling in the section at any particular time; it is improbable to have 500 vehicles in a half-mile three-lane section simultaneously.

Next, we studied the upstream section (Guadalupe Street to Lamar Boulevard). In this case, flow-in-process and delayed-flow demonstrate a horizontal trend from 14:00 to 16:00. However, from around 16:15, both flow-in-process and delayed-flow dropped significantly, resulting in negative values. In other words, more vehicles are leaving the section than vehicles entering the section, a logically impossible scenario.

The above analysis revealed that the detector station at Lamar Boulevard recorded more vehicles than those at the Guadalupe Street station and the Lazy Lane station. It is perhaps due to faulty detectors on Lamar Boulevard only. Thus, we ignored the data of the Lamar Boulevard station and plotted the flow-in-process and delayed-flow against time for the Guadalupe-Lazy section in Figure 29.

In Figure 29, both flow-in-process and delayed-flow show an upward trend, which indicates an incident that lasted for a couple of hours. However, there is no incident logged during that period. Therefore, we suspect that the detectors may not provide an accurate volume

69

count. To further investigate the issue, we applied the methodology to another site, Tweed-Pavilion.
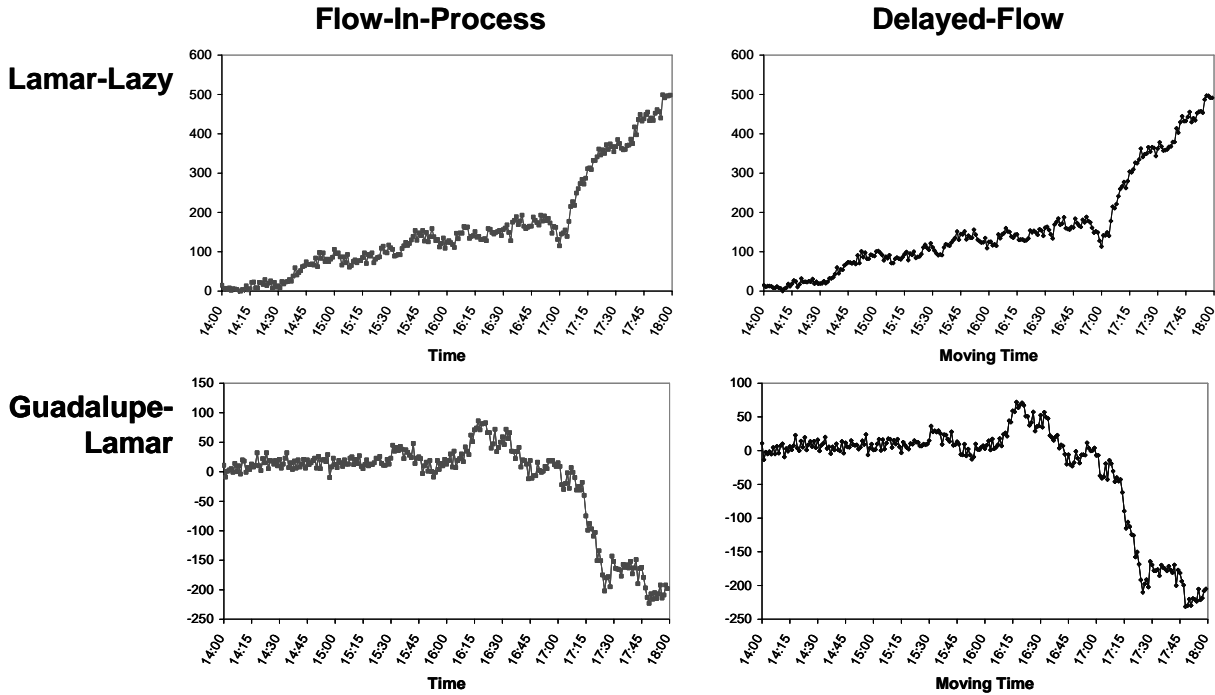
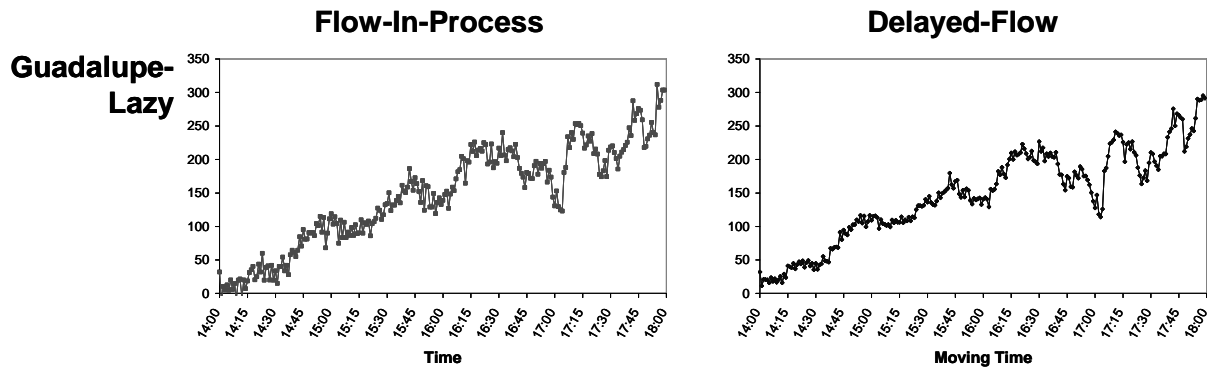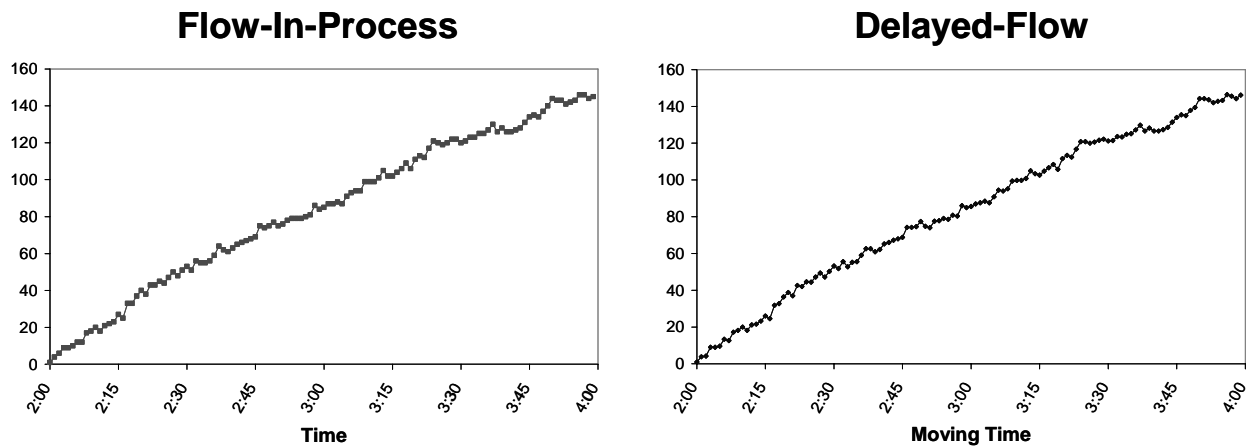**Figure 28. Flow-in-Process and Delayed-Flow of Guadalupe-Lamar-Lazy Site.**

**Figure 29. Flow-in-Process and Delayed-Flow of Guadalupe-Lazy.**

*Tweed-Pavilion Site*

The section between detector stations located at Tweed Court and Pavilion Boulevard is a basic freeway section (i.e., there are no ramps in this section). Figure 30 presents plots of flow-in-process and delayed-flow for this site. Here, both flow-in-process and delayed-flow increase with the passage of time. Note that data used here are from a non-peak period with volumes of less than 1000 vehicles recorded at both locations during the two-hour period. In addition, logs contained no record of an incident. These findings lead us to conclude that the volume counts are inaccurate and that there are inconsistencies between detector stations. We also noticed such inconsistencies by randomly inspecting data from other sections on US 183.

**Flow-In-Process**

**Delayed-Flow**

**Figure 30.  Flow-in-Process and Delayed-Flow of Tweed-Pavilion Site.**

**Data Integrity**

In a previous section, we used computer simulation to demonstrate that flow-in-process and delayed-flow can be useful in detecting different operating states along a freeway. However, as demonstrated in the previous section, the proposed methodology fails when faulty data are used. Application of the proposed methodology to a small subset of US 183 in Austin, Texas, revealed inconsistencies in volume counts from adjacent detector locations. Further investigation of Austin data revealed other inconsistencies such as very low freeway speeds (30 mph) during low-volume early-morning periods.

Figure 31 illustrates partial data collected from Carver Avenue and Chevy Chase Drive on US 183, where Carver Avenue is located immediately upstream of Chevy Chase Drive. Here,

the upstream location recorded no vehicles, while the downstream location recorded positive volume count.

Also, the upstream entrance ramp reported "–1" for speed and truck percentage, which indicates the detector is not functioning. However, volume and occupancies are "0" but not "–1." It is not clear how to interpret these data given that the speed and truck percentages are flagged with negative values. We need further information to determine if part of the data should be accepted as valid when some fields are flagged with values of "–1," or if all data for that detector should be considered invalid.

*Upstream Freeway Station (Carver Avenue)*

| Detector | Vol | Occ. | Speed | %Tr | Detector | Vol | Occ. | Speed | %Tr | Detector | Vol | Occ. | Speed | %Tr |
|---|---|---|---|---|---|---|---|---|---|---|---|---|---|---|
| 2001011 | 0 | 0 | 0 | 0 | 2001012 | 0 | 0 | 0 | 0 | 2001013 | 0 | 0 | 0 | 0 |
| 2001011 | 0 | 0 | 0 | 0 | 2001012 | 0 | 0 | 0 | 0 | 2001013 | 0 | 0 | 0 | 0 |
| 2001011 | 0 | 0 | 0 | 0 | 2001012 | 0 | 0 | 0 | 0 | 2001013 | 0 | 0 | 0 | 0 |
| 2001011 | 0 | 0 | 0 | 0 | 2001012 | 0 | 0 | 0 | 0 | 2001013 | 0 | 0 | 0 | 0 |
| 2001011 | 0 | 0 | 0 | 0 | 2001012 | 0 | 0 | 0 | 0 | 2001013 | 0 | 0 | 0 | 0 |

*Upstream Entrance Ramp Station (Carver Avenue)*

| Detector | Vol | Occ. | Speed | %Tr |
|---|---|---|---|---|
| 2001015 | 0 | 0 | 0 | 0 |
| 2001015 | 0 | 0 | 0 | 0 |
| 2001015 | 0 | 0 | 0 | 0 |
| 2001015 | 0 | 0 | 0 | 0 |
| 2001015 | 0 | 0 | 0 | 0 |

*Downstream Freeway Station (Chevy Chase Drive)*

| Detector | Vol | Occ. | Speed | %Tr | Detector | Vol | Occ. | Speed | %Tr | Detector | Vol | Occ. | Speed | %Tr |
|---|---|---|---|---|---|---|---|---|---|---|---|---|---|---|
| 2000511 | 0 | 0 | 0 | 0 | 2000512 | 6 | 2 | 47 | 0 | 2000513 | 0 | 0 | 0 | 0 |
| 2000511 | 0 | 0 | 0 | 0 | 2000512 | 1 | 0 | 49 | 0 | 2000513 | 0 | 0 | 0 | 0 |
| 2000511 | 1 | 0 | 49 | 0 | 2000512 | 1 | 0 | 49 | 0 | 2000513 | 0 | 0 | 0 | 0 |
| 2000511 | 0 | 0 | 0 | 0 | 2000512 | 2 | 1 | 43 | 50 | 2000513 | 0 | 0 | 0 | 0 |
| 2000511 | 0 | 0 | 0 | 0 | 2000512 | 0 | 0 | 0 | 0 | 2000513 | 0 | 0 | 0 | 0 |

**Figure 31.  Data on Carver Avenue and Chevy Chase Drive.**

**Summary**

This paper presented a methodology for assessing the operating states of a freeway using volume data from pairs of adjacent detectors along the freeway. The methodology compares the differences in cumulative flows from two neighboring detector locations to identify volume changes and incidents. The advantages of the methodology are its scalability, robustness in modeling different freeway configurations, and the limited amount of information required.

To demonstrate the methodology, we created a four-section freeway in VISSIM. Using the data generated by VISSIM, we demonstrated that the methodology successfully identifies changes in volume and the occurrence of an incident and the effects of the resulting shock wave.

Although the proposed methodology is promising, it fails when faulty data are used. An analysis of existing data collected from stations along US 183 revealed the presence of inconsistent or faulty data in numerous cases. Some examples of such data are:

- inconsistent volume counts in that the total number of vehicles recorded at an upstream station does not match with volumes recorded at an immediate downstream location in a basic freeway segment,

- very low speeds during early morning hours with light traffic, and

- zero volumes for a significant period of time.

There is a need to investigate and correct the causes of these inconsistencies because accurate data are needed to successfully achieve the objectives of this project.

**Other Work Underway**

As an ongoing subtask, researchers also are developing software for implementing selected traffic assessment/prediction models for this project and to serve as a basis for the prototype software to be developed during the second fiscal year.

As mentioned previously, we are developing additional simulation scenarios that will allow us to verify the proposed methodology for different freeway-section configurations. Furthermore, we plan to modify the proposed methodology to model freeway sections where the location of the entrance/exit ramp detector is significantly different from the closest freeway detector location.

**NON-CONTINUUM MODELING OF TRAFFIC MOVEMENT**

Traffic is modeled as a countable infinite collection of homogeneous interconnected dynamical systems, with each vehicle being considered as a dynamical system of finite state space dimension. Analogous to the limit of a sequence of numbers, we define a limit of the collection of dynamical systems as a "representative" dynamical system of same state space dimension as any other system (vehicle) in the collection. The choice of the limit of a collection as an aggregate is motivated by the need to convert from a Lagrangian description (vehicle

following) to an Eulerian description (dynamics at a fixed point on the freeway) since traffic operations are performed at fixed points on the freeway.

**Traffic Movement Model**

Since we consider each vehicle in the traffic as a dynamical system of fixed state space dimension, it is appropriate to consider the potential measurable and/or inferable state variables that can adequately describe the movement of traffic on the freeway. For this, we divide the freeway into sections and index them in an increasing order as we traverse toward the upstream sections. Thus if any section is indexed as *i*, the immediate upstream section is indexed as *i+1*. We develop the traffic movement model for each individual section, and thus, we have a representative vehicle for each section. Figure 32 shows a schematic for a typical division of a freeway into sections and their numbering. The sections can have any number of entrance and exit ramps.

*Variables That Are Used to Describe the Traffic Movement*

We use the number of vehicles in any section at any given time, aggregate following distance, and the aggregated speed of traffic as the variables that can describe the traffic dynamics in a section of a freeway. The aggregate following distance and number of vehicles are considered as different state variables for the following reasons:

- We believe that the psychology/inconsistency of drivers can render aggregate following distance and number of vehicles as independent variables.

- Should a traffic model of higher fidelity, involving distinct classes of vehicles, be developed, there will be two variables representing the aggregated following distance for each class of vehicle. Hence, to be consistent with possible future refinements, it makes sense to consider the two as independent variables.

- Observations made from traffic data suggest the existence of different traffic regimes (for example congested and uncongested), and thus, there is a switch in the driving behavior of drivers. This switch potentially can be made on the basis of the number of vehicles in a section as aggregated following distance is problematic, especially with different classes of vehicles and driving behavior.
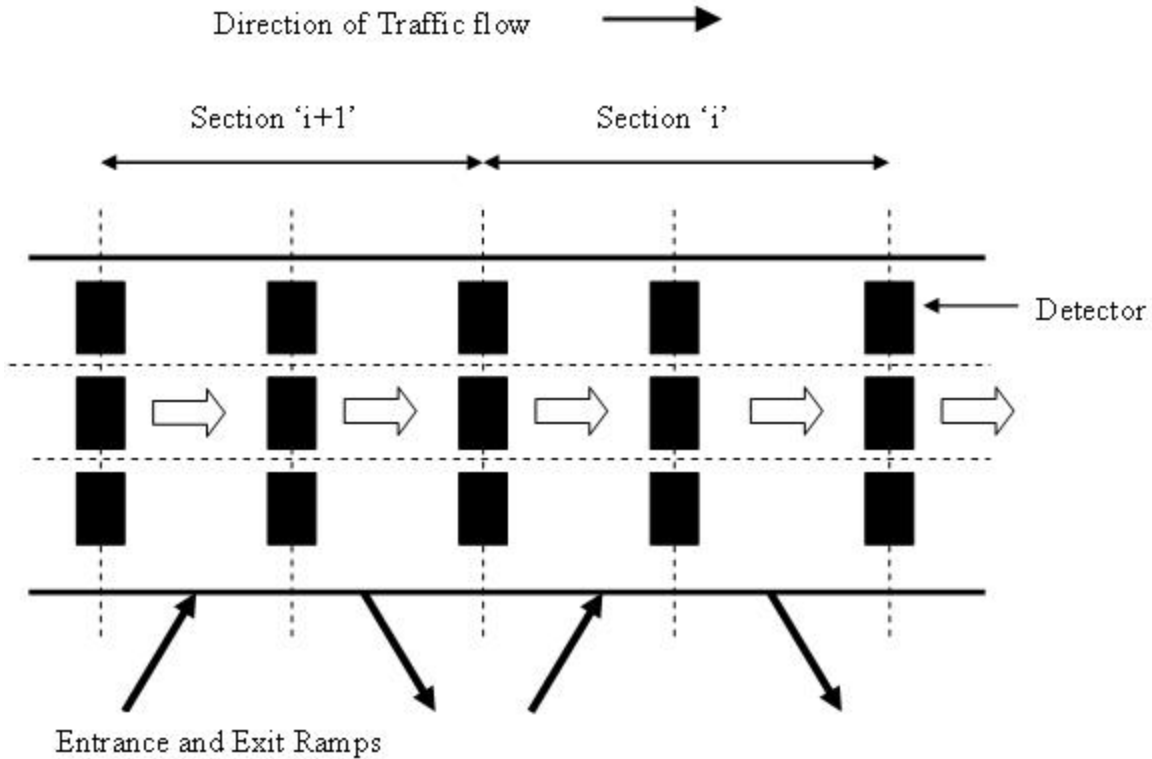
**Figure 32. Schematic Showing Division of a Freeway into Sections.**

It is reasonable to assume that vehicles on a freeway react to changes in the following distance and the relative velocity to maintain a safe distance from their preceding vehicles on a freeway. One may model the vehicle following behavior of a non-automated vehicle on the freeway as:

$$\dot{v} = f\left(v, \Delta, \dot{\Delta}\right) \qquad (23)$$

where,

$\dot{v}$ = the rate of change of vehicle speed with respect to time,

$\Delta$ = the following distance, and

$\dot{\Delta}$ = the rate of change with respect to time of the following distance of a vehicle traveling on a freeway.

This model of vehicle following neglects variations in the driving behavior of a variety of drivers; nevertheless, this is a reasonable model for the following reasons:

- We are interested in the aggregate behavior of vehicles on the freeways. Also, observation of stable maximum throughput on a number of freeway sections

75

suggests that the aggregate behavior of vehicles is well defined, although the behavior of individual vehicles may not be.

- The granularity of the model required dictates the heterogeneity of vehicle following behavior to be considered at the microscopic level.

We also make an important assumption that the vehicle following behavior is either string stable (in the case of current traffic) or can be engineered to be string stable (in the case of automated traffic). This assumption enables us to approximate the vehicle following dynamics of each of the vehicles in a section of a freeway with that of a "representative" vehicle. In physical terms, it enables us to approximate the evolution of traffic speed from the dynamics of representative vehicles in the traffic.

*The Model*

Let $\dot{N}_i$ denote the rate of change of number of vehicles with respect to time of the number of vehicles in $i$ section. Then $\dot{N}_i$ is computed using the balance of vehicles on the freeway as follows:

$$\dot{N}_i = \dot{N}_i^{en} - \dot{N}_i^{ex} + \dot{\tilde{n}}_i \qquad (24)$$

where,

$\dot{N}_i^{en}$ = the rate of vehicles entering the section from its upstream section,

$\dot{N}_i^{ex}$ = the rate of vehicles exiting the given section into a downstream section (if there is one), and

$\dot{\tilde{n}}_i$ = the net inflow into the section from the ramps.

If there are $l$ sections under consideration and they are indexed in an increasing order from the downstream end to the upstream end, the following must be true to ensure compatibility:

$$\dot{N}_{i+1}^{ex} = \dot{N}_i^{en}, i = 1, 2, ..., l-1 \qquad (25)$$

The constitutive equation for $\dot{N}_i^{ex}$ is:

$$\dot{N}_i^{ex} = \frac{\bar{v}_i N_i}{L_{s,i}} \qquad (26)$$

where,

$L_{s,i}$ = the length of the $i^{th}$ section.

Putting everything together, the traffic movement model for the $i^{th}$ section of a freeway is:

$$\dot{N}_i = \dot{N}_i^{en} - \dot{N}_i^{ex} + \dot{\tilde{n}}_i \tag{27}$$

$$\dot{\overline{\Delta}}_i = -\frac{\left(\overline{L}_{car} + \overline{\Delta}_i\right)^2}{L_{s,i}} \dot{N}_i \tag{28}$$

$$\dot{\overline{v}} = f\left(\overline{v}_i, \overline{\Delta}_i, \dot{\overline{\Delta}}_i\right) \tag{29}$$

$$\dot{N}_i^{ex} = \frac{\overline{v}_i N_i}{L_{s,i}} \tag{30}$$

$$\dot{N}_i^{en} = N_{i+1}^{ex} \tag{31}$$

**Traffic Data**

Typical traffic sensors like cameras and inductive traffic loop detectors are local in nature, as they are installed at specific locations on a freeway. With a camera, one can obtain the measurements of speed and following distance of a vehicle as it crosses a point on the highway and the rate at which vehicles enter and exit a section of a freeway. The typical measurements that one can obtain from a dual trap inductive loop detector are the speed of a vehicle as it crosses a specific point and the number of vehicles passing through the point at regular intervals of time.

*US 183 Dual Loop Detector Data*

For this project, we have utilized loop detector data from the US 183 freeway in Austin, which were collected by the Texas Department of Transportation. The data were made available by the TransLink® Laboratory at the Texas Transportation Institute. The measurements that are available from the loop detector data on US 183 are:

- number of vehicles passing through the detector location,
- average speed of vehicles that pass through the detector location,
- occupancy, and
- percentage of trucks.

These data are aggregated into one-minute intervals. Upon careful observation of data for working days on many freeway locations, we observe that the aggregate behavior of traffic does show a stable maximum throughput. By stable maximum throughput, we mean that values close to this maximum are observed on a number of days and in a repeatable manner.

Figure 33 shows typical aggregate speed, number of vehicles passing per minute, and the occupancy (in percentage) at the detector station (number 13) at Lamar Boulevard North on US 183 northbound (NB) in Austin. The same kinds of plots are observed at many different locations for all the weekdays. Figure 34 shows the same data for a weekend (Sunday in this figure) for the same location.
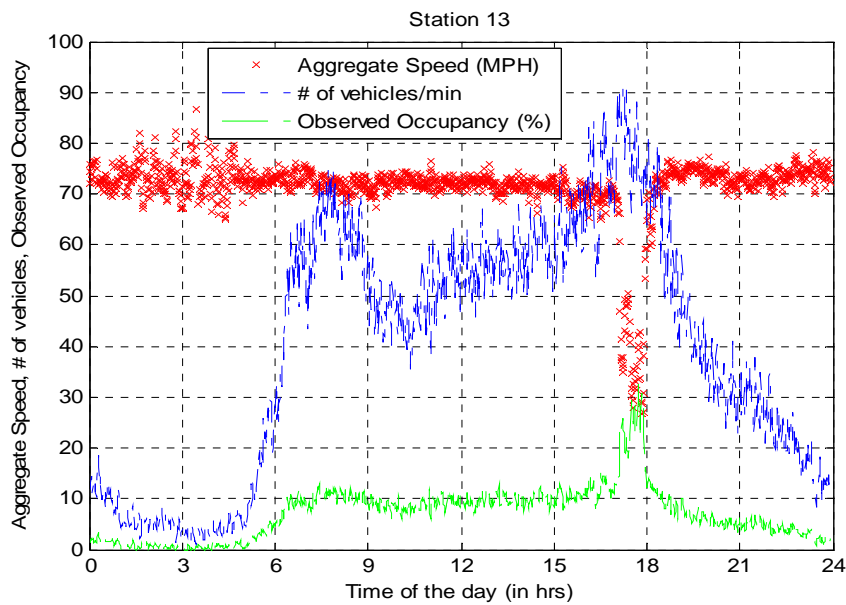


**Figure 33.  Traffic Data for 05/17/2004 at a Location on US 183 NB (Station Number 13).**
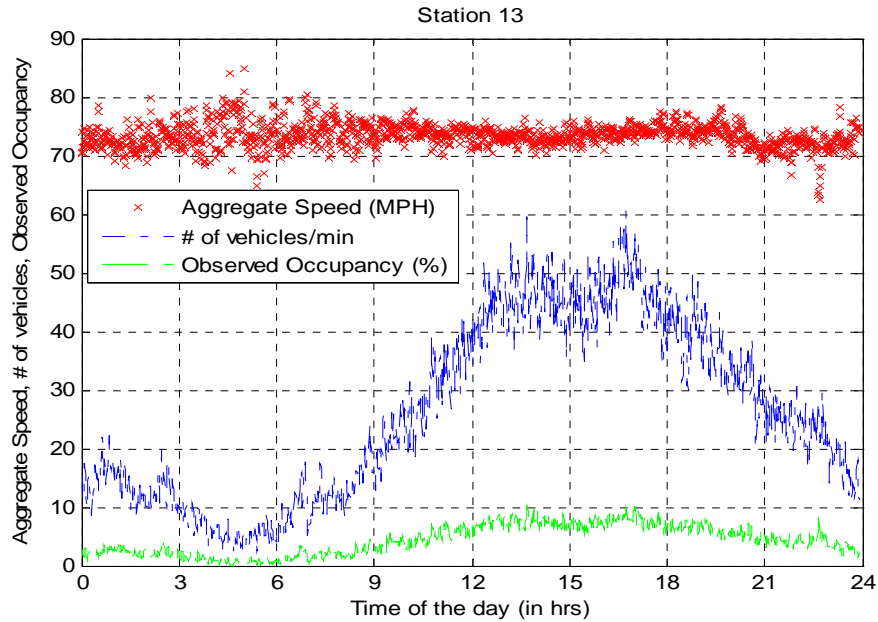
**Figure 34. Traffic Data for 05/16/2004 at a Location on US 183 NB (Station Number 13).**

Upon observation of the traffic data for many days for the years 2002, 2003, and 2004 we make the following deductions:

- Traffic movement is different for weekdays (working days) and weekends (including holidays). This difference may be observed in terms of the number of vehicles passing per minute and the occupancy levels.

- There seems to be different traffic movement regimes for traffic movement on weekdays, i.e.:

  - almost constant aggregate speed for almost the whole day besides the time period from 4:30 PM to 7:00 PM; and

  - a sharp drop in the speed around 4:30 PM to 7:00 PM, with an increase in the number of vehicles passing per minute and the occupancy levels.

- There seems to be a threshold occupancy level for the sharp drop in the aggregate speeds. This threshold occupancy level is location specific and varies from 15 to 25 percent.

- Periods of almost constant aggregate speed and of sharp speed drops suggest the existence of different driving behaviors as a reaction to the number of vehicles that

79

are trying to use the same section of the freeway at the same time. Typically, for weekdays, we can distinguish the traffic movement into the following regimes:

- *Free Regime:* observed during early morning hours and late night hours, typically from 9:30 PM to 7:00 AM;
- *Regime 1:* observed from 7:00 AM to 4:30 PM and 7:00 PM to 9:30 PM; and
- *Regime 2:* observed from 4:30 PM to 7:00 PM.

By different traffic regimes, we mean that different vehicle following behaviors can be hypothesized. During the *Free Regime*, high aggregate speeds and very few vehicles per minute passing through a location are measured on the freeway. This can be deduced both from the occupancy and number of vehicles per minute data. The vehicles being driven in this regime can be thought of as being driven with their desired speeds without any interaction with the fellow vehicles. During *Regime 1* and *Regime 2* there is an interaction between the vehicles as far greater occupancy levels and the number of vehicles passing through per minute are observed. These observations are repeatable for different working days and locations during the same time durations.

## Free Regime: Discrete Traffic State Propagation

During the *Free Regime*, there is no interaction between the vehicles, and the behavior of all the vehicles is fairly random. All the vehicles can drive at their desired speeds. Thus, the idea of a "representative" vehicle does not hold, and no specific vehicle following law can be generalized to describe the driver behavior for the current traffic. In this research project we are trying to model the current traffic, so we treat the movement of traffic in *Free Regime* as a case of "discrete traffic state propagation."

We develop a state propagation model to predict traffic state (number of vehicles) at a fixed downstream location on a freeway. The predictions are made by using real-time dual trap detector data on the number of vehicles passing through a fixed upstream location and their average speeds. The modeling framework involves considering the freeway as being divided into multiple links with the two detector stations making up the two ends of a link. Vehicles entering and exiting through the ramps are also taken into account. The prediction of traffic state at a downstream location is based on the information of traffic state at upstream locations on a freeway. To predict the number of vehicles at a downstream end of a link, we use the real-time

average speed of the traffic and the number of vehicles exiting the upstream detector station. For simulation studies, an upstream detector location is made the *source,* and then consecutive estimates of the number of vehicles at each downstream detector locations are made for a network of links. The number of vehicles moving toward the downstream end of a link is computed using the estimate of the number of vehicles at the current end (upstream end) of the link and the net vehicle inflow/outflow from the ramps. Following are the assumptions made while modeling the *Free Regime* using discrete state propagation:

- We assumed a single lane straight freeway. This is done by aggregating the vehicles on all the lanes of the freeway.

- We assumed zero initial conditions for the number of vehicles in a link. This is a reasonable assumption because during the *Free Regime* times, there are not many vehicles in any section at a given time.

- Vehicles while traversing a link maintain the speed at which they enter the link.

- Since the location of the entry and exit ramps is unknown, we assumed them to be located very near the upstream detector station.

- Exiting vehicles exit the freeway without affecting the movement of traffic on the freeway. Similarly, we assumed the entering vehicles to merge with the mainline freeway traffic and attain the average freeway speed in the current link almost instantaneously.

- The traffic data information from the ramps (both entry and exit) is used in real time. This is done since no origin-destination information of the traffic on the freeway is assumed.

Below we provide some results of the simulations done for a network of three consecutive links, covering 1.76 miles (from Lazy Lane to Mopac South on US 183 northbound). The extreme upstream detector is station number 23. The extreme downstream detector location is station number 33. Thus, the network is station numbers: 23-25-29-33. The network under consideration has two exit and one entry ramps.

Figure 35 shows the schematic of the network under consideration. Figure 36 shows the number of vehicles passing per minute through the originating ("source") station. Figure 37 through Figure 39 show the estimated and observed number of vehicles passing through stations

25, 29, and 33, respectively. On observing the plots, we see that the discrete state propagation model estimates the traffic state fairly well.
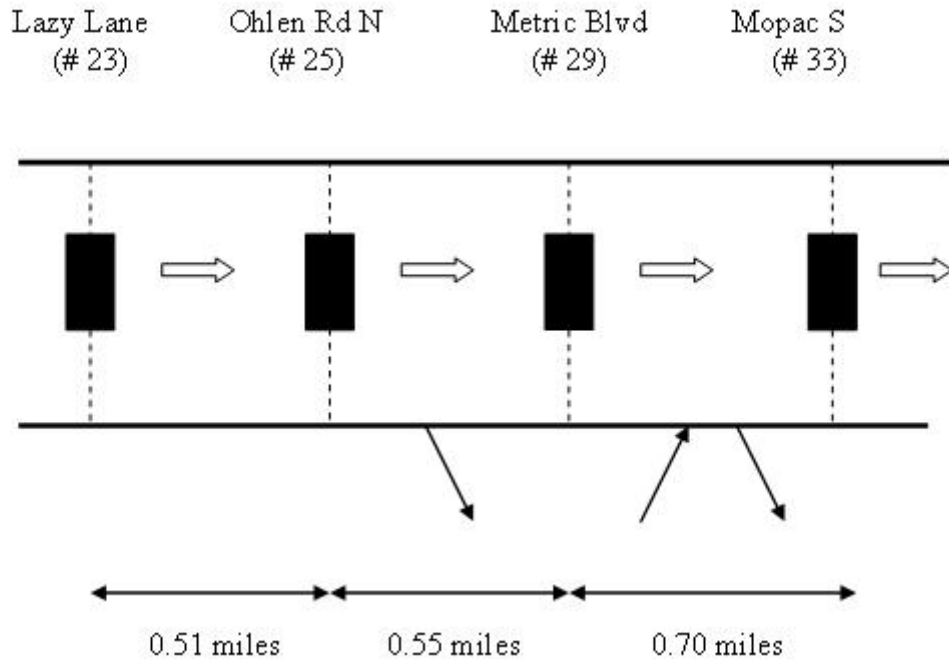


**Figure 35. Schematic of the Network under Consideration for Simulating the Free Flow on US 183 NB.**
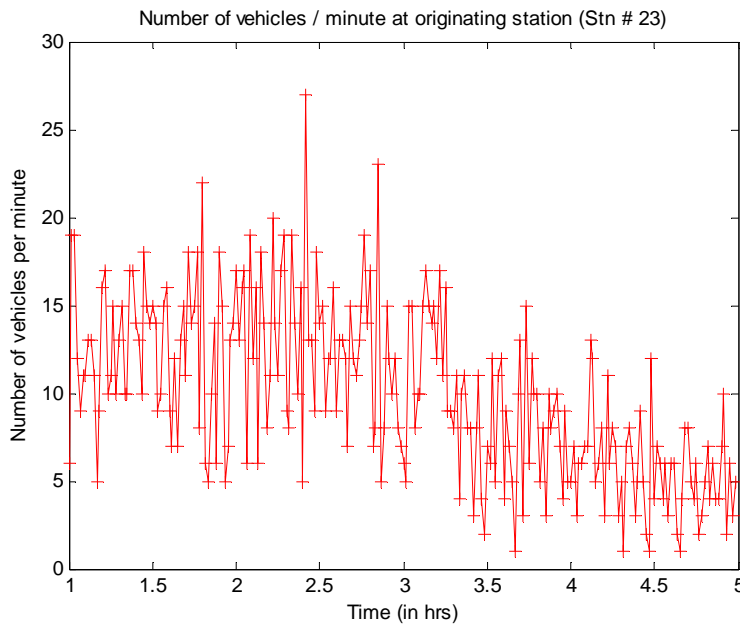


**Figure 36. Plot of Number of Vehicles Passing per Minute at Source Station #23.**
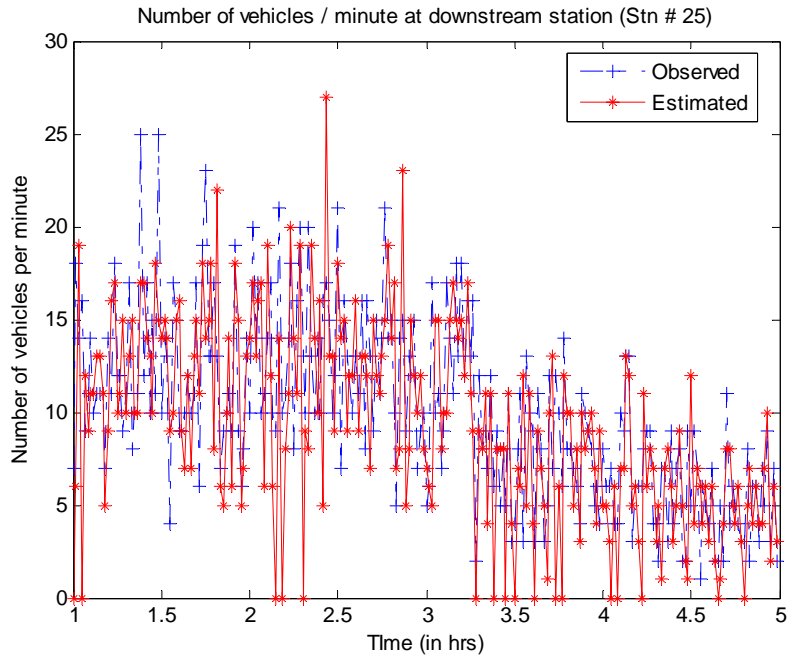
**Figure 37. Plot of Number of Vehicles Passing per Minute at Station #25.**



**Figure 38. Plot of Number of Vehicles Passing per Minute at Station #29.**

**Figure 39.  Plot of Number of Vehicles Passing per Minute at Station #33.**

Table 9 shows the cumulative number of vehicles data for a particular day, when the simulations were carried out for a time duration during the *Free Regime* (1:00 AM to 5:00 AM). The numbers of vehicles 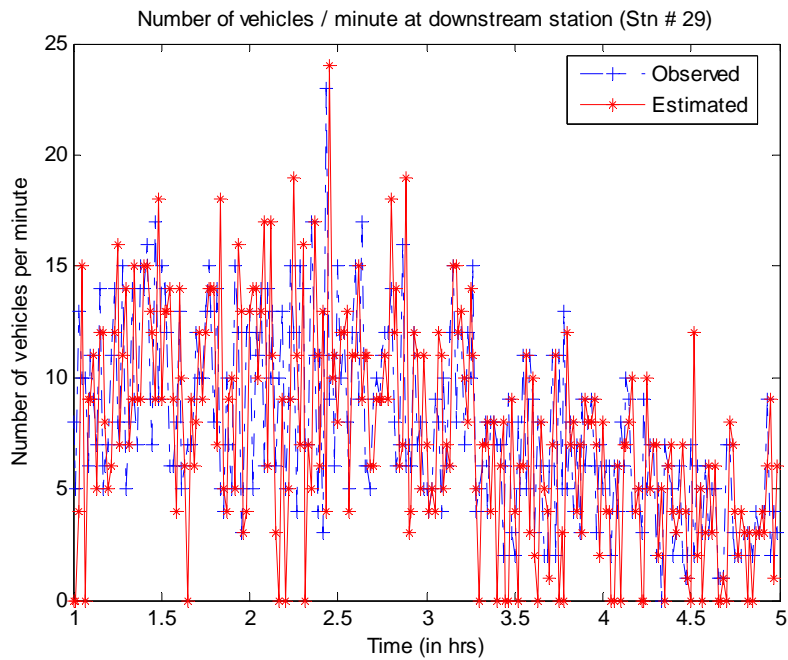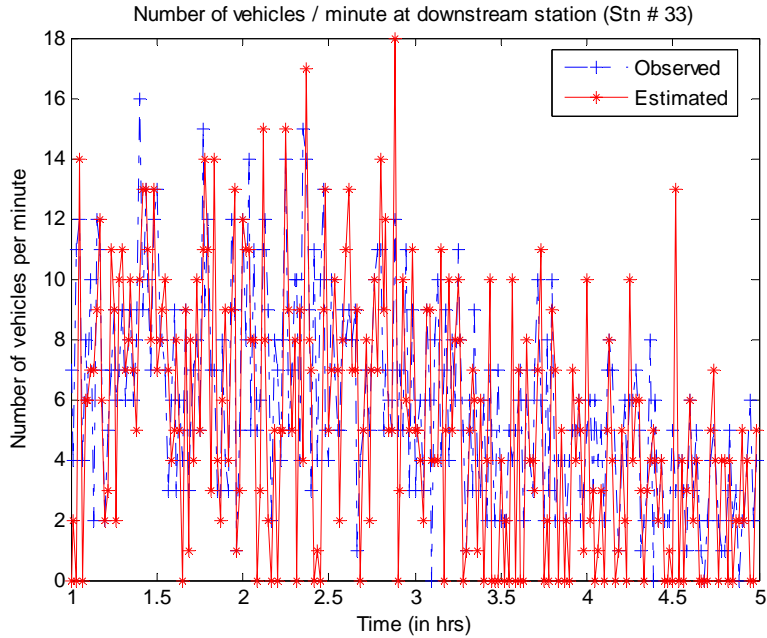leaving and entering through the ramps also are included in the simulations. From the results we observe that some vehicles are "lost" in the section. This can be due to the fact that we do not know the initial conditions of the traffic state in the network. Also, not knowing the exact location of the entry and exit ramps is a potential reason for the error in predicting the traffic state.

**Table 9.  Cumulative Count for the Number of Vehicles during *Free Regime* for the Network 23-25-29-33.**

| Station Number | Observed | Predicted | Error % |
|---|---|---|---|
| 23 | 2400 | NA | NA |
| 25 | 2417 | 2240 | 7.3231 |
| 29 | 1857 | 1799 | 3.1233 |
| 33 | 1430 | 1274 | 10.9091 |

**Regimes 1 and 2: Estimation of Traffic Parameters and Traffic State Prediction**

The traffic model that we developed is primarily based on the idea of representing the aggregate behavior of traffic movement with a "representative" vehicle, the dynamics of which

84

are based on the interactions between the vehicles in the traffic. In this section we corroborate the non-continuum traffic model with the real traffic data obtained from the Austin freeways.

*Use of Historic Traffic Data to Identify the Structure of Vehicle Following for Regimes 1 and 2*

From traffic loop detector data, repetitive patterns are observed in traffic throughput with respect to the time of the day. The traffic data for the number of vehicles passing through a location and their aggregate speeds are used to identify the structure of vehicle following for the traffic movement in *Regimes 1* and *2*. The following state space model is constructed for identification purposes:

$$N_i(k+1) = N_i(k) + h\left[ N_i^{en}(k) - \left[\frac{\overline{v}_i(k)N_i(k)}{L_{s,i}}\right] + \tilde{n}_i(k) \right] \tag{32}$$

$$N_{i,sum}^{ex}(k+1) = N_{i,sum}^{ex}(k) + h\left[\frac{\tilde{v}_i(k)N_i(k)}{L_{s,i}}\right] \tag{33}$$

$$\overline{\Delta}_i(k+1) = \overline{\Delta}_i(k) - h\left[\frac{\left(L_{car}+\overline{\Delta}_i(k)\right)^2}{L_{s,i}}\right]\left[ N_i^{en}(k) - \left[\frac{v_i(k)N_i(k)}{L_{s,i}}\right] + \tilde{n}_i(k) \right] \tag{34}$$

where,

$N_i$ = the number of vehicles in the section,

$N^{ex}{}_{i,sum}$ = the cumulative number of vehicles exiting a section,

$\overline{\Delta}_i$ = the state vector of the aggregate following distance, and

$h$ = the time step.

The system takes $(N^{en}{}_i + \tilde{n}_i)$, the net inflow of vehicles into the section in each time step as the input. The system output is taken to be $N^{ex}{}_{i,sum}$, the cumulative number of vehicles exiting the section. Thus, the model assumes that the rate of change of number of vehicles with respect to time in a section is known. Since we do not know the initial conditions of the states $N_i$, $N^{ex}{}_{i,sum}$, and $\overline{\Delta}_i$, we design a state estimator using the extended Kalman filtering technique.

*Structure of Vehicle Following Dynamics for Traffic under Different Regimes*

We apply the extended Kalman filtering methodology to identify the states in the state space model described above. Use of the Gaussian white noise sequences in the state transition equation helps to treat the aggregate following distance and the number of vehicles in the section as different state variables. The aggregate speed data are used to estimate the states at each time instant. The simulations for estimating the number of vehicles in the section and the aggregate following distance for *Regimes 1* and *2* are done for many weekdays. Figure 40 shows the aggregate following distance, and Figure 41 shows the estimated number of vehicles in a section. We conducted simulations for a section stretching from Lamar Boulevard North to Ohlen Road North on US 183 northbound in Austin. The section length under consideration is 2.84 lane miles (data for all the three lanes was aggregated). A fixed length of a vehicle is taken as 15 feet for the purposes of these simulations.
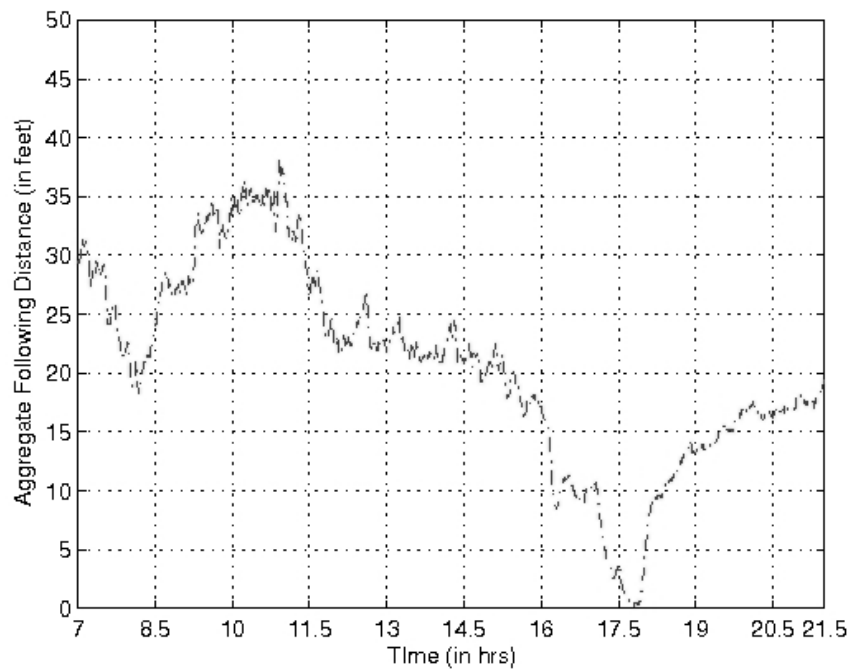


**Figure 40.  Estimated Aggregate Following Distance in a Section on US 183 NB
on May 18, 2004.**

86
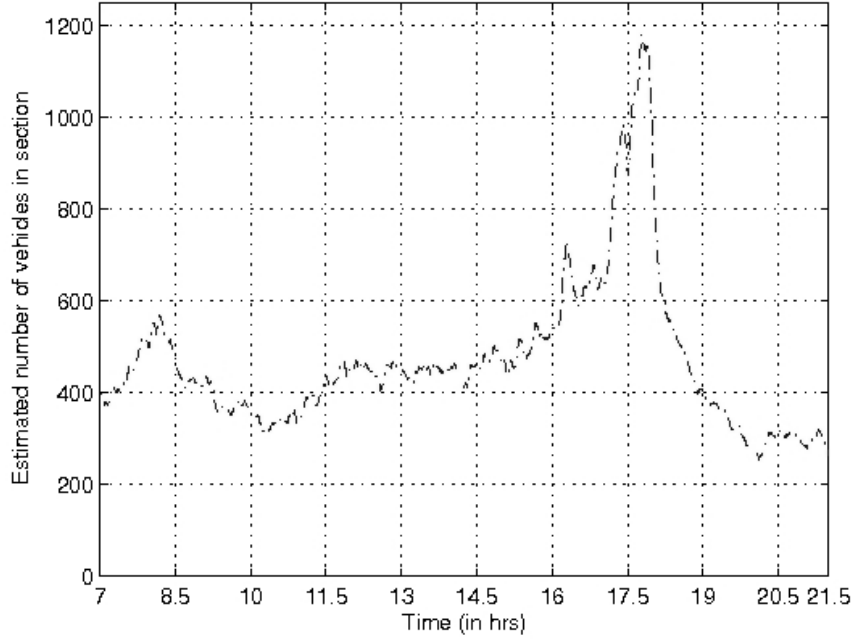
**Figure 41. Estimated Number of Vehicles in a Section on US 183 NB on May 18, 2004.**

Upon careful observation of the plot of estimated aggregated following distance we can distinguish two "sub-regimes" in *Regime 1*:

- varying aggregate following distance and
- almost constant aggregate following distance.

Also, we note that the following distance reacts quite sharply to the sharp drop and rise in the aggregate speeds between 4:30 PM to 7:00 PM (*Regime 2*). We now give the following structure to the vehicle following.

- *Regime 1:* Observed from 7:00 AM to 4:30 PM and 7:00 PM to 9:30 PM. We have the following sub-regimes:

1. *Regime 1 (a):* Observed from 7:00 AM to 11:30 AM and 7:00 PM to 9:30 PM:

$$\dot{v}_i = \frac{1}{h_w}\left[\dot{\Delta}_i + \lambda(\Delta_i - h_w v_i)\right] \tag{35}$$

2. *Regime 1 (b):* Observed from 11:30 AM to 4:30 PM:

$$\dot{v}_i = \lambda_1\dot{\Delta}_1 + \lambda_2(\Delta_i - (\frac{L_{s,i}}{N_i} - L_{car})) \tag{36}$$

87

- *Regime 2:* Observed from 4:30 PM to 7:00 PM. (Work is still under progress to model this traffic regime.)

In traffic *Regime 1 (a),* it *is hypothesized* that the drivers tend to maintain a following distance that varies with the speed of the vehicle. This hypothesis also substantiates the observation that the drivers tend to accept smaller following distances while maintaining almost constant speeds. This happens when there is an increase in the demand on utilization of the freeway (more number of vehicles are driving). On the other hand, during *Regime 1 (b),* it is hypothesized that the drivers tend to maintain a "constant" following distance. Work is still under progress to model the vehicle following behavior for *Regime 2*.

In the above equations, the parameters $\lambda$, $\lambda_1$, and $\lambda_2$ reflect the time constants associated with driving in their respective traffic regimes. These along with $h_w$ are estimated from the traffic data. The numerical values of parameters associated with this structure are specific to the freeway section under consideration.

*Estimating the Traffic Parameters Associated with Different Traffic Regimes*

The values of estimated states, the aggregate following distance and the number of vehicles in the section, and the aggregate speed data are used to estimate the parameters. The principle of least squares is then applied to estimate the parameters. The estimated parameters show consistent repetitive values for different working days. Table 10 gives the estimated values of parameters for *Regime 1 (a).*

**Table 10.  Estimated Parameters for *Regime 1 (a).***

| Regime 1 (a) | | | | | | | | | |
|---|---|---|---|---|---|---|---|---|---|
| Monday | | Tuesday | | Wednesday | | Thursday | | Friday | |
| $\lambda$ | $h_w$ | $\lambda$ | $h_w$ | $\lambda$ | $h_w$ | $\lambda$ | $h_w$ | $\lambda$ | $h_w$ |
| 7.71E-4 | 0.0623 | 7.79E-4 | 0.0522 | 4.87E-4 | 0.1036 | 2.81E-4 | 0.1007 | 6.89E-4 | 0.0607 |
| 8.81E-4 | 0.0579 | 1.09E-3 | 0.0526 | 6.26E-4 | 0.0858 | 5.59E-3 | 0.0817 | 9.24E-4 | 0.0558 |
| 4.84E-4 | 0.0610 | 3.35E-4 | 0.0572 | 5.03E-4 | 0.1509 | 6.24E-4 | 0.1117 | 3.98E-4 | 0.0894 |
| 1.25E-4 | 0.0650 | 4.32E-4 | 0.0590 | 4.93E-4 | 0.0997 | 3.24E-4 | 0.0862 | 2.80E-4 | 0.0608 |
| 4.16E-4 | 0.0589 | 7.15E-4 | 0.0613 | 3.39E-4 | 0.0840 | 7.92E-4 | 0.0791 | 4.86E-4 | 0.0747 |

The units of $\lambda$ and $h_w$ are *minute$^{-1}$* and *minute,* respectively. The parameters show repetitive trends with respect to the day of the week. The time headway $h_w$ varies from about three to nine seconds. For example, on Mondays the time headway is about three to four seconds. These numbers are fairly reasonable for the current traffic. The small values of $\lambda$ and typical values of time headway and speed in the section suggest that drivers are ready to accept shorter following distances so that they can drive with almost constant speeds and that the rate of change of speed is more dependent on the relative speed.

Table 11 gives the estimated values of parameters for *Regime 1 (b)*. From the values of $\lambda_1$ and $\lambda_2$ we deduce that the rate of change of aggregate speed for the section considered is more dependent on the relative velocity.

**Table 11. Estimated Parameters for *Regime 1 (b)*.**

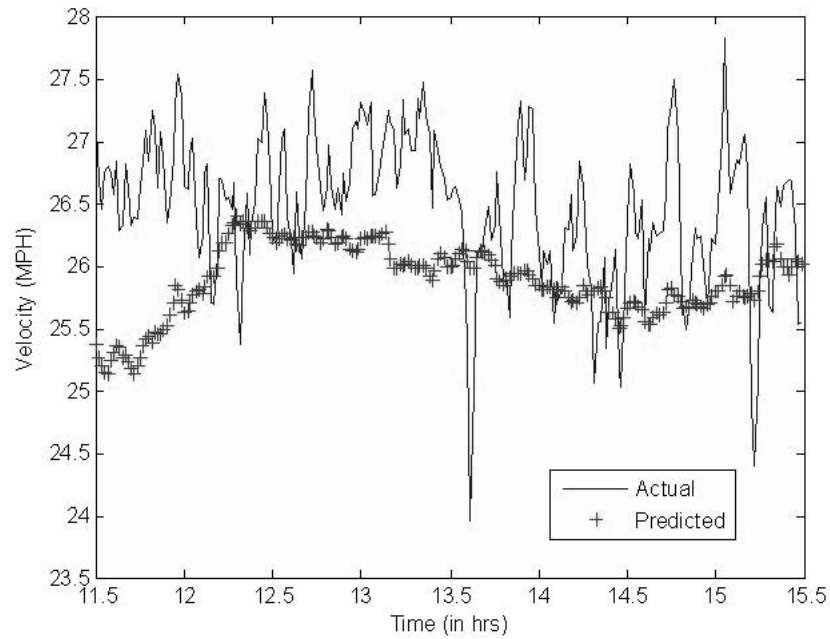| Regime 1 (b) | | | | | | | | | |
|---|---|---|---|---|---|---|---|---|---|
| **Monday** | | **Tuesday** | | **Wednesday** | | **Thursday** | | **Friday** | |
| $\lambda_1$ | $\lambda_2$ | $\lambda_1$ | $\lambda_2$ | $\lambda_1$ | $\lambda_2$ | $\lambda_1$ | $\lambda_2$ | $\lambda_1$ | $\lambda_2$ |
| 26.296 | 0.6611 | 40.508 | -0.0357 | 19.969 | 0.1377 | 19.298 | -0.0456 | 40.323 | 0.0182 |
| 21.758 | 0.0157 | 35.356 | -0.0228 | 19.540 | 0.0342 | 19.167 | -0.0258 | 37.487 | 1.0640 |
| 23.328 | 0.0454 | 33.811 | -0.0301 | 19.940 | 0.0219 | 17.788 | -0.0234 | 43.110 | 0.0905 |
| 26.539 | 0.1996 | 32.425 | -0.0094 | 22.483 | 0.1452 | 18.032 | -0.0101 | 43.229 | 0.1748 |
| 28.557 | 0.5011 | 31.643 | -0.0193 | 20.254 | 0.1215 | 26.297 | -0.1239 | 40.369 | 0.1328 |

*Estimation of Traffic State in Real Time*

After estimating the time constants associated with the different traffic regimes from historical data, we use them to predict the traffic state. Extended Kalman filtering is again used to estimate the states of traffic in real time, but now the state vector also includes the aggregate speed of the traffic (speed of the "representative" vehicles for the particular section). The input to the system is taken to be the net inflow of vehicles into the section $(N^{en}{}_i + \tilde{n}_i)$. The output of the system is again taken to be the cumulative number of vehicles exiting the section. To validate the estimated states, we plotted the predicted aggregate speed against the observed aggregate speed for the time duration on the particular day. The predictions made by this filtering technique are one step predictions. Since the time step used is one minute (the traffic data are available in one-minute intervals), the model is able to predict aggregate speeds one minute in advance.

Below we give a few results for the estimation of traffic state in real time. In the plots below, the predicted speed is plotted against the observed traffic speed for traffic *Regime 1 (b)*.

The results are for the same section for which the parameter results have been presented. The values of traffic parameters (estimated from historic data) are used in real-time estimation of the traffic state. We predicted the aggregate traffic speed on a one-minute basis. Figure 42 and Figure 43 show the one step predicted aggregate traffic speed for congestion in *Regime 2* for two working days in the year 2004. It is important to note the scale used in the plots. The vertical scale is about four miles per hour. From the plots, we can see that the model is able to predict the aggregate traffic speed very well, and in this sense the estimation is fairly accurate.
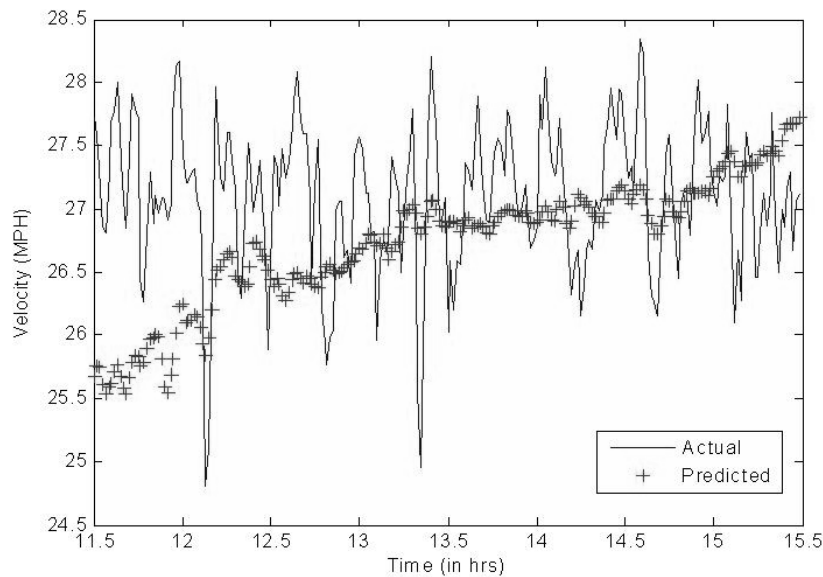


**Figure 42.  Plot of Aggregate Traffic Speed in the Section for Thursday, April 15, 2004.**

**Figure 43. Plot of Aggregate Traffic Speed in the Section for Friday, February 13, 2004.**

## Conclusion and Work in Progress

The driving behavior for traffic in *Regime 2* is yet to be modeled. Work also is underway to increase the prediction window to be on the order of five to ten minutes, which can be more beneficial in predicting both the recurring and non-recurring congestion. The switching of modes of traffic regimes also warrants attention, so that control algorithms can be developed for Advanced Traveler Management Systems and Advanced Traveler Information Systems applications.

91

# CHAPTER IV. HIGH-LEVEL SPECIFICATIONS FOR PROTOTYPE TOOL

Figure 44 shows a schematic functional diagram of the prototype tool. A more detailed functional description of each of the components follows. This more detailed discussion falls short of providing a detailed description of component (module) interfaces and associated formats, but it does indicate where those details need subsequently to be defined in detail.
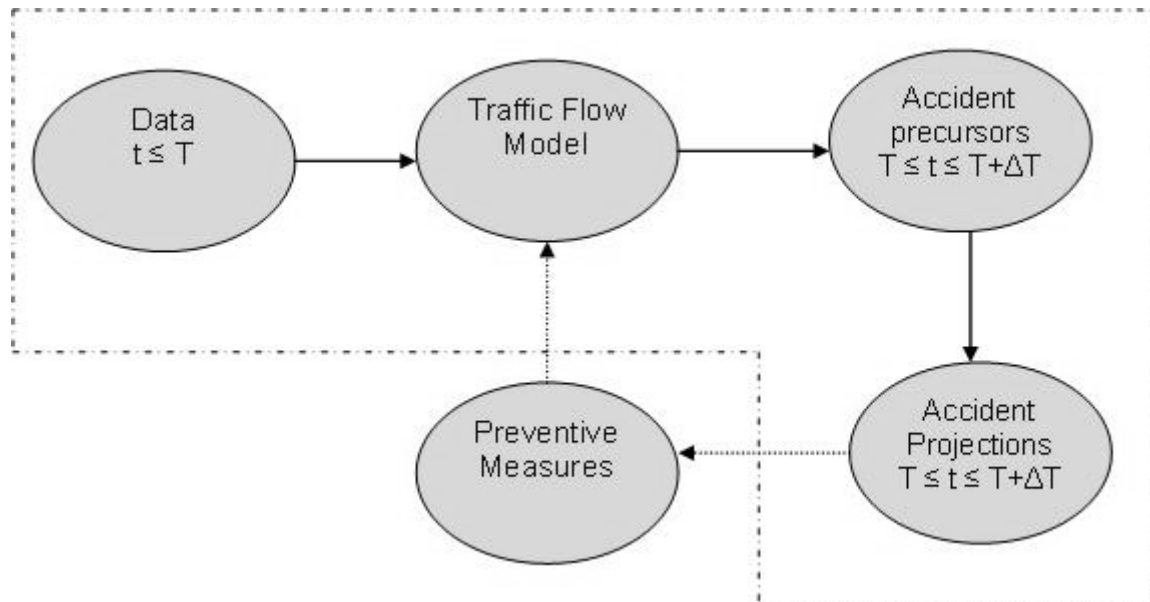


**Figure 44.  High-Level Schematic Function Diagram of On-Line System.**

## ASSUMPTIONS

The objective is to use the best available data, at some arbitrary time $T$, to predict the probability of an incident, as a function of time and position, for a designated section of freeway ("target section"), and over the "prediction interval" $T$ to $T+\Delta T$. The "prediction duration" $\Delta T$ must be long enough to permit countermeasures to be undertaken, but sufficiently short that the predictions will be reasonably accurate. Predictions will be updated at "updating horizons" $\delta t < \Delta T$.

**DATA**

The function of the data module is to provide appropriately formatted input data to the traffic flow module. Input data required by the traffic flow model include suitable representations of both observed data on the current day up to time *T,* and historical data, presumably in some mean sense, with allowance for time of day, day of week, etc. Of course, historical data are always available; however, the key hypothesis of the project is that use of current data as available, rather than mean historical data, will permit a more precise projection of probability of an incident. For implementation, detailed decisions regarding formatting of both historical data and current data *need to be undertaken*. For the historical data, we need to develop corresponding reference archives for designated target sections of freeway. The data module will have access to both these historical reference archives and the current detector data, and on demand from the traffic flow module will provide the appropriate data in a format to be determined in detail.

**TRAFFIC FLOW MODEL**

The "traffic flow model" is the system module that will acquire the requisite data from the data module, and produce therefrom a representation of the state of traffic flow over the target section and the prediction interval that is native to the methodology of the particular traffic flow model. Possible instances of a traffic flow model that are under consideration include:

- a traffic flow model based on the kinematic-wave model, in which case the output would be some representation of the time and position variation of density (or flow or speed) over the target section and the prediction interval;

- a traffic flow model based on vehicle car following dynamics; and

- any other current or future model (for example, DYNASMART or one of the other currently available models).

This design permits the traffic flow model to be developed independently of the data module, provided both respect the defined interface. The interface between traffic flow model and incident precursor model will not be independent of the details of the traffic flow model, but defining them as separate modules will permit their development in parallel and will permit decoupled version development for these two modules. The driving force behind the design decision not to "lock into" a single uniform interface between traffic flow models and incident

precursor modules is the desire to retain maximum flexibility and modularity regarding the choice of traffic flow model, thereby providing the ability to adapt rapidly to developments in the fast-paced field of computational simulation of traffic flow.

## INCIDENT PRECURSORS

The function of the incident precursor module is to accept as input the traffic flow representation native to a particular traffic flow model, for the designated target section of freeway and over the prediction interval under consideration, and produce from that the time and position dependency of the selected incident precursors (e.g., longitudinal speed variation and density). Thus, the incident precursor module must be tailored to the particular traffic flow model, but its output must conform to a uniform interface between incident precursor modules and incident projection modules. Details of the incident-precursor/incident-projection interface remain to be developed.

## INCIDENT PROJECTIONS

The incident precursor module takes as its input the output of the incident precursor module, which is to say a representation, in a format to be decided subsequently in detail, of the time and position dependency of the selected incident precursors, over the designated target section and prediction interval. As its output it produces a suitable representation of the predicted frequency of incidents over the target section and prediction interval. Details of the format of these incident projections remain to be determined, but a hard requirement is that this representation be suited to an intuitive graphical representation for quick grasp by control center operators.

## PREVENTIVE MEASURES

The details of the preventive measures that might be undertaken are outside the scope of the project itself. However, we do require some input from TxDOT on the possibilities because the time scale required to implement preventive measures materially affects the required prediction duration (i.e., $\Delta T$ in the preceding development).

# REFERENCES

1. Gribe, P. (2003). "Accident Prediction Models for Urban Roads." *Accident Analysis and Prevention,* Vol. 35, pp. 273-285.
2. Hiselius, L. W. (2004). "Estimating the Relationship between Accident Frequency and Homogeneous and Inhomogeneous Traffic Flows." *Accident Analysis and Prevention,* Vol. 36, pp. 985-999.
3. Cedar, A., and M. Livneh (1982). "Relationships between Road Accidents and Hourly Traffic Flow—I." *Accident Analysis and Prevention*, Vol. 14, pp.19-34.
4. Davis, G. A. (2005). "Collective Responsibility in Freeway Rear-End Collisions. An Application of Casual Models." Presented at Transportation Research Board Annual Meeting, Washington, D.C.
5. Oh, J.-S., C. Oh, S. G. Ritchie, and M. Chang (2005). "Real-Time Estimation of Accident Likelihood for Safety Enhancement." *Journal of Transportation Engineering*, ASCE, Vol. 131, No. 5, pp. 358-363.
6. Lee, C., F. Saccomanno, and B. Hellinga (2002). "Analysis of Crash Precursors on Instrumented Freeways." *Transportation Research Record 1784*, TRB, National Research Council, Washington, D.C., pp. 1-8.
7. Lee, C., B. Hellinga, and F. Saccomanno (2003). "Real-Time Crash Prediction Model for Application to Crash Prevention in Freeway Traffic." *Transportation Research Record 1840*, TRB, National Research Council, Washington, D.C., pp. 67-77.
8. Abdel-Aty, M., A. Pande, N. Uddin, H. Al-Deek, and E. Radwan (2004). *Linking Crash Patterns to ITS -Related Archived Data*. Final Report, University of Central Florida, Orlando.
9. Kockelman, K. M., and J. Ma (2004). „Freeway Speeds and Speed Variations Preceding Crashes, within and across Lanes." Presented at ITS America 2004, 14th Annual Meeting and Exposition, San Antonio, Texas.
10. Golob, T. F., and W. W. Recker (2004). "A Method for Relating Type of Crash to Traffic Flow Characteristics on Urban Freeways." *Transportation Research, Part A*, Vol. 38, No. 1, Elsevier, pp. 53-80.
11. Guiliano, G. (1989). "Incident Characteristics, Frequency, and Duration on a High Volume Urban Freeway." *Transportation Research, Part A,* Vol. 23, No. 5, pp. 387-396.
12. Madanat, S., P. Liu, H. Pan, and H. Teng (1997). "Freeway Incident Likelihood Prediction and Response Decision-Making." In *Joint Highway Research Project Report FHWA/IN/JHRP-96/6*, Project No. HPR-2090, Purdue University, West Lafayette, Indiana.
13. Khattak, A. J., P. Kantor, and F. M. Council (1998). "Role of Adverse Weather in Key Crash Types on Limited-Access Roadways: Implications for Advanced Weather Systems." *Transportation Research Record 1621*, TRB, National Research Council, Washington, D.C., pp. 10-19.
14. Greene, W. H. (2002). *Econometric Analysis.* 5th Ed., Prentice Hall, Pearson Education, Inc., Upper Saddle River, New Jersey.
15. Washington, S., M. Karlaftis, and F. Mannering (2003). *Statistical and Econometric Methods for Transportation Data Analysis*. CRC Press, Boca Raton, Florida.

16. Shankar, V., F. Mannering, and W. Barfield (1995). "Effect of Roadway Geometrics and Environmental Factors on Rural Freeway Accident Frequencies." *Accident Analysis and Prevention*, Vol. 27, No. 3, pp. 371-389.
17. Brodsky, H., and A. S. Hakkert (1988). "Risk of a Road Accident in Rainy Weather." *Accident Analysis and Prevention*, Vol. 20, No. 3, pp. 161-176.
18. http://cdo.ncdc.noaa.gov/ulcd/ULCD, accessed August 25, 2005.
19. Chandrasekaran, P. (1998). *Prediction of Traffic Flow for Real-Time Control*. Master's Thesis, Texas A&M University, College Station, Texas.
20. Zhang, L., and D. Levinson (January 2004). *Some Properties of Flows at Freeway Bottlenecks*. Transportation Research Board Annual Meeting CD-ROM, Washington, D.C.
21. Persaud, B., S. Yagar, D. Tsui, and H. Look. *Study of Breakdown-Related Capacity for a Freeway with Ramp Metering*. http://www.civil.ryerson.ca/staff_fac/publications/persaud/bdowntrb012revnov.htm, accessed August 25, 2005.
22. http://www.trafficlab.utah.edu/research/projects/current/acrobat/IncidentDet.pdf, accessed August 25, 2005.
23. Koppelman, F. S., and W. Lin (August 1996). *Development of an Expressway Incident Detection Algorithm for the ADVANCE Area Based on the California Algorithm Set*. Path Project Report TRF-ID-311/312, The Transportation Center, Northwestern University, Evanston, Illinois.
24. Browne, R., S. Foo, S. Huynh, B. Abdulhai, and F. Hall (January 2005). "AID CAAT: The Automatic Incident Detection Algorithm Comparison and Analysis Tool." Transportation Research Board Annual Meeting CD-ROM, Washington, D.C.
25. Chen, C., A. Skabardonis, and P. Varaiya (January 2004). "A System for Displaying Travel Times on Changeable Message Signs." Transportation Research Board Annual Meeting CD-ROM, Washington, D.C.
26. Coifman, B. (2002). "Estimating Travel Times and Vehicle Trajectories on Freeways using Dual Loop Detectors." *Transportation Research, Part A,* Vol. 36, No. 4, pp. 351-364.
27. Newell, G. (1993). "A Simplified Theory of Kinematic Waves in Highway Traffic, Part II: Queuing at Freeway Bottlenecks." *Transportation Research, Part B*, Vol. 27, pp.289-303.
28. *CORSIM, Version 1.03, User's Manual* (Apr 1997). Kaman Science Corporation, Colorado Springs, Colorado.
29. Parker, M. (2002). "Zooming In on Traffic Microsimulation." *Traffic Technology International*, Dorking, Surrey, United Kingdom.
30. Smith, M., S. Druitt, G. Cameron, and D. McArthur (July 1994). *PARAMICS Final Report*. Report No. EPCC-PARAMICS-FINAL, University of Edinburgh, Parallel Computing Center, Scotland.
31. Mahmassani, H., and K. Abdelghany (2003). *"*DYNASMART-IP: Dynamic Traffic Assignment Meso-simulator for Intermodal Networks." In *Advanced Modeling for Transit Operations and Service Planning*, pp. 201-229, Elsevier Science Publishers, Amsterdam, Netherlands.

32. Ben-Akiva, M., D. Cueno, M. Hasan, M. Jha, and Q. Yang (2003). "Evaluation of Freeway Control Using Microscopic Simulation Laboratory." *Transportation Research, Part C: Emerging Technologies*, Vol. 11, No. 1, pp. 29-50.

33. Foo, S., B. Abdulhai, and M. Elbagoury (January 2005). "Information Theoretic Analysis of Loop Detector Data." Transportation Research Board Annual Meeting CD-ROM, Washington, D.C.

34. *Highway Capacity Manual 2000.* Transportation Research Board, National Research Council, Washington, D.C.

35. Lighthill, M. J., and G. B. Whitham (1955). "On Kinematic Waves II—A Theory of Traffic Flow on Long Crowded Roads." In *Proceedings Royal Society, London,* Vol. A229, pp. 317-345.

36. Richards, P. I. (1955). "Shockwaves on the Highway." *Operations Research*, Vol. 4, pp. 42-51.

37. Papageorgieu, M. (1998). "Some Remarks on Macroscopic Traffic Flow Modeling." *Transportation Research A 32,* pp. 323-329.

38. Drake, J., J. Schofer, and A. May. (1967). A Statistical Analysis of Speed Density Hypotheses. *Highway Research Record 154*, pp. 53-87.

39. Koshi, M., M. Iwasaki, and I. Okhura (1983). "Some Findings and an Overview on Vehicular Flow Characteristics." In *Proceedings of the Eighth International Symposium on Transportation Traffic Theory*, V. F. Hurdle et al., eds., University of Toronto Press, Toronto, pp. 403-426.

40. Cassidy, M. J., and J. R. Windover (1995). "Methodology for Assessing Dynamics of Freeway Traffic Flow." *Transportation Research Record 1484*, TRB, National Research Council, Washington, D.C., pp. 73-79.

41. Greenshields, B. N. (1934). "A Study of Traffic Capacity." In *Proceedings of the 14th Annual Meeting of the Highway Research Board,* Highway Research Board, Washington, D.C., pp. 448-474.

42. Ross, P. (1988). "Traffic Dynamics." *Transportation Research B 22,* pp. 421-435.

43. Ross, P. (1989). "Response to Newell." *Transportation Research B*, *23B,* pp. 390-391.

44. Newell, G. F. (1989). "Comments on Traffic Dynamics." *Transportation Research B*, *23B,* pp. 386-389.

45. Nelson, P., and N. Kumar (2004). "Point Constrictions, Interface and Boundary Conditions for the Kinematic-Wave Model." Proceedings TRB 2004 (published in CD format), Washington, D.C.

46. Lebacque, J. P. (to appear). "Intersection Modeling, Application to Macroscopic Network Traffic Flow Models and Traffic Management. In *Proceedings of the Workshop on Traffic and Granular Flow 2003*.

47. Bui, D. D., P. Nelson, and S. L. Narasimhan (1992). *Computational Realizations of the Entropy Condition in Modeling Congested Traffic Flow*. Texas Transportation Institute, College Station, Texas.

48. Daganzo, C. F. (1994). "The Cell Transmission Model: A Dynamic Representation of Highway Traffic Consistent with the Hydrodynamic Theory." *Transportation Research B*, Vol. 28, pp. 269-287.

49. Buisson, C. (1997). "Découpage objets de Strada." Internal report Licit, Entre-Inrets, France.

50. Head, K. L. (1994). "Event-Based Short-Term Traffic Flow Prediction Model." *Transportation Research Record 1510*, TRB, National Research Council, Washington D.C, pp. 45-52.

51. Yang, F., Z. Lin, H.X. Liu, and B. Ran (2004). "Online Recursive Algorithm for Short-Term Traffic Prediction." *Transportation Research Record 1879*, TRB, National Research Council, Washington D.C, pp. 1-9.

52. *VISSIM 4.00 User Manual* (2004). PTV, Stumpfstraβe 1, D-76131 Karlsruhe, Germany.

# APPENDIX: SOFTWARE TOOL DEVELOPMENT

The primary objective of this project is to develop freeway traffic assessment and prediction models and a prototype software implementation of selected models. To provide for efficient testing and development of these models, researchers are developing a software package. The objective is to produce an off-line research tool that would provide a basis for the prototype software to be delivered to TxDOT at the end of this project. To fulfill the above requirements, the following functionality, graphically shown in Figure A-1, is needed:

1. Read a freeway configuration file and create the precedence relationships for all detectors in the freeway system.

2. Mimic real-time operation by reading data of the entire freeway system in one-minute steps.

3. After reading new data at each one-minute step:

   a. Invoke selected traffic assessment/prediction models, and

   b. Display/output key indicators/measurements regarding the status (locations of congestion and incidents, travel times, etc.) of the freeway.

## SOFTWARE DESCRIPTION

### Freeway System

In this software (currently named 0-4946 Data Analyzer), a freeway system is modeled using four basic objects: system, station, detector, and record. The "system" is composed of "stations," which in turn contain "detectors" at the same location. A "record" contains minute-by-minute volume, occupancy, speed, and truck percentage data for each detector. Figure A-2 illustrates these relationships.
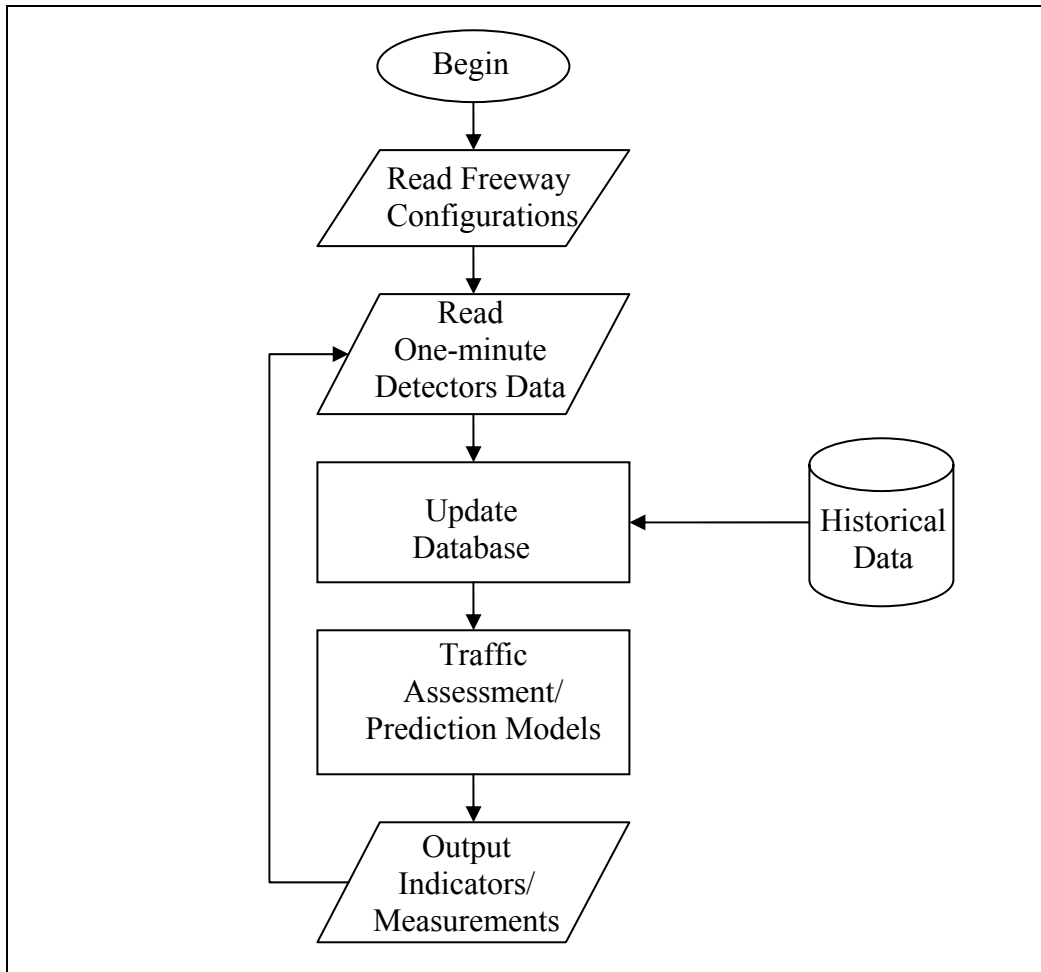
**Figure A-1.  Software Flow Chart.**
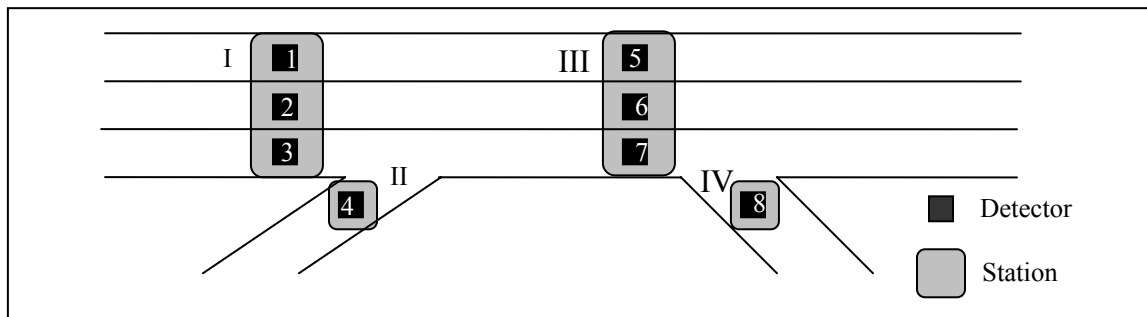


**Figure A-2.  Freeway System.**

The freeway system shown in Figure A-2 has eight detectors and four stations. Station I has detectors 1, 2, and 3; station II has detector 4; station III has detectors 5, 6, and 7; and station IV has detector 8. Table A-1 presents the data definitions.

**Table A-1. Data Definitions.**

| System | |
|---|---|
| **Data Name** | **Description** |
| System Name | Freeway name. |
| Direction | Traffic flow direction. |
| Station Vector | List of all the stations in the system. |
| Time Stamp | Time stamp of the last data record read. |
| Record Interval | Interval between each data record. |

| Station | |
|---|---|
| **Data Name** | **Description** |
| Station ID | Unique station identification number. |
| Station Name | Name of the cross street identifying the station. |
| X-Coordinate Y-Coordinate | Station's geographic coordinates (for distance calculation). |
| Link Speed | Free-flow speed of the section from current station to the next downstream station on the freeway. |
| Detectors Vector | Detectors associated with the station. |
| Upstream Station Vector | Set of immediate upstream stations. |
| Downstream Station Vector | Set of immediate downstream stations. |

| Detector | |
|---|---|
| **Data Name** | **Description** |
| Detector ID | Unique detector identification number. |
| Record Vector | Minute-by-minute data records. |

| Record | |
|---|---|
| **Data Name** | **Description** |
| Time Stamp | Time stamp of the record. |
| Volume | One-minute volume. |
| Occupancy | Occupancy, 0–100%. |
| Speed | Average speed, mph. |
| Truck Percentage | Average truck percentage, 0–100%. |

**Input Data**

The software requires two data input sources, namely freeway configurations and detectors data. All data input files are in comma-separated format.

*Freeway Configurations File*

The freeway configurations file contains the information necessary to define the freeway system. The data format is shown in Table A-2.

**Table A-2.  Data Format of Freeway Configurations File.**

| Line 1 | |
|---|---|
| **Data Name** | **Description** |
| System Name | Name of the freeway. |
| Direction | Traffic bound. |
| Record Interval | Interval between each data record, in seconds. |

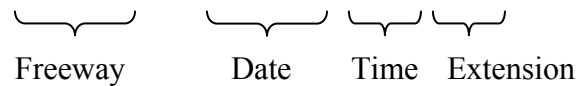| Line 2+ | |
|---|---|
| **Data Name** | **Description** |
| Station ID | Unique station identification number. |
| Station Type | Station Type: FWY (freeway station), ENT (entrance ramp station), EXT (exit ramp station), and SER (service road station). |
| Station Name | Name of the cross street that identifies the station. |
| Link Information Identifier | Value: "L." |
| Latitude | X-coordinate of the station. |
| Longitude | Y-coordinate of the station. |
| Link Speed | Free-flow speed, in mph. |
| Detector Identifier | Value: "D." |
| Detector IDs | Set of detector IDs that belong to the station. |
| Downstream Station Identifier | Value: "S." |
| Downstream Station IDs | Set of immediate downstream station IDs. |

As shown in Table A-2, the first line of the file contains general information about the freeway, i.e., system name, freeway direction, and record interval that is the time between successive data collection points. Currently, this value is 60 seconds.

Each following line (lines 2 through *n*) defines a station. Each of these lines has three elements: link information identifier, detector identifier, and downstream station identifier. Since the number of detectors and number of downstream stations vary, identifiers are also used to mark the beginning and ending of the corresponding data.

For program development, *Traffic Detector Mapbook: Traffic Operations Detector Locations in Austin, Texas* prepared by the Texas Transportation Institute was used to derive information on station ID, detector type, cross street name, and detector ID, and to define the precedence relationships of the stations on the freeway. TxDOT's Austin District provided the information on estimated free-flow speed of each freeway system and latitude and longitude for each detector using State Plane Central Zone (4203), NAD83 datum, high accuracy regional network (HARN) grid coordinates. Latitude and longitude of each detector provide the x- and y-coordinates of each station. If a station has more than one detector, we use the coordinates for the detector in the rightmost lane as an approximation.

*Detector Data*

Historic detector data files used were provided by TxDOT. Each data file contains one-hour data for all detectors for which data are being collected. Files are named following a specific naming convention that contains the freeway name, year, month, date, and time of the data collected. For example, the following file contains detector data for US 183 for the "0900" hour (09:00–09:59) on January 2, 2004:

US 0183 SCU 20040102 0900.DET

       Freeway       Date    Time  Extension

In each file, the first line contains data that defines the number of the detector for which data are being collected, detector IDs, and the station name and has the following format:

nnn,xxxxx,yyyyyyyyyyyyyyyyyyyyyyyyyyyyyyyy, xxxxx,yyyyyyyyyyyyyyyyyyyyyyyyyyyyyyyy, ……

where:

nnn = number of detectors for which data are being collected,

xxxxx = detector ID, and

yyyyyyyyyyyyyyyyyyyyyyyyyyyyyyyy = station name string.

The next 60 lines provide minute-by-minute volume, occupancy, speed, and truck percentage data for each detector and have the following format:

hhmmss,xxxxx,vvv,ooo,sss,ttt,xxxxx,vvv,ooo,sss,ttt,…

where,

hhmmss = time stamp (hh = hour, mm = minute, ss = second) of the data recorded,

xxxxx = detector ID,

vvv = one-minute volume,

ooo = occupancy, 0–100%,

sss = average speed, mph, and

ttt = average truck percentage, 0–100%.

**CURRENT STATUS OF 0-4946 DATA ANALYZER**

Currently, the software has the capabilities of creating the precedence relationships of all the stations on a freeway system by reading a freeway configuration file and mimicking real-time operation by reading minute-by-minute data for the entire freeway system. Researchers have started using the software for calculating entropy and mutual information of volume, occupancy, and speed to gain understanding of these variables. Also, the software is able to calculate and output cumulative volume counts of all or selected detectors for analysis. A snapshot of the software is shown in Figure A-3.
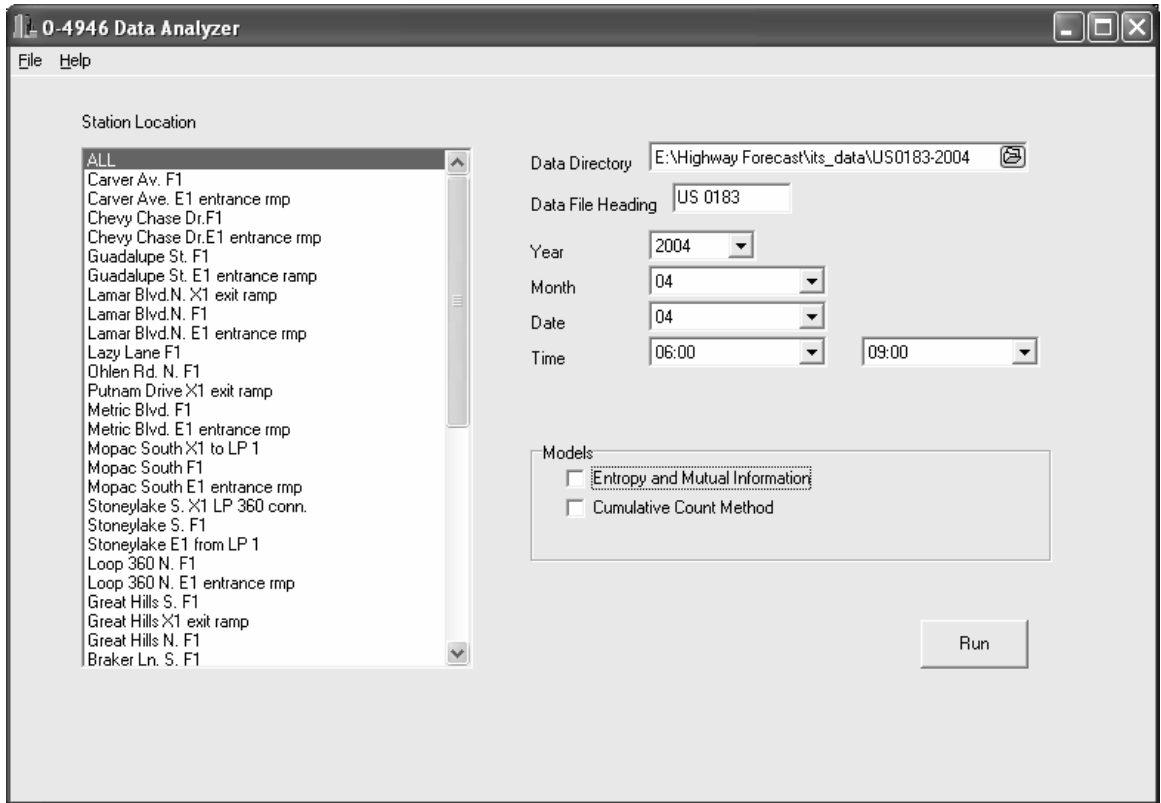
**Figure A-3.  Snapshot of the Prototype Software.**